

NEOTECTONICS OF ALTINTAŞ (ARABAN, GAZİANTEP) BASIN,
SE TURKEY

A THESIS SUBMITTED TO
THE GRADUATE SCHOOL OF NATURAL AND APPLIED SCIENCES
OF
MIDDLE EAST TECHNICAL UNIVERSITY

BY

AYDIN ÇİÇEK

IN PARTIAL FULFILLMENT OF THE REQUIREMENTS
FOR
THE DEGREE OF DOCTOR OF PHILOSOPHY
IN
GEOLOGICAL ENGINEERING

MAY 2016

Approval of the thesis:

**NEOTECTONICS OF ALTINTAŞ (ARABAN, GAZİANTEP) BASIN,
SE TURKEY**

submitted by **AYDIN ÇİÇEK** in partial fulfillment of the requirements for the degree of **Doctor of Philosophy in Geological Engineering Department, Middle East Technical University** by,

Prof. Dr. Gülbin Dural Ünver
Dean, Graduate School of **Natural and Applied Sciences**

Prof. Dr. Erdin Bozkurt
Head of Department, **Geological Engineering**

Prof. Dr. Ali Koçyiğit
Supervisor, **Geological Engineering Dept., METU**

Examining Committee Members:

Prof. Dr. Erdin Bozkurt
Geological Engineering Dept., METU

Prof. Dr. Ali Koçyiğit
Geological Engineering Dept., METU

Prof. Dr. Uğur Doğan
Department of Geography, Ankara Univ.

Prof. Dr. Kadir Dirik
Geological Engineering Dept., Hacettepe Univ.

Assist. Prof. Dr. A. Arda Özacar
Geological Engineering Dept., METU

Date: 11/03/2016

I hereby declare that all information in this document has been obtained and presented in accordance with academic rules and ethical conduct. I also declare that, as required by these rules and conduct, I have fully cited and referenced all material and results that are not original to this work.

Name, Last name: Aydın ÇİÇEK

Signature:

ABSTRACT

NEOTECTONICS OF ALTINTAŞ (ARABAN, GAZİANTEP) BASIN,
SE TURKEY

Çiçek, Aydın

PhD., Department of Geological Engineering

Supervisor: Prof. Dr. Ali Koçyiğit

May 2016, 195 pages

Altıntaş basin is an approximately 6-9 km wide, 50 km long and E-W-trending depression located in the northwestern margin of the Arabian Plate. The Study area is bounded by the Kırkpınar fault zone to the west, by the Güllüce Fault Zone to the north, by the Bağlıca, Akdurak, Erenbağ and Fıstıklıdağ Fault Sets to the northeast, by the Kemerli Fault set to the east and Karasu Fold Set to the south.

Altıntaş Basin comprises two distinct basin fills separated by a clear angular unconformity. (1) Middle Eocene-Pliocene deformed fill and (2) Early Quaternary to recent nearly flat lying fill. Field observations reveal that Middle Eocene to Pliocene units developed inside a foreland system under the control of dominantly NNW-trending mainly contractional deformation. This phase is named as “phase-1”. In addition to this, the pre-modern Altıntaş ramp-basin formed due to separation of the Araban Block from the northwestern margin of the Arabian

Plate at the end of Phase-1. Later, NNW-trending maximum principal stress axis was modified into NW to E-W-trends with strike-slip tectonic regime. This term has been regarded as Phase-2. During this phase, the basin configuration did not change significantly. Later, the maximum principal stress axis has become dominantly NNE-trends in relation to onset of escape of the Anatolian Collage. This phase has been regarded as Phase-3 or the neotectonic period. During this period, the Altıntaş basin restricted to a smaller area due to formation of a strike-slip basin.

Key words: basin, inversion, paleotectonics, neotectonics, Altıntaş.

ÖZ

ALTINTAŞ HAVZASININ NEOTEKTONİĞİ (ARABAN, GAZİANTEP), GD TÜRKİYE

Çiçek, Aydın
Doktora, Jeoloji Mühendisliği Bölümü
Danışman: Prof. Dr. Ali Koçyiğit

Mayıs 2016, 195 sayfa

Altıntaş (Gaziantep) havzası yaklaşık 6-9 km genişliğinde, 50 km uzunluğunda yaklaşık D-B gidişli bir çöküntü olup Arabistan Plakasının kuzeybatı kenarında yer alır. Çalışma alanı, batıdan Kırkpınar fay zonu ile kuzeyden Güllüce Fay Zonu ile, kuzeybatıdan Bağlıca, Akdurak, Erenbağ ve Fıstıklıdağ Fay Setleri ile, doğudan Kemerli fay seti ile güneyden ise Karadağ Kıvrım Seti ile sınırlanmaktadır.

Altıntaş havza dolgusu açısız uyumsuzlukla sınırlanmış ve birbirinden ayrılan iki farklı havza dolgusundan oluşmaktadır. Bunlar (1) Orta Eosen-Pliyosen yaşlı belirgin şekilde deformasyona uğramış havza dolgusu ve (2) yaklaşık yatay karakterli Erken Kuvaterner yaşlı havza dolgusudur. Arazi gözlemlerine göre, Orta Eosen-Pliyosen yaşlı dolgu yaklaşık önce KKB-gidişli maksimum eksene sahip büzüşmeli karakterli tektonik sistem altında bir foreland sisteminde gelişmiş ve deformasyona uğramıştır. Bu döneme faz-1 denmiştir. Bu deformasyon sonucunda Araban Bloğu Arabistan Plakasının kuzeybatı ucundan ayrılmış ve ilişkili olarak Altıntaş dağarası havzası gelişmiştir. Daha sonrasında ise maksimum stress ekseni KKB'dan KB ile D-B arasında yayılım gösteren doğrultu atım faylanma karakteri

kazanmıřtır. Bu dneme faz-2 denmiřtir. Bu deformasyon fazı ile Altıntař havzasının řekli belirgin bir deęiřime uęramamıřtır. Daha sonrasında ise Anadolu bloklar topluluęunun batıya kamaya bařlaması ile birlikte stress rejimi hemen hemen eski konumuna geri dnmř fakat strike-slip karakteri kazanmıřtır. Bu dneme faz-3 veya neotektonik dnem denmektedir. Bu dnemde Altıntař havzası daha dar bir alan ile sınırlanmıřtır. Bu fazda havza doęrultu atımlarla sınırlı bir havza grnm almıřtır.

Anahtar kelimeler: havza, terlenme, paleotektonik, neotektonik, Altıntař

To My “the one and only” Wife, Aysun and “prankish little son”, U. Ali Emir

ACKNOWLEDGMENTS

Studying under the supervision of Prof. Dr. Ali KOÇYIĞİT was a great chance to learn more about Geology and Tectonics. I am grateful to him for supervising me and sharing his scientific experience with me during my studies. I also would like to express my great appreciation to committee members Prof. Dr. Erdin BOZKURT, Prof. Dr. Kadir DİRİK, Assoc. Prof. Arda ÖZACAR, and Prof. Dr. Uğur DOĞAN for the guidance they have provided and for being excellent teachers.

I would like to give my endless thanks to my “the one and only” wife, Aysun ÇİÇEK and my “prankish little son”, U. Ali Emir. In addition, I would like to thank my parents Recep ÇİÇEK and Habibe ÇİÇEK, my brother Erol ÇİÇEK and sister Ayşe ÇELEBİ. Without them, it was impossible to complete such an exhausting work.

I also give my special thank to Ayten KOÇ who prevented me when I decide to withdraw in the most stressful times of such an exhausting study. Without her support, it was not possible to complete such a nice study done in 100 day full field work of 1500 km on foot in many dangerous places inside the study area.

At last but does not mean the least, I would also want to thank to Hacı KARAKOCA, Nezahat KARAKOCA, Samet KARAKOCA, Murat KARAKOCA, Emine KARAKOCA, Seydi ÖZYIĞİT, Fatih ÖZTÜRK, Hacı DARICI, Musa KAYA, Mustafa İLİK, Bayram İLİK, for their great hospitality and help during my field work in Araban. Moreover, I would like to acknowledge my great pleasure to İlker ÇANDIR, M. Can CANOĞLU, Arif M. EKER, F. Mehmet VEKLİ, Serhad AKYOL, Orhan KILINÇ, Adnan GÜVEN, Ahmet ÖZGÜVEN, Halil YUSUFOĞLU, Murat ÖZKAPTAN, Erhan GÜLYÜZ, Mehmet Fatih ÖZİÇLİ, Kemalettin TOKATLI, Niyazi TOK, Assoc. Prof. Atilla ERGİN, Remiz AKSU, Assist. Prof. Dr. Abdülkadir GÜZEL, Bülent TOKAY, Mustafa

KAPLAN, Maaşallah KOÇMAN, Cevdet ARSLANOĞLU, Özgür KANDEMİR, Muhammed ÇOBAN and other friends I could not remember their names exactly right now for their adding hope, color, a new insight to my life, patience, making me laugh whenever I was in despair and encouragement during my studies.

TABLE OF CONTENTS

ABSTRACT	V
ÖZ.....	Vii
ACKNOWLEDGMENTS.....	X
TABLE OF CONTENTS	Xii
LIST OF FIGURES.....	XV
CHAPTERS.....	1
1 INTRODUCTION	1
1.1. Purpose and Scope	1
1.2. Method of Study.....	2
1.3. Location and Accessibility	3
1.4. Previous works	3
1.5. Regional Tectonic Setting	17
2- STRATIGRAPHY	25
2.1. Paleotectonic Unit	25
2.1.1. Allochthonous Units	25
2.1.2. Autochthonous Units.....	29
2.1.3. Pre-Modern Basin Fill.....	30
2.1.3.1. The Cingife Formation (Tc)	32
2.1.3.2. Yavuzeli Volcanics (Ty)	42
2.1.3.3. Şelmo Formation (Tş)	50
2.2.1. Neotectonic Units (or Modern Basin Fill)	53
2.2.1.1. Lahti Group (Q).....	53
3- STRUCTURAL GEOLOGY	61
3.1. Altıntaş Basin	62
3.2. Paleotectonic Structures	63

3.2.1. Beds	63
3.2.2. Unconformities	64
3.2.3. Mesoscopic Structures	65
3.2.3.1. Tension gashes	65
3.2.3.2. Stylolites.....	74
3.1.3.3. Conjugate Shear Fractures	76
3.2.4. Macroscopic Structures.....	83
3.2.4.1. Folds.....	83
3.2.4.1.1. E-W-Trending Fold System.....	83
3.2.4.1.2. NNE and NW-Trending Fold System.....	102
3.2.4.1.3. NE-Trending Fold System	104
3.2.4.2. Paleotectonic Faults	110
3.2.4.2.1. Çatboğazı Thrust Fault Zone	110
3.2.4.2.2. Karadağ Fault Zone.....	111
3.2.4.2.3. Erenbağ Fault Set.....	112
3.3. Neotectonic Faults.....	112
3.3.1. Yavuzeli Fault.....	112
3.3.2. Güllüce Fault Zone	113
3.3. 3. Kırkpınar Fault Zone	123
3.3.4. Dağdağancık Fault Zone.....	124
3.3.5. Yakuplu Fault Set	129
3.3.6. Çatlaklar Fault Set	132
3.3.7. Taşdeğirmen Fault Set.....	132
3.3.9. Akdurak Fault Set.....	133
3.3.8. Bağlıca Fault Set.....	138
3.3.10. Fıstıklıdağ Fault Set.....	141
3.3.11. Kemerli Fault Set.....	144
4- DEVELOPMENT HISTORY OF THE ALTINTAŞ BASIN.....	149
4.1. Middle Eocene-Early Pliocene Real Contractional Phase (phase-1)	150
4.2. Pliocene Strike-slip Phase (Phase-2).....	152

4.3. Quaternary Strike-slip Neotectonic Phase (Phase-3)	157
5- DISCUSSION.....	161
6- CONCLUSION	165
REFERENCES	167
APPENDICES:.....	191
Appendix-A:.....	191
Appendix-B:	193
CURRICULUM VITAE	195

LIST OF FIGURES

FIGURES

Figure 1. a) Map of Turkey with major geological structures. b) Location map of the study area and close vicinity.....	21
Figure 2. Simplified neotectonic map of Turkey which includes the study area (Koçyiğit and Özacar, 2003; Koçyiğit, 2009).....	22
Figure 3. Digital Elevation Model showing the study area (Altıntaş basin) and some major structures around it.....	23
Figure 4. Geologic cross-section across the western sector of the SE Anatolian orogenic belt, showing tectonic units and their relationships (adapted from Yiğitbaş and Yılmaz, 1996a).....	24
Figure 5. Generalized tectonostratigraphic columnar section of the study area and its neighborhood.	26
Figure 6. G.....	28
Figure 7. Ballık measured type section of the Cingife Formation (nearly 500 m north of the Ballık Village).....	34
Figure 8. General view of the Yavuzeli Volcanics, Fırat Formation and Cingife Formation and the site of Ballık measured section (view towards WNW; nearly 500 m north of the Ballık Village).....	35
Figure 9.....	36
Figure 10. Dağdağancık measured type section of the Cingife Formation (nearly 1 km SE of the Dağdağancık Village).	37
Figure 11. General view of the boundaries among the Fırat Formation, Cingife Formation and the Yavuzeli Volcanics and the site of Dağdağancık measured section (view towards WNW, nearly 1 km SE of the Dağdağancık Village).	38
Figure 12. Close-up view of the boundary between Fırat Formation and Cingife Formation and the site of measured section (view towards SE; nearly 1 km SE of the Dağdağancık Village)	39

Figure 13. The photograph illustrating contact relationship between the Fırat Formation and the Yavuzeli Volcanics near Karadağ passage located in the south central section of the study area (view towards SW, nearly NE of the Küçükkarakuyu Village).....	40
Figure 14. The field photograph illustrating contact relationship and its nature between the Stage 1 levels of the Yavuzeli Volcanics and the Cingife Formations (view towards NE, nearly 2 km NW of Yavuzeli (Gaziantep) District).....	41
Figure 15. Measured stratigraphic column of both the Stage 2 levels of Yavuzeli Volcanics and the Şelmo Formation (Ziyaret village 5 km north of Altıntaş).....	45
Figure 16. General view of the Ziyaret measured section site (view towards S, nearly 700 m N of the Ziyaret Village).....	46
Figure 17. Close-up view of mudstone and volcanic levels of Stage 2 levels of the Yavuzeli Volcanics (view towards S, nearly 700 m N of the Ziyaret Village).....	47
Figure 18. The field photograph illustrating the close-up view of the faulted contact (the Akkuyu Fault) between the Stage 2 levels of the Yavuzeli Volcanics and the Fırat Formation (view towards WNW, a few hundred meters NE of the Küçükkuyu Village). 48	
Figure 19. Close-up view of the boulder-block conglomerates comprising the Middle Miocene-Early Pliocene Şelmo Formation (approximately 900 m ESE of Ziyaret village located along the northern margin of the Altıntaş basin).	52
Figure 20. Close-up view of the nearly flat-lying Plio-Quaternary Lahti Formation (a few hundreds meters N of the Adıyaman-Gaziantep Highway).	55
Figure 21. General view of the Quaternary alluvial sediments in the northern margin of the Altıntaş basin between Sarıl and Güllüce Villages (veiw towards N, nearly 1 km W of the Güllüce Village).	56
Figure 22. General view of the fluvial sediments (view towards, NW, between Dipçeşni and Gümüşpınar Villages in SE margin of the Altıntaş basin).	57
Figure 23. Terraced flat lying Quaternary sediments.....	59
Figure 24. Types of Tension and hybrid (tension and shear) fractures. (“A”, “B”, “C” modified from www.files.ethz.ch/structuralgeology/JPB/files/English/4joints.pdf “ and “D” adapted from https://structuredatabase.wordpress.com/brittle-shear-sense-indicators/).....	66
Figure 25. General view of an unfilled tension fractures nearly 1.5 km SE of Dağdağancık Village (Araban District).....	67

Figure 26. Close-up view of a filled tension gash (~1750 m NE of Aşağı Mülk settlement).	68
Figure 27. Close-up view of some mesoscopic tension and hybrid (combination of tension and shear features) fractures (~1750 m S of Akkuyu Village).	69
Figure 28. Types of conjugate en echelon tension gashes (Adapted from www.files.ethz.ch/structuralgeology/JPB/files/English/4joints.pdf).	71
Figure 29. General view of some mesoscopic tension and hybrid (combination of tension and shear) fractures nearly inside the Dağdağancık Village (Araban-Gaziantep) located due South of the study area.	72
Figure 30. Close-up view of fiber crystals (Çatalboğazı area along northern margin of the Altınbaş basin).	73
Figure 31. A block diagram the relationship between local stress and mesoscopic structures such as tension gashes, stylolites and shear fractures (modified from Eyal and Reches, 1983).	78
Figure 32. Classification of stylolites according to pure geometry. (1) Simple or primitive wave-like type, (2) Sutured type, (3) Up-peak type (rectangular type), (4) Down-peak type (rectangular type), (5) Sharp-peak type (tapered and pointed), (6) Seismogram type (Redrawn from Park and Scot, 1968).	79
Figure 33. General view of two stylolite presenting abutting relationship nearly 1.5 km NE of Köklüce Village (Araban-Gaziantep).	80
Figure 34. General view of some bedding parallel (or diagenetic) stylolites nearly 1 km NE of Köklüce Village (Araban-Gaziantep).	81
Figure 35. General view of tectonic, diagenetic and the stylolites developed around of nearly rounded objects located nearly several hundreds meters west of Köklüce Village (Araban-Gaziantep) (This photo has been taken from a vertical Wall of a stone quarry).	82
Figure 36. Field photograph showing a conjugate shear fracture exposed in the Çatboğazı area along the northern margin of the Altıntaş basin.	84
Figure 37. Simplified structure map of the study area.	85
Figure 38. Unsimplied GAD-86-303 seismic section illustrating contact relationships among various rock units and the sub-surface structure of the Altıntaş basin (Adapted from Sonel and Sarbay, 1988).	88

Figure 39. GAD-86-303 seismic section illustrating contact relationships among various rock units and the sub-surface structure of the Altıntaş basin (Modified from Sonel and Sarbay, 1988).	89
Figure 40. Unsimplified GAD-86-102 seismic section illustrating contact relationships among various rock units and the sub-surface structure of the Altıntaş basin. (Adapted from Sonel and Sarbay, 1988).	90
Figure 41. GAD-86-102 seismic section illustrating contact relationships among various rock units and the sub-surface structure of the Altıntaş basin. (Modified from Sonel and Sarbay, 1988).	91
Figure 42. Field photograph illustrating an anticline comprising the Suvarlı Fold Set (view towards, SE, nearly 1.5 km SE of the Kesmetepe Village located nearly 5 km north of the Altıntaş basin).	93
Figure 43. Field photograph illustrating an anticline comprising the Karadağ Fold Set (view towards ESE, nearly 1.5 km W of Keşreobası Village located southwestern margin of the Altıntaş basin).	95
Figure 44. Unsimplified GAD-86-102 seismic section illustrating contact relationships among various rock units and the sub-surface structure of the Altıntaş basin. (Modified from Sonel and Sarbay, 1988).	96
Figure 45. GAD-87-206 seismic section illustrating contact relationships among various rock units and the sub-surface structure of the southwestern margin of the Altıntaş basin (Modified from Sonel and Sarbay, 1988).	97
Figure 46. Unsimplified GAD-87-206 seismic section illustrating contact relationships among various rock units and the sub-surface structure of the southwestern margin of the Altıntaş basin (Adapted from Sonel and Sarbay, 1988).	98
Figure 47. GAD-86-312 seismic section illustrating contact relationships among various rock units and the sub-surface structure of the southwestern margin of the Altıntaş basin (Modified from http://www.getfilings.com/sec-filings/120628/TRANSATLANTIC-PETROLEUM-LTD_8-K/d374244dex991.htm).	99
Figure 48. Unsimplified GAD-87-201 seismic section illustrating contact relationships among various rock units and the sub-surface structure of the southwestern margin of the Altıntaş basin (Modified from http://www.getfilings.com/sec-filings/120628/TRANSATLANTIC-PETROLEUM-LTD_8-K/d374244dex991.htm).	100

Figure 49. GAD-87-201 seismic section illustrating contact relationships among various rock units and the sub-surface structure of the southwestern margin of the Altıntaş basin (Modified http://www.getfilings.com/sec-filings/120628/TRANSATLANTIC-PETROLEUM-LTD_8-K/d374244dex991.htm).	101
Figure 50. Field photograph illustrating an anticline exposed around Saritepe Village (view to NE).	107
Figure 51. Field photograph illustrating an anticline and syncline included in the Saritepe-Tarlabası fold set exposed around the Dipçepni village (view towards WSW).	108
Figure 52. Field photograph illustrating a large scaled gentle anticline cut and reformed by the Kemerli fault set (1 km E of Çiftkeoz Village, view to NE).	109
Figure 53. Field photograph illustrating the trace of northward steeply dipping Yavuzeli Fault and its south-facing steep scarp.	114
Figure 54. close-up view of the set of nearly horizontal slip-lines printed over the older set of steeply-plunging slip-lines (nearly 1750 m east of the Ballık Village).	115
Figure 55. Field photograph illustrating various morphotectonic features produced by the master fault segment of the Güllüce Fault Zone (view towards north).	117
Figure 56. Field photograph illustrating the faulted contact between the Fırat Formation and the Cingife Formations exposed across near the Güllüce Village (view towards north).	118
Figure 57. Field photograph illustrating Close-up view of the Güllüce Fault Zone that cuts both Fırat and Cingife Formations and displaced them in vertical direction (view towards ENE).	119
Figure 58. Close-up view of the Güllüce master fault which cuts across the Quaternary basin fill and displaced it in both lateral and vertical directions (nearly 1 km WSW of the Köklüce Village).	120
Figure 59. A Google earth image showing the antecedent Ardıl stream which existed before the uplift of the Kızıldağ Mountain.	121
Figure 60. A Google earth image showing some paleovalleys which were active before the uplift of the Kızıldağ Mountain.	122
Figure 61. Field photograph illustrating both the Sadakalar and Ganıdağ Fault Sets comprising the Kırkpınar Fault Zone.	125

Figure 62. Close-up view of the fault plane of the fault segment included in the Ganıdağ Fault Set (nearly 300 m SW of the Ganıdağ Village, view towards NE).....	126
Figure 63. Field photograph illustrating the linear mountain, steep fault scarp and the sudden break in slope due to motion on the Turunçlu Fault Set. (nearly 1 km SW of the Hörüklü Village).	127
Figure 64. Close-up view of the Turunçlu Fault Set (nearly 300 m of Hörüklü Village, view to N).....	128
Figure 65. Field photograph illustrating the Dağdağancık section of the Dağdağancık Fault Zone (nearly 1 km SE of the Dağdağancık Village, view to SE).....	130
Figure 66. Close-up view of the Dağdağancık Fault Zone (nearly 300 m of Hörüklü Village, view to N, nearly 1 km SE of the Dağdağancık Village, view to SE).....	131
Figure 67. Field photograph illustrating the trace and the scarp of the Taşdeğirmen Fault Set (Taşdeğirmen Village, view to S).	134
Figure 68. Close-up view slip-plane (fault slickenside) with overprinting relationship. (nearly 1750 m east of the Ballık Village).	135
Figure 69. Close-up view of another slip-plane (fault slickenside) with overprinting relationship. (nearly 1750 m east of the Ballık Village).	136
Figure 70. A Google earth image overlain by the geology map along the Taşdeğirmen Fault Set. (see Appendix-A for the legend of the geology map).....	137
Figure 71. Field photograph illustrating the tectonic contact (Bağlıca master fault). Between the Karadut Complex and the firat Formation (Çatboğazı area, view towards SE).	139
Figure 72. Close-up view of the fault plane of the Bağlıca master fault in Çatboğazı area (view towards SE).	140
Figure 73. Field photograph illustrating the Akkoç Fault and Akdurak F.S. Note that the pre modern basin fill is cut and displaced and tectonically juxtaposed to each other by the Akdurak Fault Set. (nearly 2.5 km SW of Akdurak Fault Village, view towards east)...	142
Figure 74. Close-up view of the fault plane of the Akdurak master fault nearly in 2.5 km SW of Akdurak Fault Village (view towards east).	143
Figure 75. General view of the Kemerli Fault Set's scarp and plane (nearly 1 km east of the Çiftekoz Village, view towards S).....	145

Figure 76. Close-up view of the fault slickenside of the the Kemerli Fault Set (nearly 1 km east of the Çiftekoz Village, view towards SW).....	146
Figure 77. Sketch block diagram depicting development history of the pre-modern Altıntaş basin during Late Miocene (?)-Early Pliocene.....	154
Figure 78. Sketch block diagram depicting development history of the pre-modern Altıntaş basin during Pliocene.	155
Figure 79. Sketch block diagram depicting development history of the pre-modern Altıntaş basin during the Quaternary.	156

CHAPTER 1

INTRODUCTION

1.1. Purpose and Scope

Turkey is a geologically very complex area. For this reason, that it is regarded as a unique natural geological laboratory by both national and international geoscientists. Hundreds of papers were published to get deeper insight into the nature of this geologically complex terrain. One of the major geological debates is the onset age of the neotectonic regime in this country. In the present, there is a large number of data related to the neotectonics of all over Turkey, except for SE Anatolia. It is a part of northern margin of the Arabian plate. Although the geological data related to basic geological concepts of SE Anatolia is very much due to significant petroleum exploration studies, there is no detailed geological study about the neotectonics of this region. For this reason, it seems to very difficult to answer satisfactorily the mode, style, initiation age of the neotectonic period in SE Anatolia.

It is widely accepted that the neotectonics of Turkey is the result of interference between complex subduction processes in the Mediterranean sea, opening of the Red sea, Gulf of Aden and East African rift, collision between Arabian plate and Anatolian platelet (or collage), escape of Anatolia, collapse of Southwestern Anatolian lithosphere and related differential plate velocities. But initiation age of the neotectonic regime, deformational phases and nature of deformation are still under debate. It is aimed to bring some solutions to the above-mentioned neotectonic problems in the frame of this PhD study carried out in Altıntaş Basin by means of field geological mapping and observations including stratigraphic, structural and geophysical aspects of the Altıntaş basin located at the

junction of Adiyaman, Kahramanmaraş, Gaziantep and Şanlıurfa cities in the western part of SE Anatolia.

1.2. Method of Study

In order to achieve the above mentioned, a research has been carried out at three stages; (1) office work, (2) field work, and (3) laboratory and office work. During the office work, first of all, available literature was surveyed and reviewed. Thereafter, available borehole data was picked up from General Directorate of Mineral Research & Exploration of Turkey (MTA) and Turkish Petroleum (TPAO). These borehole data was also used to determine the thickness of the paleotectonic units and Quaternary sedimentary sequence (whole modern basin infill).

During the field work, lithological boundaries, geological structures such as strike/dip of bedding planes, fold axis, fault traces, local fault plane measurements, some other mesoscopic and macroscopic structures such as stylolites, tension gashes, conjugate shear fractures, fiber crystal growths were measured and mapped in 1/25000 scale. Those features were also documented by photography. In addition to this, detailed stratigraphy of the latest paleotectonic and neotectonic fill of the basin (Eocene and Quaternary rocks) were studied in order to distinguish the deformational patterns of paleotectonic and neotectonic periods. For these purposes, the latest paleotectonic and the neotectonic sedimentary sequences were studied and analyzed in terms of measured stratigraphic sections.

Subsequent to the field work, laboratory and office works have been started. At this stage, the structural data have been assessed by some computer programs such as Stereonet Version 8.9.2 developed by (Allmendinger et al 2013; Cardozo and Allmendinger, 2013) which allows many structural data processing, Global Mapper 15, 'Tector' developed by (Angelier, 1990) which provides stereographic plots of fault planes and orientations of stress tensors including operation directions of the stresses at the time of sedimentation and after

the sedimentation. Consequently, this thesis has been prepared by using some softwares of Tector, 5.42, Stereonet, 8.9.2, Freehand 11 Mx, Surfer 10, and Microsoft Office 2007 Professional.

1.3. Location and Accessibility

The study area is the Altıntaş basin. It is located approximately between 4131000-4151000 latitudes and 356000-412000 longitudes at the junction of Adıyaman, Kahramanmaraş, Gaziantep, Şanlıurfa cities in the western part of SE Anatolia (along the northern margin of the Arabian Plate). It falls into the Gaziantep N38 b2-b3, N39 a1, a2, a3, a4, b1, b2, b3, b4 topographic base maps and covers an area of more than 1200 km². The Altıntaş basin is an almost E-W-trending depression with the maximum relief of approximately 875 m between the lowest level and the highest peak of the margin-bounding highlands.

The accessibility to the study area is provided by Gaziantep-Adıyaman and Kahramanmaraş-Pazarcık highways running through the study area (Figure 1). There are also some other suborder roads such as asphaltic, stabilized and earthy roads cutting or joining to the main road. By means of these roads, all margins of the basin are accessible.

1.4. Previous works

SE Turkey is one of the most important natural laboratory for the understanding of continent-continent collision processes in the world. Therefore, it attracted attention of many researchers. This is because the area has a great potential to study all branches of geology, especially tectonics and petroleum exploration.

The SE Turkey or northern margin of the Arabian plate is an area of intercontinental collision related to active strike-slip deformation. The area is bounded by sinistral strike-slip East Anatolian and the Dead Sea Transform fault

systems to the west and northwest, Bitlis suture zone to the north, northeast and east (Figure 2) and neighbouring country borders to the south. It comprises a series of real compression and strike-slip deformation related diagnostic features such as almost E-W-trending folds, thrust to reverse faults, N-S-trending normal faults to tension fissures, NE-trending sinistral and NW-trending dextral strike-slip faults (Figure 2).

SE Anatolia is a region characterized by strike-slip neotectonic regime with dominantly reverse-component (Koçyiğit and Özacar, 2003) (Figure 2). The area includes some well-developed E-W, NE-SW, and NW-SE superimposed strike-slip basins. Their sizes range from a few square kilometers to up to hundreds of square kilometers. One of the most significant one is the Altıntaş basin, which is the study area. It is approximately 6-9 km wide, 50 km long and E-W-trending lens shaped depression located inside the SE Anatolian region (Figure 3). The basin includes two distinct basin fills, separated by intervening regional angular unconformity. The Altıntaş basin is bounded by the Kırkpınar fault zone to the west, by the Güllüce fault zone to the northwest, by the Bağlıca fault set to the northeast, by the Kemerli fault set to the east and Karadağ Fold Set to the south (Appendix-A).

Despite the fact that the neotectonic characteristics of the Altıntaş Basin have been poorly studied, some data about paleotectonic, stratigraphical, sedimentological and paleontological features have been collected to some extent by both native and foreigner researchers, particularly, since the second half of the 20th century. The contributions to the geology of the vicinity of the Altıntaş Basin are mainly in Turkish to English languages. They are summarized below.

First attempt related to the geology of the vicinity of Altıntaş Basin was done by (Stchephsy, 1943a). **(Stchephsy, 1943a)** studied the general geological properties of the Gaziantep and Kahramanmaraş areas and established basic stratigraphic relationships of some rock units, their depositional environmental characteristics and ages by using the field and paleontological studies. He also first claimed the existence of Oligocene units in this region.

(**Stchephsy, 1943b**) studied Oligocene rocks of the Gaziantep area and defined a number of new endemic and nonendemic fossils indicating the Oligocene time and marine units deposited in the Gaziantep area.

(**Tromp, 1943**) studied the Turonian to younger deposits in the Gaziantep and Şanlıurfa areas, and identified a number of fossil assemblages. Later on, he established the basic stratigraphic relationships among various lithofacies. He also defined the basaltic lavas and assigned Quaternary age to them. However, they were re-dated to be Miocene by (Çemen, 1987; Arger et al. 2000; Tatar et al, 2004).

(**Tolun, 1956**) studied general geological properties of the Pazarcık (Kahramanmaraş), Birek (Şanlıurfa) and Gaziantep areas including the Altıntaş basin. He prepared 1/100.000 scaled geological map including some basic geological structures such as synclines and anticlines in his study area.

(**Quennel, 1958**) studied the Dead Sea Rift located between Jordan and Palestine. According to the author, this basin is controlled by the Dead Sea Fault System. He suggested that the Miocene to recent evolutionary history of the basin is episodic. The first episode occurred in Miocene to Pliocene time interval and controlled strike-slip tectonic regime. Author also reported that the total displacement along margin boundary faults was 62-km during the first time interval. The first episode was followed by a quiescence period for a short time slice. Later, this quiescence period was followed by again a dominantly strike-slip tectonic regime during the second episode of Quaternary time. According to the author, a 42-km strike-slip displacement accumulated along the margin boundary faults during the second episode.

(**Arpat and Şaroğlu, 1972**) studied some large scale active sinistral strike-slip faults between Karlıova and Lake Hazar in east to southeast Anatolia. They first named this gigantic structure as a whole as East Anatolian Fault (EAF). The authors also subdivided the EAF into two segments between Karlıova and Lake Hazar as Karlıova-Bingöl and Pazı-Lake Hazar segments. They also claimed that the EAF is at least post-Miocene in age.

(**Ercan, 1979**) studied the microseismicity around of Malatya-Pötürge section of the East Anatolian Fault System (EAFS). The author reported that nearly 5 earthquakes took place smaller than magnitude 3 inside the study area during 105 days observation period. The author also claimed that the focal mechanism solutions originated from the main strand and subsidiary strands of this section of the EAFS dominantly imply that maximum compression stress axis is nearly N-S-trend and the character is sinistral strike-slip. Moreover, he also claimed that the main energy release occurred along the main strand of EAFS near the junction of Fırat River and Şiro stream.

(**Yalçın, 1979**) studied the Karaağaç-Türkoğlu (Kahramanmaraş) section of the East Anatolian Fault System (EAFS) by detailed field geological mapping and field observations. He identified some first order and second order faults with approximately N68E-trending sinistral strike-slip faults. He reported nearly 1750 m-2000 m Quaternary sinistral displacements, 20 m-50 m vertical Quaternary displacements and more than 1000 m vertical pre-Quaternary displacements. He claimed that there is no direct relationship between Dead Sea Fault System (DAFS) and EAFS and argued that the EAFS and DSFS are two different faults which cross-cut each other with an acute angle.

(**Biddle et al. 1987**) studied some significant folds and thrust faults of SE Anatolian region. They used seismic sections and field data to define the origin, geometry and type of the folds and thrust faults of Diyarbakır area. According to the authors, some major folds located in Diyarbakır area have two origins related to faulting. These are fault-bend folds and fault propagation folds.

(**Çemen, 1987**) studied the area bounded by the Fırat River to the east, Gaziantep city center to the south, Pazarcık (Kahramanmaraş)-İslahiye (Gaziantep) line to the west and Gölbaşı (Adıyaman) to the north. He studied the faults, folds and petroleum possibilities of the study area. He mapped many previously unrecognized structures and discussed the origin of folds exposing in his study area.

(**Gülen et al .1987**) studied the deformation related to continent-continent collision in Kahramanmaraş area and its environs. They reported that the internal stress in the Arabian plate, the indenter block, has been accommodated along some kink folds such as Palymyra and Kırıkhan-Gaziantep kink folds along the Dead Sea Fault System and the thrust fronts, namely Bitlis-Pötürge thrust front. The authors also proposed that the stress is first accommodated by folding and thrusting, later by lateral escape of nearly triangular shaped blocks along large scale strike-slip faults.

(**Perinçek et al .1987**) studied the strike-slip faults in east and southeast Anatolia. They identified a number of new strike-slip faults. The authors also claimed that the EAFS occurred during Middle Miocene and many of the segments belonging to them are clearly active in the present. In addition to this, they also reported that some of the sections of the Dead Sea Fault System join with the Amanos Fault Zone near Kırıkhan (Hatay) and Hassa (Hatay) while some others enter into the Syrian border towards north, later again appear in the Turkish terranes and finally joins with the EAFS in the east of Narlı (Kahramanmaraş) to the north. They also claimed that some depressions occurred as a result of post-Serravalian deformation and later filled with Plio-Quaternary sediments. One of these depressions is the Altıntaş basin.

(**Yoldemir, 1987**) studied the area bounded by Altıntaş basin (Araban) to the east, Gaziantep city to the south, Narlı (Kahramanmaraş) district to the west and Gölbaşı (Adıyaman) district to the north. He studied the general geology, structures and petroleum possibilities of the study area, and then established the stratigraphy of this area. In addition, he also mapped some major faults and folds including the western part of the Altıntaş basin.

(**Yoldemir, O. 1988**) studied the stratigraphy, structural geology and petroleum possibilities of western part of the Gaziantep City. He first established the stratigraphy and mapped some important folds. Later, he subdivided the tectonic structures into two categories, namely the paleotectonic and the young tectonic (Middle Miocene to recent) structures. He also subdivided the young

tectonics into two phases. The first phase took place during the middle Miocene to Pliocene time and second phase took place Pliocene to recent time interval according to the author. The major structures governing the young deformation existed as a result of the formation of the East Anatolian Fault System.

(**Çemen et al. 1990a**) studied the area between Altıntaş (Araban) basin to the west, Halfeti (Şanlıurfa) to the south and Atatürk Dam to the north and east. They conducted detailed field geological mapping focusing mostly on structural features. They reported that the Bozova Fault was a reverse fault. According to the authors, later on, the Bozova fault zone has reactivated as a dextral strike slip fault. They also reported that the Gemrik, Karababa and Tutluca anticlines with axis running parallel to the Bozova fault zone are older structures. They also claimed that the folds being oblique to Bozova fault zone are en echelon in pattern and probably formed as a result of the dextral motion on the Bozova fault zone.

(**Perinçek and Çemen, 1990**) studied northern section of the Dead Sea Fault System and the southwestern section of the East Anatolian Fault System in the area between Lake Hazar (Elazığ) and Hatay. They claimed that Dead Sea and East Anatolian Fault Systems meet to each other in the Amik plain (Hatay) in the southwest. They also claimed that the N-S-trending Amanos fault connects the East Anatolian Fault System with the Cyprus arc in the south. This relationship leads to development of Hatay Graben as a transtensional basin along the East Anatolian Fault System. They published a regional map including Altıntaş basin and its close vicinity where reverse faults, major folds and some major lineaments are observed.

(**Yoldemir and Perinçek, 1990**) studied in a very broad area including Pazarcık (Kahramanmaraş) and Kömürler (Gaziantep) to the west, Altıntaş plain (Gaziantep) to the east, Sakçagöze, Sarıkaya, Yaylacık villages (Gaziantep) to the south and Belveren, Suvarlı towns (Adıyaman) to the north. They studied the tectonostratigraphic units in their study area. Consequently, they reported the existence of some Paleocene basins and horst systems. They also claimed that these horst and basin systems have a relationship with the Dead Sea Fault System.

(**Taymaz et al. 1991**) studied the source parameters of the large earthquakes took place along the East Anatolian Fault System (EAFS). They used P and SH-wave forms of four largest earthquakes took place during the last 35 years. The authors reported that only one of the earthquakes yielded NE-SW-trending fault, which is probably originated from the EAFS and all the other earthquakes yielded steeply dipping NNW-trends, which is not related with the EAFS. In addition to these, the fault plane solutions correspond to either 10° to 63° degree slip vectors or the average slip on the EAFS, which must be between 25-35 mm/yr with 29 mm/yr average value.

(**Lyberis et al. 1992**) studied the western part of the East Anatolian Fault System by using the satellite images and fault slip plane analysis. They concluded that the neotectonic maximum principal stress axis is almost N-S in direction and the style of deformation in the area is strike-slip in nature. They also reported some major lineaments corresponding to faults in the western part of the Altıntaş basin.

(**Şaroğlu et al. 1992**) studied the East Anatolian Fault Zone. They reported that the EAFS is a 10-m to 4-km wide, 580-km long, NE-SW-trending active zone of deformation with maximum 20-25 km sinistral displacement. In addition to this, the authors proposed that the deformation zone consists of 6 main segments. Moreover, they claimed the age of the EAFS is Late Pliocene. Furthermore, the researchers finally concluded that the reoccurrence period of earthquakes with the magnitude 7 was calculated as 300 to 400 years for the EAFS.

(**Terlemez et al. 1992**) studied inside the area bounded by Gaziantep to the east, Syria border to the south, Sakçagöze town to the west and Pazarcık district to the north. They reevaluated the stratigraphy and the structural geology of the study area, and re-dated some rock units exposing in this region.

(**İmamoğlu, 1993**) studied the neotectonics of the Narlı (Pazarcık-Kahramanmaraş)-Gölbaşı (Adıyaman) section of the East Anatolian Fault System (EAFS) by field and laboratory based detailed structural geologic, stratigraphic, petrographic and paleontologic studies and observations. Firstly, he established the stratigraphy of the study area and then mapped some significant structures such as

faults and folds in detail. The author also assigned the depositional environments of the neotectonic and paleotectonic units in detail. Moreover, he identified prominent regional angular unconformity between Late Pliocene units and the older units. Based on those observations, he concluded that the neotectonic period commenced during the late Pliocene time in relation to the formation of presentday sinistral EAFS.

(**Yılmaz, 1993**) studied the evolution of the SE Anatolian region. He established the stratigraphy and main structural units such as folds and faults in his study area. He also mapped some folds with ENE-trending axis. He reported that these folds disappeared at the Late Cretaceous thrust front. According to the author, the thrust front subdivides the Altıntaş basin into two different geological settings.

(**Chorowicz et al. 1994**) studied the area between Kahramanmaraş to the north, Gaziantep and Syria border to the east, Amanos Mountains to the west and Hatay city to the south by using digital elevation models, satellite images, fault slip plane measurements and some field observations carried out in the Plio-Quaternary units. They concluded that the Maraş area is a triple junction between Arabia, Africa, and Anatolia. Moreover, they defined the Amanos fault to be a structure with a reverse component.

(**Yiğitbaş and Yılmaz, 1996a**) studied the significance of the strike-slip tectonic tectonics and its relation to the development of the SE Anatolian Orogenic (SEAO). The authors claimed that three main orogenic phases controlled the development of the SEAO since Late Cretaceous. These are Late Cretaceous, Eocene and Miocene thrusting phases. According to the researchers, the orogene is basically made up of three major tectonic zones. These are Nappe region, imbricate zone and Arabian Platform from north to south, respectively. In addition to this, they also reported that the strike-slip tectonics played a key role in the development of the orogene during Eocene in a very similar fashion of presentday tectonic development of the western United States of America due to ridge subduction processes.

(**Westaway and Arger, 1996**) examined the Gölbaşı (Adıyaman) basin based on the geological studies and quantitative analysis. They claimed that they identified and named a new fault (Kırkpınar fault) comprising the African and Arabian plate boundary. Authors also reported 17-km displacement accumulated on the Kırkpınar fault. According to these authors, this fault runs up to Gölbaşı (Adıyaman) basin and meets with the Gölbaşı-Türkoğlu section of the East Anatolian Fault System.

(**Yürür and Chorowicz, 1998**) studied in a broad area bounded by Kahramanmaraş to the north, Gaziantep city to the east, Syrian border to the south and east, and Gulf of İskenderun (Hatay) to the west. Based on the data related to satellite images, volcanic fissures, tension fractures and fault slip analysis, they reported that three significant tectonic events took place in the study area after Middle Miocene. The first event operated in the time interval between Middle Miocene and Early Quaternary. The second event became prominent during Early Quaternary to recent. However, no data was presented related to the third event.

(**Arger et al. 2000**) studied the Neogene and Quaternary volcanics exposed in the area of Malatya, Gaziantep and Osmaniye. They determined that these volcanics formed at two distinct episodes. The first episode volcanics are tholeiitic in composition while the second episode volcanics are mainly alkaline in nature. These researchers also reported that the first and second episode volcanics occurred in a time intervals of 19-15 Ma and 2.3 to 0.6 Ma, respectively. Arger and his colleagues proposed that both volcanics occurred due to far field effects of the glacial loading in the poles and sea level changes. According to them, the first global event intensified about at the beginning of Early Miocene and second global event intensified about 2.5 Ma.

(**Coşkun and Coşkun, 2000**) studied the area bounded by Pazarcık (Kahramanmaraş) to the west, Yavuzeli District of Gaziantep to the north, Şanlıurfa to the east and Elbeyli district of Kilis to the south. They used field geological observations, borehole and seismic reflection data to identify the subsurface geometry of main structures. Later on, they reported that their study

area was controlled by two geological events. These are the Late Cretaceous and Late Miocene thrusting events, respectively. During the first event, the late Cretaceous Koçali and Karadut mélanges were emplaced on the Arabian plate, whereas during the second event, the Dead Sea Fault System propagated upto the Gaziantep basin and led to the deformation, volcanic activity and Tertiary transgression in this region.

(Demirel et al. 2001) studied the petroleum systems of Adıyaman region in SE Anatolia. They used some borehole data to understand the maturity and quality of crude oil. Cosequently, they reported that significant oil traps developed during Late Cretaceous and Late Miocene time interval, but considerable amount of hydrocarbons were lost and the escaped petroleum might have been trapped in another region owing to the tectonic events.

(Adıyaman and Chorowicz, 2002) studied Cenozoic tectonics and volcanism in the northwestern corner of the Arabian plate. Their studies were based on radar imagery, digital elevation models and field studies. They suggested that the elongate volcanos, volcanic ridges, and linear cluster of Early Miocene volcanic vents are located along tension fractures trending nearfly N30-35E. This indicates that the least principal stress axis was operating in an approximately N55-60W during Early Miocene.

(Rojay et al. 2001) and (Toprak et al. 2002) studied the neotectonic characteristics of the Karasu Rift located mainly inside .Hatay and partly Gaziantep cities. The authors claimed that the Karasu rift is a Quaternary structure which is controlled by nearly east dipping Karasu fault zone to the west and nearly west dipping some segments of the Dead Sea Fault System (DSFS) to the east. They also obtained some radiometric ages from Quaternary volcanics. According to the authors, the slip rate along oblique-slip sinistral strike-slip fault with normal component Karasu fault zone is approximately 4.1 mm/year.

(Nalbant et al. 2002) studied the stress accumulation on the East Anatolian Fault System (EAFS), which is relatively quiescent with respect to North Anatolian Fault System during the last century. The researchers used 10 well

constrained historical devastating earthquakes since 1822. In addition to this, they did the analysis by using both seismic and tectonic loading related 3D stress perturbation tensors via numerical analysis method. Moreover, the authors obtained a good correlation between stress loading and earthquake location on corresponding segments and proposed that Kahramanmaraş-Malatya segment is the mostly likely area which is capable of producing devastating earthquakes greater than $M_w=7.3$

(Koçyiğit et al. 2003) examined the Sivrice Section or Sivrice Fault Zone (SFZ of the East Anatolian Fault System within the context of a training course. They discussed some basic neotectonic characteristics of the Sivrice fault zone. The trainers also reported that the SFZ is 3-6 km wide, 180 km long and 240°N - trending sinistral simple shear zone consisting of a series of parallel to sub parallel fault sets and isolated faults of varying lengths.

(Över et al. 2003) studied the tectonics of the area including Hatay, Osmaniye, Kahramanmaraş and Adana regions. They used the slip plane data on the faults observed in the field and the earthquake focal mechanism solutions to obtain present day style of deformation and stress regime. They concluded that the Miocene to Pliocene regime was strike-slip with reverse component while the Late Pliocene (possibly Quaternary) to recent regime is strike-slip with normal component.

(Kuzucuoğlu et al. 2004) studied the Holocene terraces between Karkamış (Gaziantep) and Birecik (Şanlıurfa) area. They reported that the pre-Holocene incised topography dates back to Late Pleistocene.

(Tatar et al. 2004) carried out both paleomagnetic and radiometric dating studies on volcanics exposed in the area of Osmaniye, Kahramanmaraş and Adana, and then reported that the volcanics of the Pazarcık-Yavuzeli area and Altıntaş plain are Early Miocene in age, not Late Miocene as has been proposed in a number of previous works.

(Westaway, 2004) studied along the Dead Sea Fault System and revised its quantitative kinematics by combining previously published data sets with the new

findings. Later on, he reported that the NNE-trending Afrin fault runs through Syria and then splays into a number of NE-trending sinistral strike-slip fault segments. One of them is Kırkpınar Fault. This segment is also the western margin boundary fault of the Altıntaş basin.

(**Çabalar, 2006**) carried out a ground response analysis in the Gaziantep area. He investigated the effects of the $M_w=7.5$ scenario earthquake to be sourced from Dead Sea Fault System and the different attenuation relationships for the Gaziantep city.

(**Yılmaz et al. 2006**) studied the kinematics of the East Anatolian Fault System between Çelikhhan (Adiyaman) and Türkoğlu (Kahramanmaraş) area. They used both the slip plane data measured on the faults and the focal mechanism solutions of some significant earthquakes took place inside their study area to determine the present day stress regime. They concluded that the stress regime is dominantly strike-slip with reverse component. They also reported that the initiation age of the East Anatolian Fault System, at least inside their study area, is Pliocene.

(**Alpaslan, 2007**) studied Early-Middle Miocene basaltic volcanics exposed in the area of Narlı (Kahramanmaraş), Pazarcık (Kahramanmaraş), Yavuzeli (Gaziantep) and Araban (Gaziantep) districts. He concluded that all of the analyzed volcanics are tholeiitic in nature and was originated from the asthenospheric mantle and purely garnet-peridotite or spinel end members. In other words, according to the author, the volcanics were not originated from a single mantle.

(**Çabalar, 2008**) assessed the earthquake hazard of Gaziantep city by using the earthquakes of magnitudes greater than 3 and took place in the period between 1973 to 2003, in the region. He also used different attenuation relationships for a scenario earthquake with $M_w=7.5$ to be sourced from the Dead Sea Fault System. In addition, he also the author evaluated the geological site conditions throughout the Gaziantep province and their effects on the strong ground motion.

(Demir et al. 2008) studied river terraces along Fırat River near Birecik (Şanlıurfa) and determined their exact positions by using Differential Global Positioning System (DGPS) studies. They estimated amounts of total uplift near Birecik area as 600 m since early Late Miocene (~ 9 Ma) represented by 270 m fluvial incision. The difference between them reflects downstream lengthening of the Fırat River channel as the coastline retreats. They also reported that the 55 m of incision had taken place since Early Middle Pleistocene when the uplift rates significantly increased.

(Herece, 2009) studied the age, offset, geometry and other characteristics of East Anatolian Fault System by using field geological mapping and observations. He synthesized that the fault system should have become a transform fault during late Pliocene. He also reported some total displacements accumulated along the Göynük section of the East Anatolian Fault System. These are the 14 ±1-km along the Göynük Section, 15-km along the Palu and Şiro section, 22.5 to 26-km along the Erkenek section and 19-26-km along the Gölbaşı section of the East Anatolian Fault System.

(Huesing et al., 2009) studied Muş, Elazığ and Maraş basins in SE Turkey in the frame of stratigraphic and paleoenvironmental interpretations. He concluded that there is no a direct relationship between the closure of the Southern branch of the Neo-Tethys and major climate changes, which took place 13.82 Ma.

(Kaymakçı et al. 2010) studied the kinematics of a broad area of the western part of the East and SE Anatolian region and determined five groups of deformation phases. They reported that the last phase of deformation occurred in Late Pliocene time and is still lasting in the nature of strike-slip faulting.

(Koçyiğit et al. 2010) presented a technical field trip guide book discussing the Gölbaşı (Adıyaman) section of the East Anatolian Fault System (EAFS). They reported that the EAFS is a nearly 700 km long, 75 km wide a system of Intracontinental transform fault with sinistral character. In addition to this, they reported that the EAFS is made up of 14 sections, 20 fault zones and a number of single faults. Furthermore, they also discussed that the EAFS occurred after the

Serravalian (nearly 12 Ma) to Late Pliocene (nearly 3 to 2.6 Ma) transitional contractional phase of tectonic regime or latest Paleotectonic regime. Hence, the initiation age of the Gölbaşı section of the EAFS and neotectonic period in their examination area is Latest Pliocene to Earliest Quaternary in age (i.e. 3 to 2.6 Ma).

(Bulut et al. 2012) studied the seismotectonics of the East Anatolian Fault System (EAFS) by using precisely relocated earthquake epicenters. The authors reported that the epicentral distribution indicates NE-SW-sinistral, E-W-trending thrust to reverse and nearly N-S-trending normal faulting related earthquake activity along the EAFS. The researchers also claimed that the observed spatiotemporal evolution of hypocenters indicates a systematic migration of micro- and moderate-sized earthquakes from the main fault into adjacent fault segments within several days documenting progressive interaction between the major branch of the EAFS and its secondary structures. Moreover, They claimed that pre- versus post-seismic phase for $M > 5$ events show that aftershock activities are initially spread to entire source region for several months but start to cluster at the central part of the main shock rupture thereafter.

(Koç and Kaymakçı, 2013) studied the kinematics of Sürgü Fault Zone located to the south of Malatya city. Based on the remotely sensed data, focal mechanism solutions of some significant earthquakes, previous GPS slip-plane vectors and fault slip data obtained from the field, they concluded that the Sürgü Fault Zone is a dextral strike-slip fault, not a sinistral strike-slip fault as reported earlier.

(Yönlü et al. 2013) mapped the Gölbaşı (Adıyaman) basin and then reported that the Göksun River has been crossed and displaced up to 16.5 km in sinistral direction by the East Anatolian Fault System.

(Kartal et al. 2014) studied the 19th September, 2012 Pazarcık-Kahramanmaraş earthquake and then determined that the style of the deformation inside the study area is strike-slip with normal component. Based on the focal mechanism solutions of main shock and aftershocks, they also suggested that the present day maximum principal stress axis is operating in NNW-direction.

Consequently, as is seen from the aforementioned previous works carried in the SE Anatolia, there is no detailed study focusing on the neotectonic evolutionary history of the basins, except for the Hazar and Gölbaşı basins. From this point of view, the Altıntaş basin will be the first study in detail.

1.5. Regional Tectonic Setting

SE Anatolian lies on the northern side of the Arabian Plate bounded on the north by Bitlis-Zagros Orogenic Belt. This belt is defined by a complex continent-continent and continent-oceanic collisional boundary. There was an oceanic realm continuing from the eastern Mediterranean to the Indian Ocean before collision (Şengör et al, 1979; Şengör, 1987a; 1987b). There are three major tectonic zones trending approximately E-W in SE Anatolia. These are: (1) the Arabian Platform, (2) a zone of imbrication, and (3) a nappe region (Yılmaz, 1993; Yiğitbaş and Yılmaz, 1996a) (Figure 4). The second and the third tectonic zone correspond to the main orogenic zones (SE Anatolian Orogen). These three zones are separated from one another by the intervening thrusts (Figure 4).

The Arabian Platform is composed mainly of autochthonous sedimentary sequences accumulated mostly in marine environments in the period of Paleozoic to Miocene (Sungurlu, 1974; Yılmaz et al. 1984; Perinçek et al 1991; Yılmaz, 1993; Yılmaz et al. 1993; Yiğitbaş and Yılmaz, 1996a). The belt lying immediately north of the Arabian Platform is an imbricated zone (Figure 4). It is a narrow zone of deformation (Up to nearly 10-km in width). It occurs between the Arabian Platform and the nappe zone, and consists of an imbricated sequence ranging from the Late Cretaceous to Middle Eocene in age. The ophiolitic nappes comprising the third tectonic zone were emplaced on to the platform during the Late Cretaceous and Eocene periods (Yiğitbaş et al. 1992; Yılmaz. 1993; Yiğitbaş and Yılmaz, 1996a, b).

The nappe region is located north of the imbricated zone, and structurally it contains the upper most tectonic units of the SE Anatolian Orogenic Belt. It

consists of metamorphic and ophiolite associations (Figure 4). The nappe region is composed of two nappe packages. These are the lower and upper nappe packages. The lower nappe package consists of metamorphosed ophiolitic rock assemblages; the upper nappe comprises the metamorphic massifs of SE Anatolia (i.e. the Bitlis, Pötürge, Malatya and Keban Massifs). These massifs may be regarded as parts of a once-united metamorphic-tectonic unit, which later were fragmented during Late Cretaceous to Miocene thrusting (Yılmaz, 1993; Yiğitbaş and Yılmaz, 1996a).

The convergence between the Arabian Plate and the northerly located Eurasian Plate produced southerly transported nappe emplacement in three major periods or phases: (1) Late Cretaceous (K_2), Late Early Eocene (Eoc), (3) Early Middle Miocene (Mio_{1-2}) (Figure 4). During the first two phases, only the ophiolitic nappes were obducted onto the Arabian Platform (Figure 3). During the third phase, a nappe package composed of ophiolitic nappes, overlain tectonically by the metamorphic massifs, moved onto the Arabian Platform (Figure 4). The nappe stacks were accreted onto the Arabian Continental Margin during the final stage of Miocene nappe emplacement (Yiğitbaş and Yılmaz, 1996a). Finally, migration of nappe packages in N-S-direction led to the strike-perpendicular thrust shortening. This real thrust shortening lasted at the end of Pliocene and then replaced by a strike-slip neotectonic regime and related structures in the Early Quaternary (Koçyiğit, 2013). The main regional tectonic event, which triggered and governed the neotectonic regime in Turkey, is the episodic break up of the Afro-Arabian unique continent and its splitting apart into two independent plates, the African and Arabian Plates (Hempton, 1987). The terminal suturing between Arabian and Eurasian Plates along the Bitlis-Zagros suture zone locked both the northward motion of the Arabian Plate and the strike-slip motion along the Dead Sea Transform Fault System during the late Serravalian (approximately 12 Ma). Accordingly, the Late Eocene-Early Miocene phase-1 extension and the sea floor spreading along the Red Sea were interrupted for a long time period from Late Serravalian to Late Pliocene (approximately for 9.4 My) (Hempton, 1987).

However, the N-S-directed intra-continental convergence continued at a relatively low rate of motion and led to the occurrence of a series of inversion and formation of some structures. These are the thickening and uplift (up to 2-km above the sea level) of the frontal part of Eurasian Plate, formation of a series of E-W-trending intramontane or ramp basins bounded by thrust to reverse faults and folds. Lastly, the frontal part of Eurasian Plate split apart into several large continental wedges, one of which was the proto-Anatolian Platelet, during this transitional period between Late Serravalian-Late Pliocene. Starting from Early Quaternary (2.588 Ma) onwards, the strike-slip neotectonic regime became prominent, two major shear zones (East Anatolian Transform Fault System-EATFS and North Anatolian Transform Fault System-NATFS) were formed and Anatolian Block began to move in WSW-direction along those two strike-slip fault systems. This last major event retriggered occurrence of some other neotectonic events such as emergence of phase-II extension along the Red Sea, strike-slip motion on the Dead Sea Transform Fault System, northward motion of the Arabian Plate and the onset of the strike-slip neotectonic regime in East and SE Anatolia.

One of major structures of Early Quaternary strike-slip neotectonic regime is the EATFS, it is an 75-km wide, nearly 700-km long and NE-trending Intracontinental sinistral transform fault bounding the SSE edge of the Anatolian Platelet (Koçyiğit et al. 2010). It is located Karlıova to the NE and the Karataş-Samandağ Counties to the SW. Whole of Quaternary units and structures of paleotectonic periods are truncated and displaced (up to 27 km) in sinistral direction by the EAFS (Arpat and Şaroğlu, 1972; Seymen and Aydın, 1972; Herece and Akay, 1992). The EATFS is characterized by a number of active fault segments and strike-slip basins originated from strike-slip complexities linking the fault segments to each other. One of the E-W-trending older ramp basins truncated and deformed by the EAFS is the Altıntaş Basin (Figure 4). It is the study area and located in the SW section of the EATFS. Originally, the earlier configuration of the Altıntaş basin is inherited from the Early Pliocene thrust to reverse faulting events due to formation of the Arabian Block (Figure 3). Starting from the Early

Quaternary onwards, older Altıntaş basin and related thrust to reverse faulting tectonics were replaced by the strike-slip neotectonic regime and related structures.

Both these development history and phases of deformation experienced by the Altıntaş basin will be analyzed in the frame of a PhD thesis.

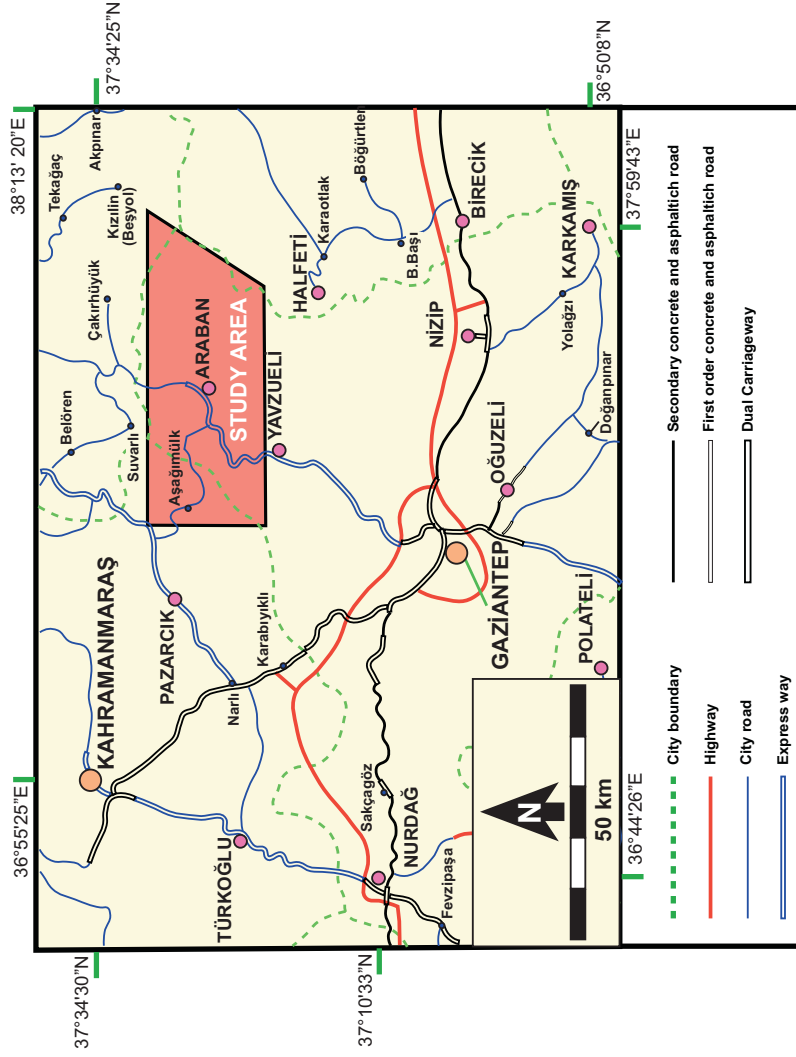


Figure 1. a) Map of Turkey with major geological structures. b) Location map of the study area and close vicinity.

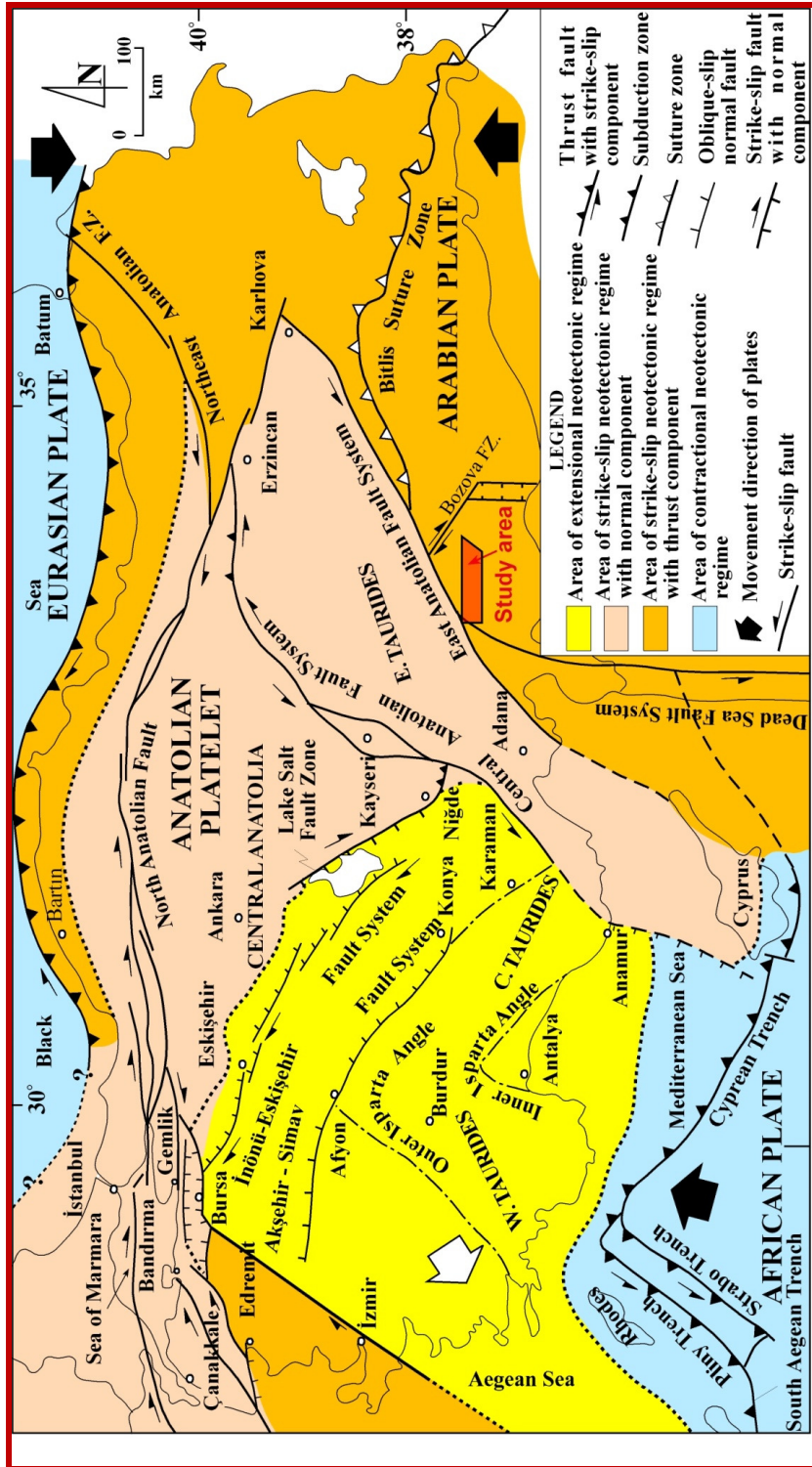


Figure 2. Simplified neotectonic map of Turkey which includes the study area (Koçyiğit and Özacar, 2003; Koçyiğit, 2009).

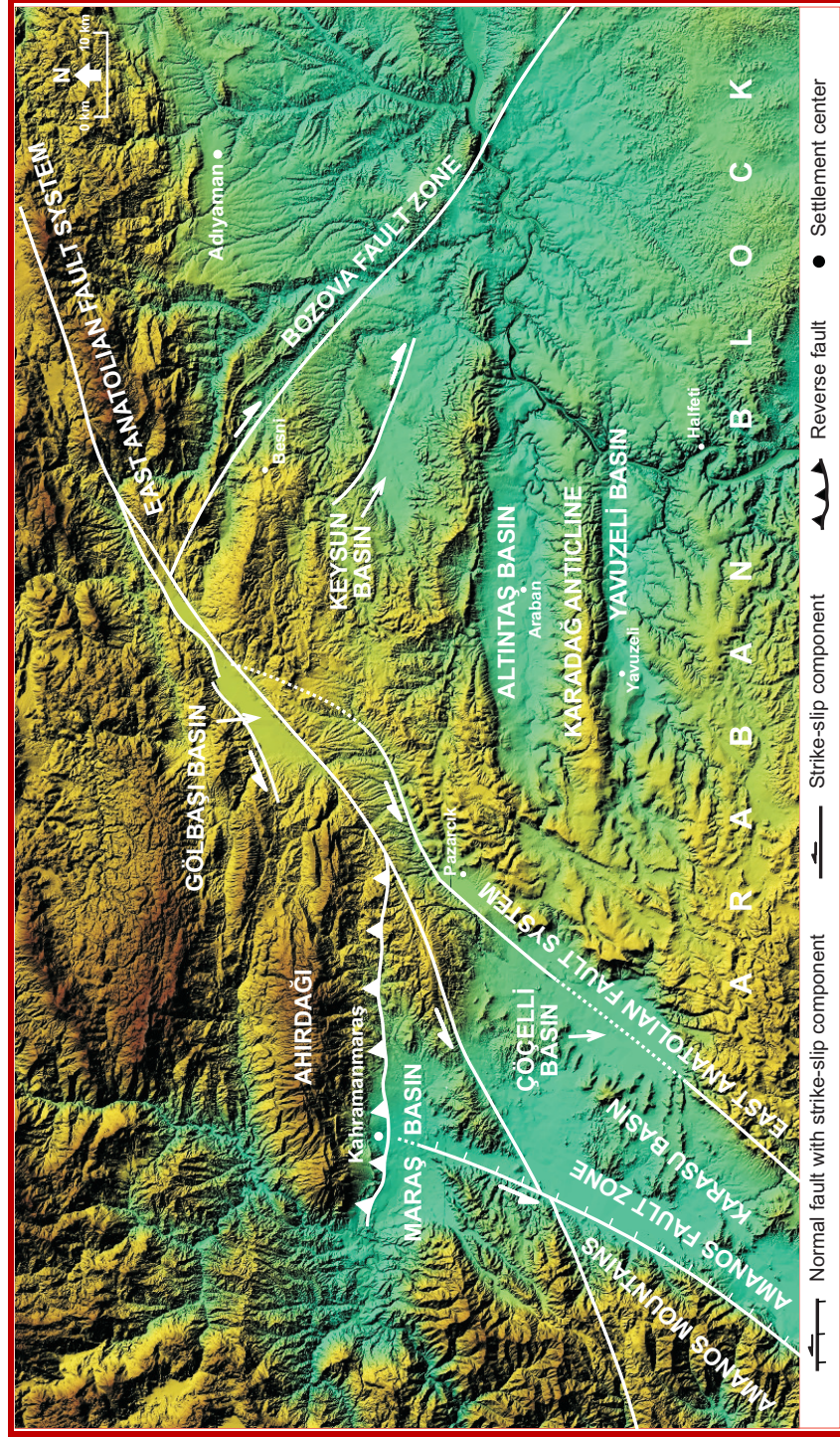


Figure 3. Digital Elevation Model showing the study area (Altıntaş basin) and some major structures around it.

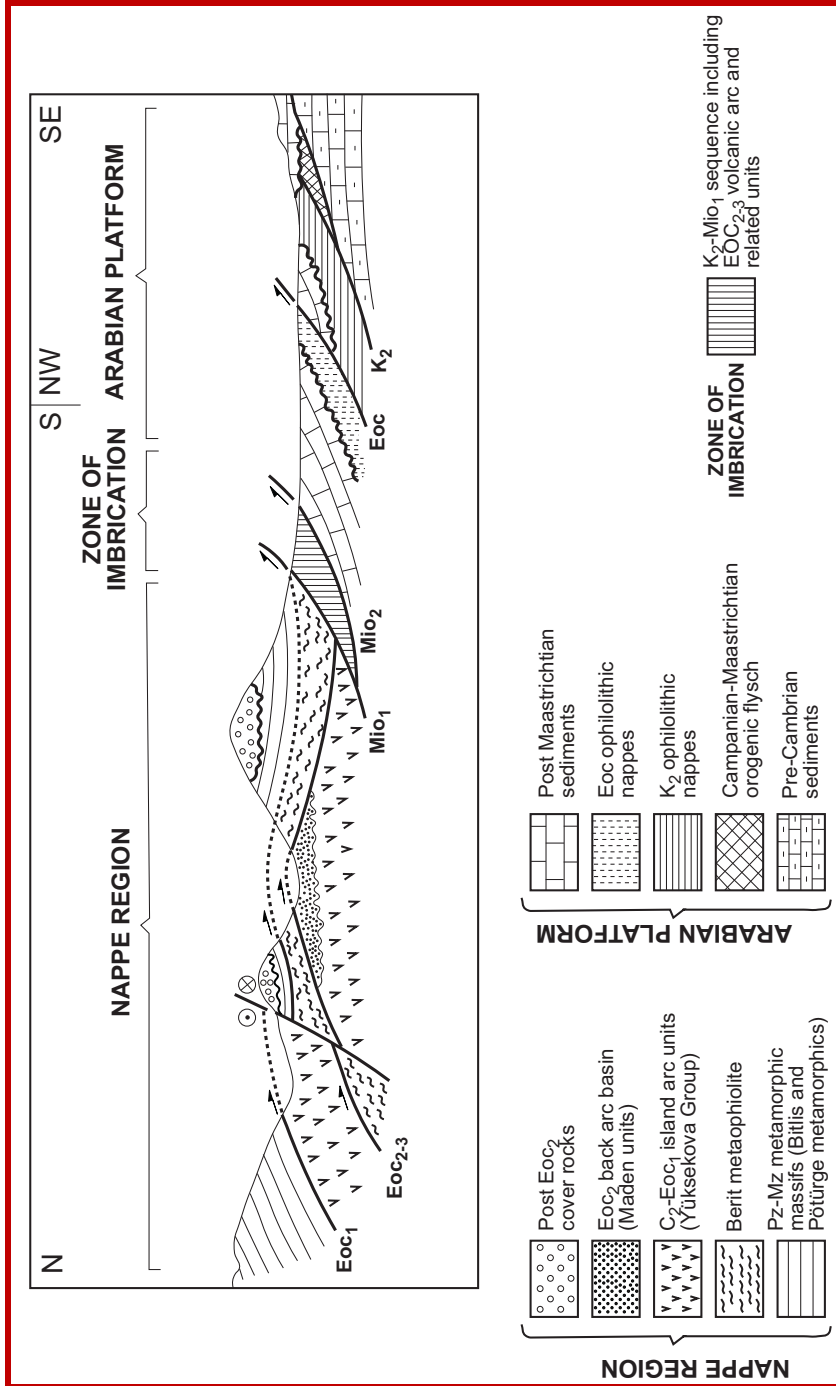


Figure 4. Geologic cross-section across the western sector of the SE Anatolian orogenic belt, showing tectonic units and their relationships (adapted from Yigitbaş and Yılmaz, 1996a)

CHAPTER 2

STRATIGRAPHY

Based on the ages and deformation patterns, the rocks exposing in and adjacent to the study area are divided into two main categories: (1) Late Cretaceous-Pliocene Paleotectonic units and (2) Quaternary neotectonic units (modern basin fill) (Figure 1).

2.1. Paleotectonic Unit

The Paleotectonic rocks exposing in and adjacent to the study area are classified into three basic sub-categories (1) Allochthonous units, (2) Older units and (3) Pre-modern basin fill.

2.1.1. Allochthonous Units

These are the units formed and emplaced during the Latest Cretaceous. During the field work, it has been observed that some of the Allochthonous units are exposing in the northern portion of the study area (Appendix-A). The units occur as two different rock formations (Appendix-A and Figure 5). They are: (a) the Karadut complex and (b) the Koçali ophiolitic mélange. They are briefly summarized as follows.

Lowermost Allochthonous unit exposing in the vicinity of the study area is the Karadut complex (Kka). This unit first was named as “*Karadut unit*” included in the “*Kevan gravity nappes*” in “Kevan-1” borehole drilled in Çermik (Diyarbakır) by (Turkish Gulf Oil, 1961). The type section is located in Karadut Village of Narince County to the northeast of the Adıyaman (Bolat, 2012). It

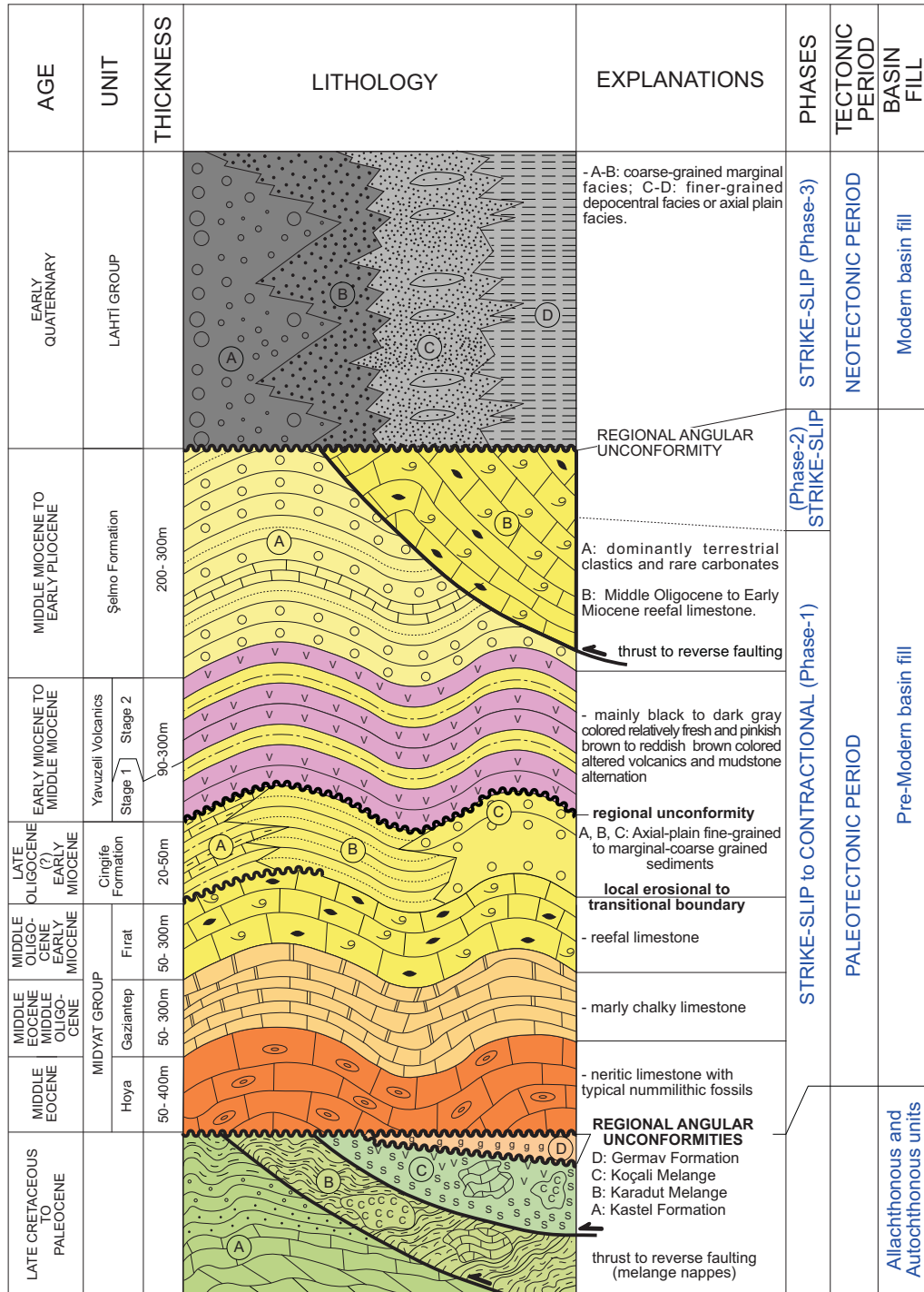


Figure 5. Generalized tectonostratigraphic columnar section of the study area and its neighborhood.

consists of silicified limestone, radiolarite, cherty and silicified shale, cherty limestone, clayey limestone, layered chert, sandstone and volcanites (Terlemez et al. 1992). The unit exposes only in the north of Çatboğazı in the study area (Appendix-A and Figure 6). Bottom boundary is not observed in the study area while the upper boundary is seen clearly in the north of the Çatboğazı area. According to the observation, the top boundary is overlain by the Koçali ophiolitic mélange with a tectonic contact in the study area. The unit was deposited as a passive margin apron representing the outer-shelf and continental slope environment (Yılmaz, 1993). The Karadut complex has two ages. One is formation age and the other one is emplacement age. There are different views about the formation age of the complex. (Yoldemir, 1987) proposed Santonian formation age to the complex while (Yılmaz, 1993) proposed Late Triassic and Campanian age for its formation. In contrast to formation age, the emplacement age of the Karadut complex is widely accepted as Latest Cretaceous (Yoldemir 1987; Terlemez et al. 1992; Yılmaz 1993).

The Koçali ophiolitic mélange (Kko) is the second observed unit of the Allochthonous complex. This unit was first observed by Dubertret (1955) in Bryant (1960), but first named by Kellog (1960) as the “*Pirik Formation*” in Diyarbakır area. Later, Sungurlu (1973) used Koçali assemblage to this rock assemblage. This name has been widely accepted by many researchers working in SE Anatolia. The type section of the unit is located in the Pamukdere area 1.5 km SW of the Koçali County in the north of the Adıyaman city. The Koçali mélange is made up of ultrabasic rocks, volcanites, serpentinite, radiolarite, cherty limestone, and limestones of various ages (Terlemez et al. 1992). The unit exposes only in the north of Çatboğazı in the study area (Appendix-A, Figures 5). According to the field observation, the unit overlies the Karadut mélange with a tectonic contact at the bottom while it is overlain by the Late Cretaceous to Early Paleocene Germav formation with an angular unconformity. The apparent thickness has been determined as 37 m in Bağlıca-1 oil well drilled at a locality nearly 2.5 km NE of

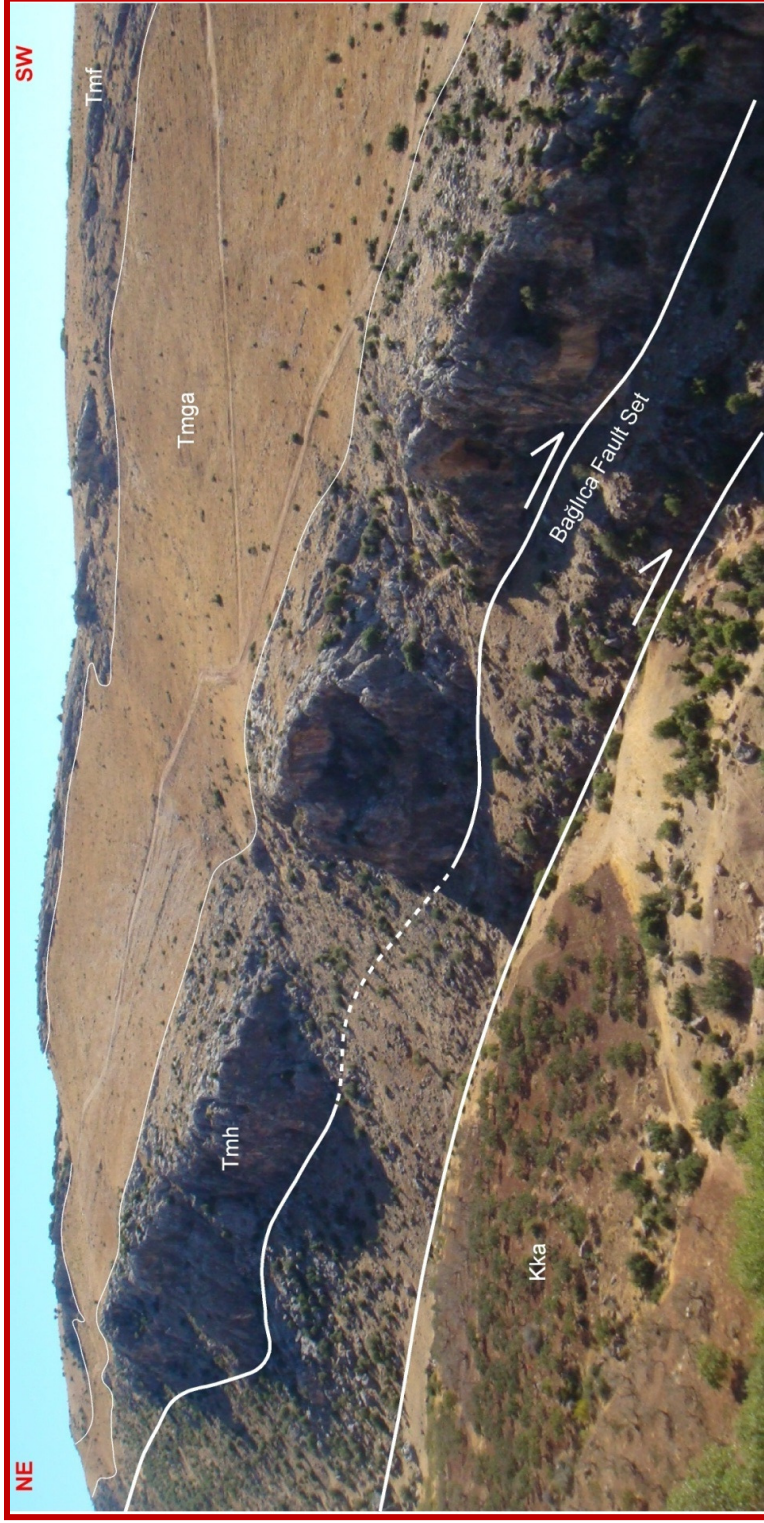


Figure 6. General view of the Karadut Complex (or mélange) and the Midyat Group (Hoya, Gaziantep and Fırat Formations) along the Bağlıca Fault Zone nearly 1.5 km NE of Çakallı Village (Araban) in the northern section of the study area (View towards SE, 1.5 km NE)

Bağlıca Village in the north of the study area (Appendix-A). The Koçali complex has two ages. One is formation age and the other one is emplacement age. Tuna (1973) assigned Late Jurassic to Early Cretaceous formation ages to the Koçali mélangé. However, a Late Cretaceous emplacement age reported for the Koçali mélangé (Yoldemir, 1987; Terlemez et al., 1992; Yılmaz, 1993; Yiğitbaş and Yılmaz, 1996a).

2.1.2. Autochthonous Units

One formation is observable belonging to this on the surface. However, some others also recorded in the oil wells drilled in the vicinity of the study area in subsurface. However, only the Late Cretaceous to Early Paleocene Germav Formation exposing in the surface have been discussed here. It is described briefly below.

Germav Formation (Ktşg) is the only stratigraphic unit belonging to the oldest autochthonous units rock package which exposes in the near vicinity of the study area (Figure 5). However, this formation has not been mapped in detail. The Germav Formation was first identified and named as the Kermav Formation by Maxson, (1936). The type section of the Germav Formation is located nearby Germav Village 40-km east of the Gercüş District (Batman) (Yılmaz and Duran, 1997). The Germav Formation is composed mostly of yellowish to bluish gray colored marls with pelagic limestone intercalations. The unit exposes around the Çatboğazi area in the northern section of the study area (Appendix-A). The Germav Formation overlies the Koçali ophiolitic mélangé with an angular unconformity at the bottom while it is overlain by the Eocene Hoya Formation with an angular unconformity at the top (Figure 5). The lithofacies of the Germav Formation indicate that it has been deposited in a deep continental slope, submarine fans and deep sea fans (Güven et al, 1991). The Age of the unit was reported to be Maastrichtian to Early Paleocene by some researchers (Yılmaz, 1993 and Terlemez et al., 1992).

2.1.3. Pre-Modern Basin Fill

Indeed these are six different rock stratigraphic units. The first three have been discussed under the Midyat Group while the other three units which are made up of a volcanosedimentary sequence named as Cingife Formation, Yavuzeli Volcanics and Şelmo Formation, respectively. However, Cingife Formation and Şelmo Formation were evaluated under the Şelmo Formation in most of previous works (Ulu et al., 1991; Terlemez et al., 1992; İmamoğlu, 1993).

The Hoya Formation (Teh) is the lowermost unit of the Midyat Group exposing in the study area (Appendix-A and Figure 5). The unit was first defined informally and named by Taşman (1930) as the “*Nummilites limestone*”. Later, various different names have been used for the same formation. The term “Hoya Formation” was first used and included in the Midyat Group by Perinçek (1978). The type section of the Hoya Formation is in the vicinity of Hoya Village located 2 km SW of the Çüngüş District (Diyarbakır). The Hoya Formation consists mostly of cream to light gray colored thick-bedded or massive limestones and dolomites. The unit is well-exposed along the northern margin of the Altıntaş basin (Appendix-A). This formation overlies older Karadut mélangé, the Koçali mélangé and the Germav Formation with an angular unconformity at the bottom and is overlain conformably by the Middle Eocene to Middle Oligocene Gaziantep Formation at the top (Appendix-A, Figures 5 and 6). The apparent thickness of the unit ranges from 100 m to 400 m based on the geological cross-section and data obtained from some oil wells drilled in the study area. Terlemez et al., (1992) proposed a Middle Eocene age for the Hoya Formation based on its some fossil content.

The Gaziantep Formation (Tmga) is the second rock stratigraphic unit of the Midyat Group exposing in the study area (Appendix-A and Figures 5 and 6). The unit was first identified by (Schmidt, 1935) as the “*Lowermost limestone, middlemost limestone and higher limestone*”, but first named by Wilson and

Krumenacher, (1959) in Gaziantep area. The type section of the Gaziantep Formation is a locality near Kilis Yılmaz and Duran, (1997). The Gaziantep Formation is made up of gray, cream to light red clayey to chalky limestone and marl at some localities. The unit exposes along both northern and southern margins of the Altıntaş basin (Appendix-A and Figure 6). The Gaziantep Formation is underlain and overlain conformably by the Hoya and Fırat Formations, respectively (Appendix-A and Figure 6). The calculated thickness of the Gaziantep Formation ranges between 100-200 m. However, its apparent thickness was determined to be 300 m in some oil wells drilled in the study area. Based on its rich fossil content, the age of the unit was reported as Middle Eocene to Middle Oligocene by Ulu et al., (1991).

The Fırat Formation (Tmf) is the third and topmost stratigraphic unit of the Midyat Group exposing in the study area (Appendix-A and Figures 5 and 7). The Fırat Formation was first identified and named by Maxon and Tromp, (1940) as a member of Midyat Formation. However, Later on, Krausert, (1958) and Wilson and Krummenacher, (1959) used the informal names the “Pirin Formation” and the “Karadağ Formation”, respectively. In addition, Duran et al., (1989) reported the name of Fırat Formation in the Silvan Group in the Diyarbakır area for their formation. Lastly, the Fırat Formation was included in the Midyat Group by Ulu et al., (1991) and Terlemez et al., (1992). The type section of the Fırat Formation is observable along the Fırat River near the Birecik (Şanlıurfa) area Ulu et al., (1991). The formation is dirty yellow, light gray and cream colored and thick-bedded to massive. The Fırat Formation is the most widespread unit inside the study area (Appendix-A). It is distributed along both northern and southern margins of the study area (Appendix-A). The unit conformably overlies the Gaziantep Formation but is overlain with a transitional contact and local unconformity by the Cingife Formation (Appendix-A, Figures 5, 6, 7, 8, 10, 11, 12). However, the Yavuzeli Volcanics display an erosional contact relationship with the Fırat Formation in some places (Appendix-A, Figures 5 and 13). Ulu et al., (1991) and Terlemez et al., (1992) have reported that the Fırat Formation has

been deposited in the shallowest part of a marine carbonate platform. The calculated thickness of the Fırat Formation ranges between 100-200 m based on geological-cross-section (Appendix-B). In addition to this, the apparent thickness of the formation was determined to be 300 m based on data obtained from oil wells drilled in the study area and its close vicinity. Middle Oligocene-Early Miocene age was assigned to the Fırat Formation based on its rich fossil content (Ulu et al., 1991).

Based on new radiometric age data coming from the Yavuzeli Volcanics and the contact relationships determined during our detailed field geological mapping, the thick volcano-sedimentary sequence are subdivided into three formations: These are the Late Oligocene (?) to Early Miocene Cingife Formation, the Early Miocene to Middle Miocene Yavuzeli Volcanics, and the Middle Miocene to Early Pliocene Şelmo Formation (Appendix-A and Figure 5). On the other hand, all of the Miocene volcanics have been discussed under the Yavuzeli Volcanics. However, they were subdivided into three stages. Only, two stages expose inside the study area. The sedimentary series are subdivided as Cingife and Şelmo Formations. They are summarized below a bit in detail, respectively. They are described separately below.

2.1.3.1. The Cingife Formation (Tc)

This formation was first named as the Cingife Formation (Ayazoğlu, 1958; Tertemiz, 1958). Bolgi (1964) renamed the unit as the Adıyaman formation. Moreover, Ulu et al., (1991) and Terlemez et al. (1992) reported the widespread distribution of the pre-modern basin fill rocks in the south of Altıntaş and Yavuzeli basins and their close vicinity.

The Cingife Formation exposes along the southwest and northwest margins of the Altıntaş basin (Appendix-A, Figures 8 and 9).

It is underlain by the Oligocene to Early Miocene Fırat Formation with a partly transitional and partly erosional contacts in some places at the bottom

(Figures 5, 7, 8, 10, 11, 12). However, it is overlain with an unconformity by the Early Miocene stage 1 Yavuzeli volcanics at the top (Figures 5, 7, 8, 10, 11, 14). The type section of the formation has been observed first and determined during this study in a few hundred meters NE of the Ballık Village of Yavuzeli (Gaziantep) District (Appendix-A, Figure 7). At this locality, the Cingife Formation starts with dominantly cream, beige and lesser amount of light brown colored and thick bedded polygenetic conglomerates on the top of the Firat Formation. Clasts forming the conglomerates are made up of red colored radiolarites, green colored ultramafic rocks, Nummulites-bearing limestones and black to dark gray colored vesicular basalts. They have been derived directly from the underlying older units such as the Midyat Group rocks and lesser amount of Koçali and Karadut ophiolitic mélanges. The pebbles or clasts are typically oblate in shape and several centimeters in diameter. They rarely exceed 25 cm in diameter. In addition to these, lower levels of the formation also include light red to cream colored massive limestone intercalations thinner than 1 meter as a whole (Figure 7). The lower clastic level of the formation is succeeded by mostly opaque light green colored dominantly well to partly sorted and well rounded pebbly clean sandstone, light gray to gray and light reddish brown colored and weakly cemented clean sandstone and fine grained conglomerate alternations. This package alternates with the tile red colored mudstones towards middle levels of the formations (Figures 7 and 9). This middle section is succeeded by mainly beige to gray colored and fine-grained clastics such as claystone, marl and less amount of tile red colored mudstones. At the top most, the Cingife Formation consists of again gray, cream, light tile red, beige colored polygenetic conglomerate and sandstone alternation. On the contrary to the Ballık section, the Dağdağancı reference section of the Cingife Formation is much more monogenic and typically made up of tile red colored mudstone and gray, beige colored argillaceous limestone alternations with gradational contact relationships (Figures 10, 11, 12).

AGE	UNIT	THICKNESS	LITHOLOGY	EXPLANATIONS
Early Miocene	Stage 1 Yavuzeli Volc.	~ 160 m		20, 88 Ma +/- 0.36 Ma - dark gray to reddish brown colored mainly layered basaltic volcanics with gas voids filled with CaCO ₃ and some clay minerals.
Late Oligocene (?) to Early Miocene	Firat Fm	44 m		- grey-cream, light tile red-beige colored polygenetic conglomerates and sandstone alternation.
				- mainly beige to grey colored claystone-marl and lesser amount of light tile red colored mudstone alternation.
				- mainly light green colored conglomerate, gray to light green colored pebbly sandstone packages and light tile red colored mudstone alternation.
				- mainly opaque light green colored and grey-beige to light reddish brown colored coarse grained sandstone and conglomerate alternation. Lesser amount of light tile red colored mudstone is also present.
				- light red to cream colored massive limestone
				- mainly light cream colored well cemented boulder block conglomerate with carbonate matrix.
				- cream-beige-light brown colored well cemented conglomerate-sandstone-marl-claystone alternation.
				- mainly light brown-red cream-beige-colored well cemented conglomerate with oblate shaped clasts.
				- mainly light brown-cream-beige colored well cemented conglomerate and lesser amount of sandstone-siltstone-marl-claystone. The clasts are oblate shaped.
			Middle Oligocene Early Miocene	Firat Fm

Figure 7. Ballık measured type section of the Cingife Formation (nearly 500 m north of the Ballık Village).



Figure 8. General view of the Yavuzeli Volcanics, Firat Formation and Cingife Formation and the site of Ballık measured section (view towards WNW; nearly 500 m north of the Ballık Village).

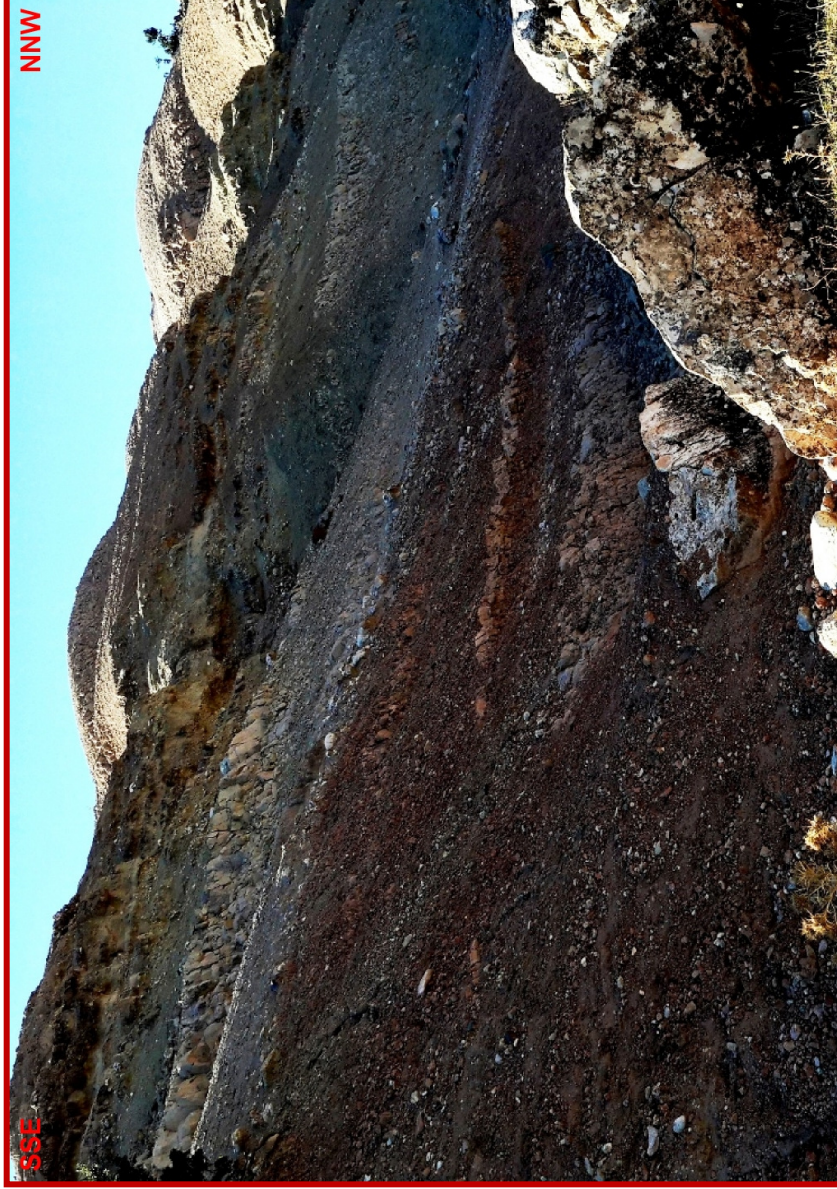


Figure 9. Close-up view of a part of middle levels of the Ballik measured section of Cingife Formation (view towards WSW, nearly 500 m north of the Ballik Village).

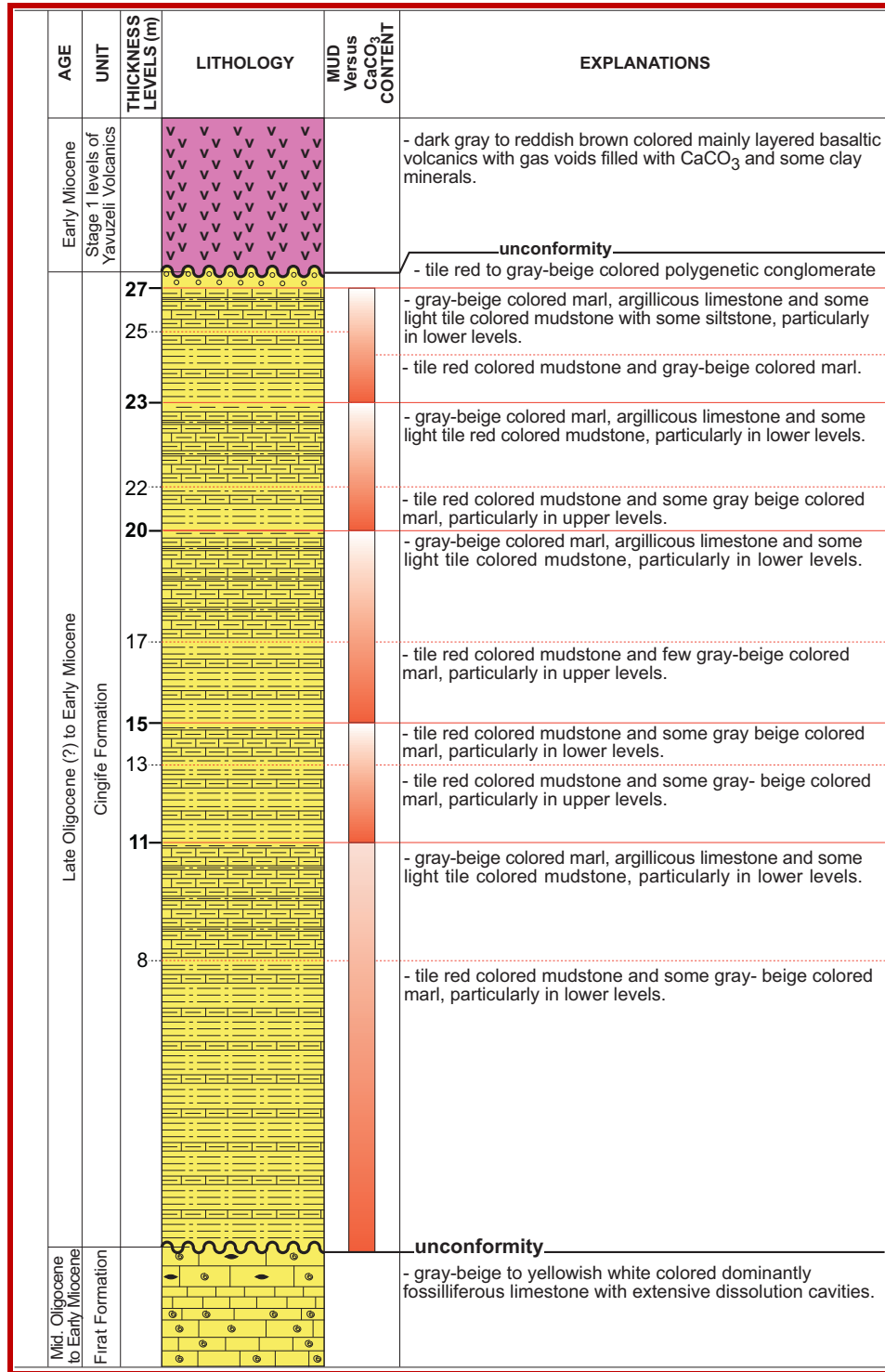


Figure 10. Dağdağancık measured type section of the Cingife Formation (nearly 1 km SE of the Dağdağancık Village).

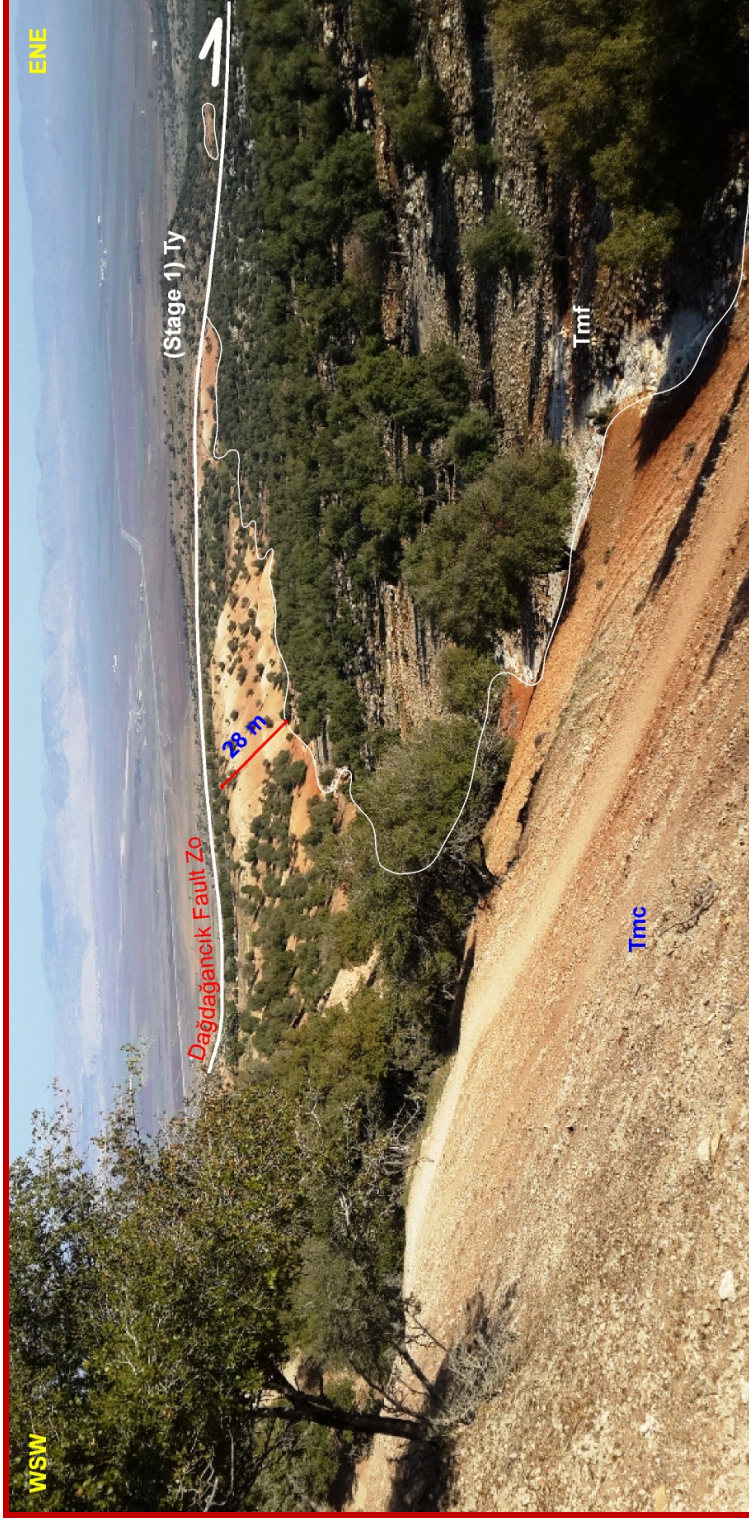


Figure 11. General view of the boundaries among the Firat Formation, Cingife Formation and the Yavuzeli Volcanics and the site of Dağdağancık measured section (view towards WNW, nearly 1 km SE of the Dağdağancık Village).



Figure 12. Close-up view of the boundary between Firat Formation and Cingife Formation and the site of measured section (view towards SE; nearly 1 km SE of the Dağdağancık Village)

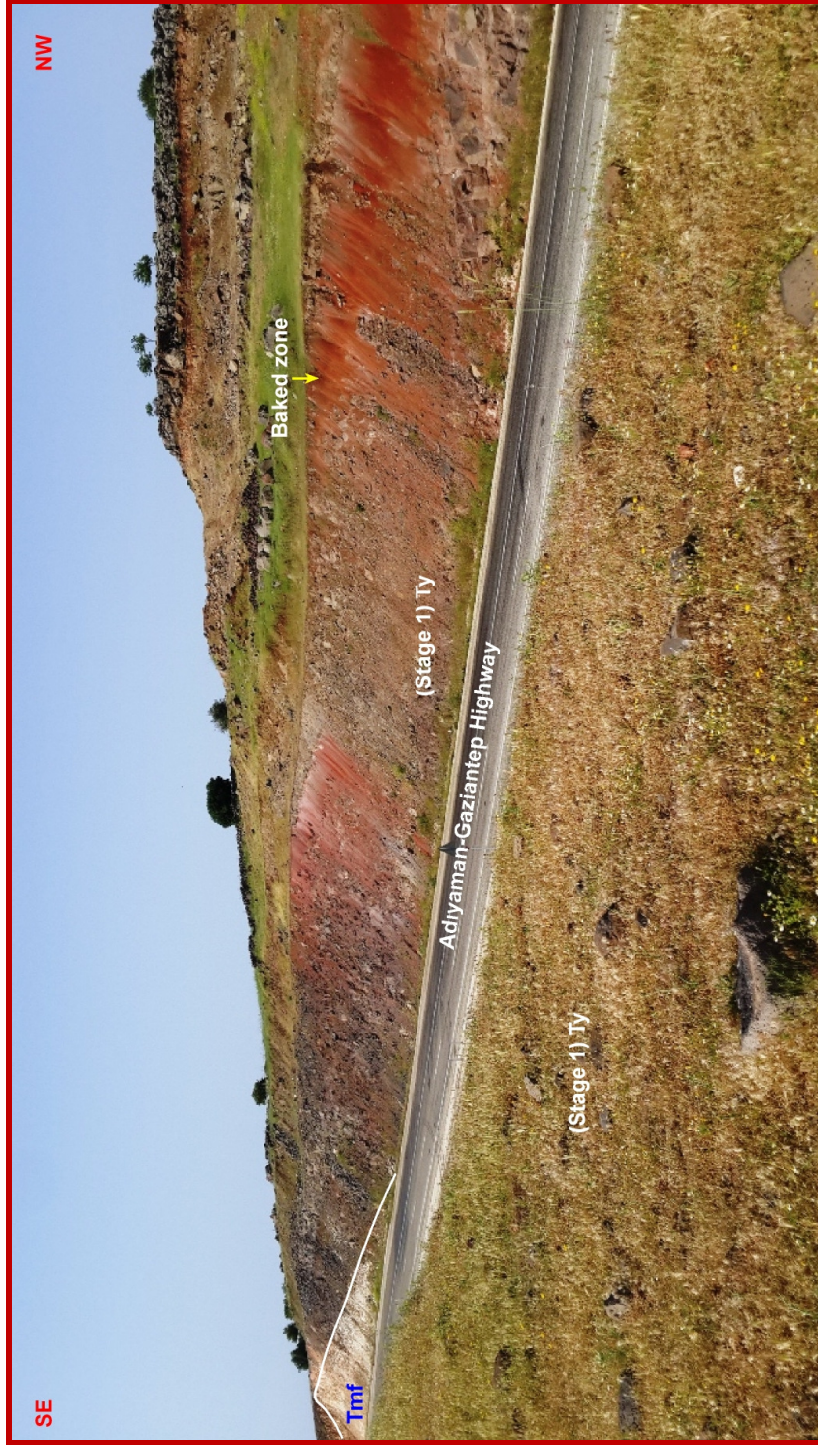


Figure 13. The photograph illustrating contact relationship between the Firat Formation and the Yavuzeli Volcanics near Karadağ passage located in the south central section of the study area (view towards SW, nearly NE of the Küçükkarakuyu Village)..



Figure 14. The field photograph illustrating contact relationship and its nature between the Stage 1 levels of the Yavuzeli Volcanics and the Cingife Formations (view towards NE, nearly 2 km NW of Yavuzeli (Gaziantep District)).

The upper most level of the Dağdağancık section ends with the coarse grained clastics such as polygenetic conglomerates in character (Figure 10).

The true thickness of the Cingife Formation was measured 44 m and 28 m in both the Ballık and the Dağdağancık measured sections respectively (Figures 5, 7, 8, 10, 11, 12). However, its apparent thickness was determined as 31 m in Bakırca-1 oil well located nearly 5 km WSW of the Yavuzeli District (Appendix-A).

No characteristic fossil could be found in the Cingife Formation. However, Arger et al. (2000) and Tatar et al. (2004) dated some samples belonging to the Stage 1 levels of the Yavuzeli Volcanics overlying the Cingife Formation by using the K-Ar and Ar-Ar dating methodologies. They found that the ages of the basaltic volcanics range between 21.24 ± 2.04 Ma and 16.32 ± 0.00 Ma. Thus, age of the Cingife Formation must be at least Early Miocene or a little bit older than i.e. Latest Oligocene based on the radiometric data and the stratigraphic relationship in the field. Therefore, Latest Oligocene (?) - Early Miocene age is used for the Cingife Formation in this study.

2.1.3.2. Yavuzeli Volcanics (Ty)

One of other widespread rock stratigraphic units exposing in and around the study area is the Yavuzeli Volcanics. It was first defined and named by Yoldemir (1987). However, these volcanics were studied, mapped and informally named by a number of researchers (Tromp, 1943; Stcephsky, 1943a, b; Güvenç, 1973). In addition, it was reported that the Yavuzeli Volcanics are same as those of the Karacadağ volcanics exposing in the east and far from the study area in these previous works. Lastly, Ulu et al. (1991) differentiated the volcanics exposing near the Çatboğazi area from the Yavuzeli Volcanics, and renamed them as the Çatboğazi basalts based on their physical characteristics and the stratigraphic relationships with the nearby rock units. In the present study, the name of Yavuzeli Volcanics was preferred and it was determined that the Yavuzeli Volcanics have

evolved at more than one stages (Appendix-A, Figures 5, 7, 10, 13, 14, 15, 16, 17, 18).

The type sections of the volcanics expose widely in the vicinity of Yavuzeli (Gaziantep) District in the south of the study area (Appendix-A, Figures 5, 7, 8, 13, 14).

Based on new field observations carried out in the frame of the present study and the published and unpublished age data obtained in and outside the study area (Çemen, 1987; Tatar et al., 2004; Arger et al., 2000), it can be concluded that these volcanics are not the products of only one eruption and evolutionary stage occurred in Middle Miocene-Late Miocene as was proposed in the earlier studies. In contrast, they evolved at least three volcanic stages during Miocene time slice. The Yavuzeli Volcanics may be the northern continuation of the Late Cenozoic Syrian Volcanics located in the further south on the Arabian Plate (Trifonov et al., 2011). In their study, the Late Cenozoic Syrian volcanics have been subdivided into three main stages based on the age and stratigraphic positions. This classification is also used for the Yavuzeli Volcanics in the study area (Altıntaş basin namely). These are the stage 1 levels of Yavuzeli volcanics, stage 2 levels of Yavuzeli Volcanics (or Çatboğazı basalts of Ulu et al. 1991) and the stage 3 levels of Yavuzeli volcanics which expose outside of the study area. Mapping separately these three stages of volcanics is beyond the scope of the present study. However, they are described briefly below.

The stage 1 levels of the Yavuzeli Volcanics were first identified and reported by Tromp (1943), Stchepshy (1943a, b) and Tolun (1956). These volcanics mapped and reported by them and defined to be basaltic volcanics without any age data. Later, Yoldemir (1987), Ulu et al. (1991), Terlemez et al. (1992) and İmamoğlu (1993) assigned a Middle Miocene-Late Miocene age to these volcanics. However, Arger et al. (2000), Tatar et al. (2004) and Gürsoy et al. (2007) roughly mapped and dated these volcanics as Early Miocene by using the K/Ar and Ar/Ar methods. Based on the radiometric ages, Stage 1 levels of the Yavuzeli volcanics correspond to the lowermost horizon of the Late Cenozoic

Syrian Volcanics (Trifonov et al., 2011). The Stage 1 levels of the Yavuzeli Volcanics are exposed widely of margins of the Altıntaş basin (Appendix-A). They are also widespread outside the study area such as the Pazarcik, Şhitkamil, Kilis and Urfa. The type section of the Stage 1 along the whole levels of Yavuzeli Volcanics are exposed well in the vicinity of Yavuzeli (Gazianstep) District in the study area (Appendix-A, Figures 5, 7, 8, 13, 14). The first stage volcanics are basically made up of black to brown colored basaltic lava flows. They are rarely observed in tile red to dark red colored along the baked zones (Figure 13). Based on the thin-section, detailed chemical analysis of the samples taken from basalts, they were defined as the olivine-ojit basalt with gas voids filled with the secondary minerals such as calcite and zeolite (Ulu et al., 1991; Terlemez et al., 1992). In addition, basalts are tholeithic in origin based on their geochemical composition (Ulu et al., 1991; Terlemez et al., 1992; Alpaslan, 2007; Telsiz et al., 2007). In general, the Stage 1 levels of the Yavuzeli Volcanics overly the Latest Oligocene-Early Miocene Cingife Formation and older rocks at the bottom, however it is overlain with an angular unconformity by the modern basin fill of Quaternary age at the top (Figures 5, 7, 8, 10, 11, 13 and 14). These field observations indicate that their age span is Early Miocene to Middle Miocene inside the study area. Various ages were used by the previous researchers such as Early Miocene, Late Miocene and Quaternary were assigned to the Stage 1 levels of the Yavuzeli Volcanics by previous workers (Tolun, 1956; Yoldemir, 1987; Ulu et al., 1991; Terlemez et al., 1992; İmamoğlu, 1993; Arger et al., 2000; Külah, 2006).

AGE	UNIT	THICKNESS	LITHOLOGY	EXPLANATIONS
Q		<50m		- Quaternary fan apron deposits.
	Middle Miocene to Early Pliocene Şelmo Formation	390 m		- light reddish brown to grey-beige-cream colored conglomerate and sandstone alternation.
	Middle Miocene Stage 2 levels of Yavuzeli Volcanics	240 m		comformable 12.1 +/- 0.4 Ma - black to dark grey colored and relatively fresh basaltic lava flows with gas voids filled with CaCO ₃ and clay minerals.
				- alternation of light pinkish brown colored basaltic lava flows with gas voids filled with CaCO ₃ and some clay minerals, and dominantly (> 90%) red colored mudstone alternation and basaltic lava flows.
Mid. Oligocene- Early Miocene	Firat Formation			15.1 +/- 0.4 Ma unconformity - gray-beige to yellowish white colored fossiliferous limestone, cherty, marly, chalky, limestone and dolomite alternation.

Figure 15. Measured stratigraphic column of both the Stage 2 levels of Yavuzeli Volcanics and the Şelmo Formation (Ziyaret village 5 km north of Altıntaş).

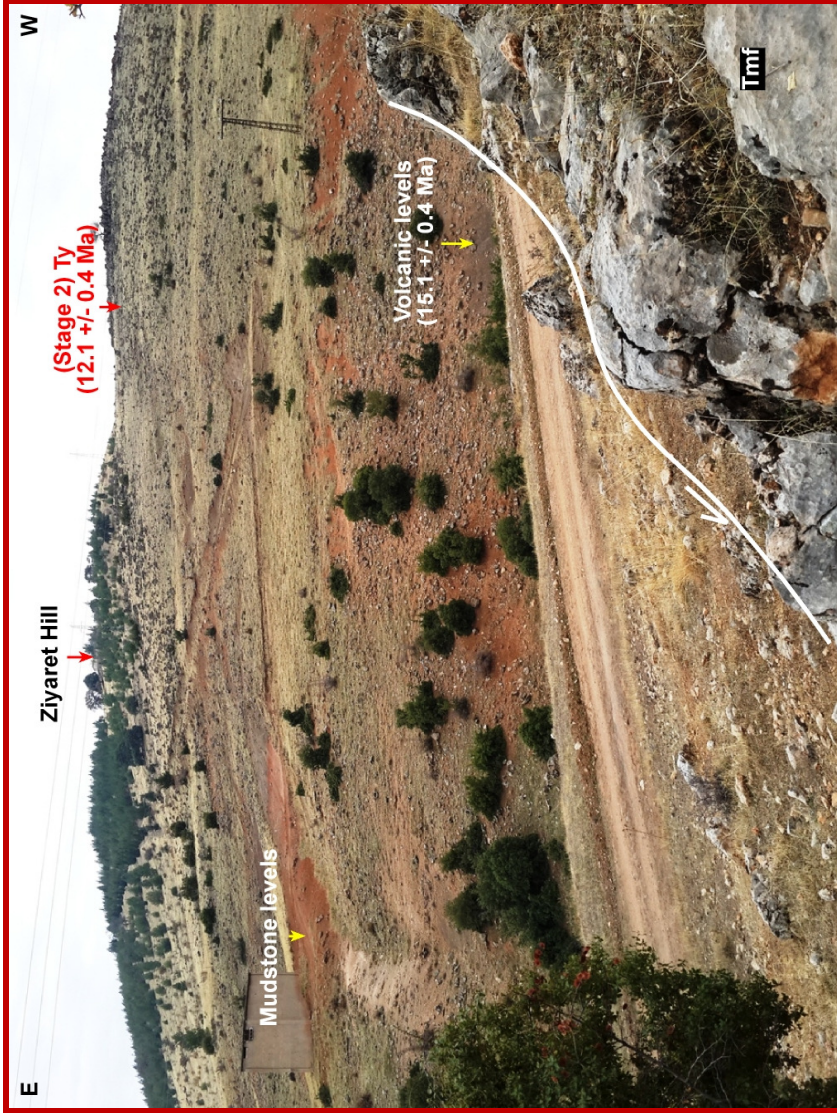


Figure 16. General view of the Ziyaret measured section site (view towards S, nearly 700 m N of the Ziyaret Village).



Figure 17. Close-up view of mudstone and volcanic levels of Stage 2 levels of the Yavuzeli Volcanics (view towards S, nearly 700 m N of the Ziyaret Village)..



Figure 18. The field photograph illustrating the close-up view of the faulted contact (the Akkuyu Fault) between the Stage 2 levels of the Yavuzeli Volcanics and the Firat Formation (view towards WNW, a few hundred meters NE of the Küçükkuşu Village).

In contrast, they are at least Early Miocene, not younger, based on both the radiometric data (Tatar et al. 2004) and the field observations carried out in the present study.

The true thickness of these volcanics was measured as approximately 50 m near the Karadağ locality along the Gaziantep-Adıyaman highway in the south of the study area (Appendix-A). However, its apparent thickness was determined to be the 93.30 m in the Altıntaş-2 well located nearly 2 km W of the Altıntaş, 178 m in the Bakırca-1 oil well located nearly 5 km WSW of the Yavuzeli district 173, 70 m in the Kızkapanı-1 oil well located nearly 43 km WSW of the Altıntaş district center, and 279 m in Karagöl-1 oil well located nearly 18 km NW of the Yavuzeli district.

The Stage 2 levels of the Yavuzeli volcanics were first identified by Yoldemir, (1987) and named as the “Çatboğazi Basalts” by Ulu et al., (1991). The type section of Stage 2 levels of the Yavuzeli Volcanics are exposed well around the Çatboğazi area along the northern margin of the Altıntaş basin (Appendix-A, Figures 5, 15, 16 and 17). They are basically represented by olivine-oid basalts with gas voids, filled with secondary minerals such as calcite and zeolite. They are tholeiitic in nature based on their geochemical composition (Ulu et al. 1991; Alpaslan, 2007; Telsiz et al. 2007). Spheroidal exfoliation structures with a pillow-like appearance are the characteristic features to recognize them in the field (Figures 5, 15, 16, 17 and 18). This property helps the geologists to distinguish it from stage 1 levels of the Yavuzeli Volcanics in the field (Figures 5, 8, 13, 14, 16, 17 and 18). The stage 2 levels of the Yavuzeli Volcanics overlie the Middle Oligocene to Early Miocene Fırat Formation with an unconformity at some localities. However, it is conformably overlain by the Middle Miocene-Early Pliocene Şelmo Formation at the top (Figures 5, 15, 16 and 17). Volcanics alternate with the lower levels of the overlying Sedimentary facies of the Şelmo Formation (Figures 5, 15, 16 and 17). The true thickness of the stage 2 levels of the Yavuzeli Volcanics were measured as 240 m in the Ziyaret measured section (Figures 15, 16, 17). However, their apparent thickness was determined as 284 m

in a geothermal well drilled nearly 1 km SE of Ziyaret Village near Çatboğazi area by Mineral Research and Exploration of Turkey (MTA 2012). There are two K/Ar ages obtained from its type locality. Age of the samples from bottom of these volcanics was determined as 15.1 ± 0.4 my while it is 12.1 ± 0.4 my for those taken from their upper horizons (Çemen, 1987) (Figure 15). Based on these results, the age of the Stage 2 levels of the Yavuzeli Volcanics are accepted as Middle Miocene in the present study.

The stage 3 levels of the Yavuzeli Volcanics are exposed outside of the study area such as the west and central parts of the Şanlıurfa, and Kilis areas and their vicinities (Güvenç, 1973; Ulu et al., 1991; Terlemez et al., 1992; Tatar et al., 2004; Gürsoy et al., 2007). Therefore, they are not described here.

2.1.3.3. Şelmo Formation (Tş)

This unit was first identified and named as the “*Adıyaman Gravel Group*” by (Gossage, 1956). Later, Bolgi (1961) renamed it as the Şelmo Formation in the Siirt and Batman areas, located outside of the study area. After Bolgi (1961), same name was used for the Miocene clastics exposing in and around the Altıntaş basin by a number of researchers (Çemen, 1987; Yoldemir, 1987; Sonel and Sarbay, 1988; Çemen, 1990; Çemen et al., 1990a; Ulu et al., 1991; Terlemez et al., 1992; İmamoğlu, 1993; Külah, 2006; Türkkan, 2011). However, the Cingife Formation was also included in the Şelmo Formation by these previous works. Whereas, as has been explained in the before mentioned sections, the Cingife Formation is older than the Şelmo Formation. This is evidenced by an intervening and most widespread rock unit (Yavuzeli Volcanics) (Figure 5).

The original type locality of the Şelmo Formation is Şelmo Village of the Sason (Batman) district outside and further east of the study area. The Şelmo Formation is exposed well along the east-northeast margin of the Altıntaş Basin, and displays various contact relationships (erosional, faulted and transitional bottom to top contacts) with both older and younger rock-stratigraphic units

(Appendix-A, Figures 5, 15, 16 and 17). The Şelmo Formation is composed mostly of orange, light red to gray colored boulder-block conglomerate, red colored mudstone, grey to light red colored claystones, gray to dirty white, beige colored marl and tuffite alternation (Appendix-A, Figure 19). The clasts (blocks, boulders, pebbles and other fragments) are made up of mainly flat to semi flat limestones, ultramafic rocks, radiolarite, cherts and basalts derived directly from the nearby older rocks. They are bounded firmly to each other by a siliceous to carbonaceous cement. Clasts range from a block in 0.5 m in diameter to a several cm (Figure 19).

Both the bottom and the top contact relationships of the Şelmo Formation with both the older rocks and the nearly flat-lying basin fill are observed well around Ziyaret, Bağlıca, Yukarıkaravaiz and Başpınar settlements located along the northeast margin of the Altıntaş basin. At these localities the Şelmo Formation displays a conformable contact, disconformable contact with the Stage 2 levels of the Yavuzeli Volcanics and the Fırat Formation, respectively, but is overlain with an angular unconformity by the Quaternary basin fill (Figure 15). Thus, the age of the Şelmo Formation can be bracketed by the Middle Miocene from bottom and the Quaternary at the top (Figure 15). However, some pollens in the upper levels of the Şelmo Formation were collected and dated by (Çemen, 1990; Çemen et al. 1990a). These are the *Pityosporites sp.*, *Tricolpopollenites sp.*, *Tricolporopollenites sp.*, *Compositae sp.*, *Hypoxylon sp.*, *Laevigatosporites sp.*, *Polyad fungal spore*. Based on these pollen assemblage, Late Miocene-Early Pliocene age is assigned to upper level of the Şelmo Formation. Therefore Middle Miocene to Early Pliocene age is used in this study.

The true thickness of the Şelmo Formation was measured as 390 m at its type section (the Ziyaret measured section) (Appendix-A, Figure 15). However, the apparent thickness (vertical borehole thickness) was determined as 336 m in a geothermal well drilled at nearly 900 m SE of the Ziyaret Village by MTA in 2012.

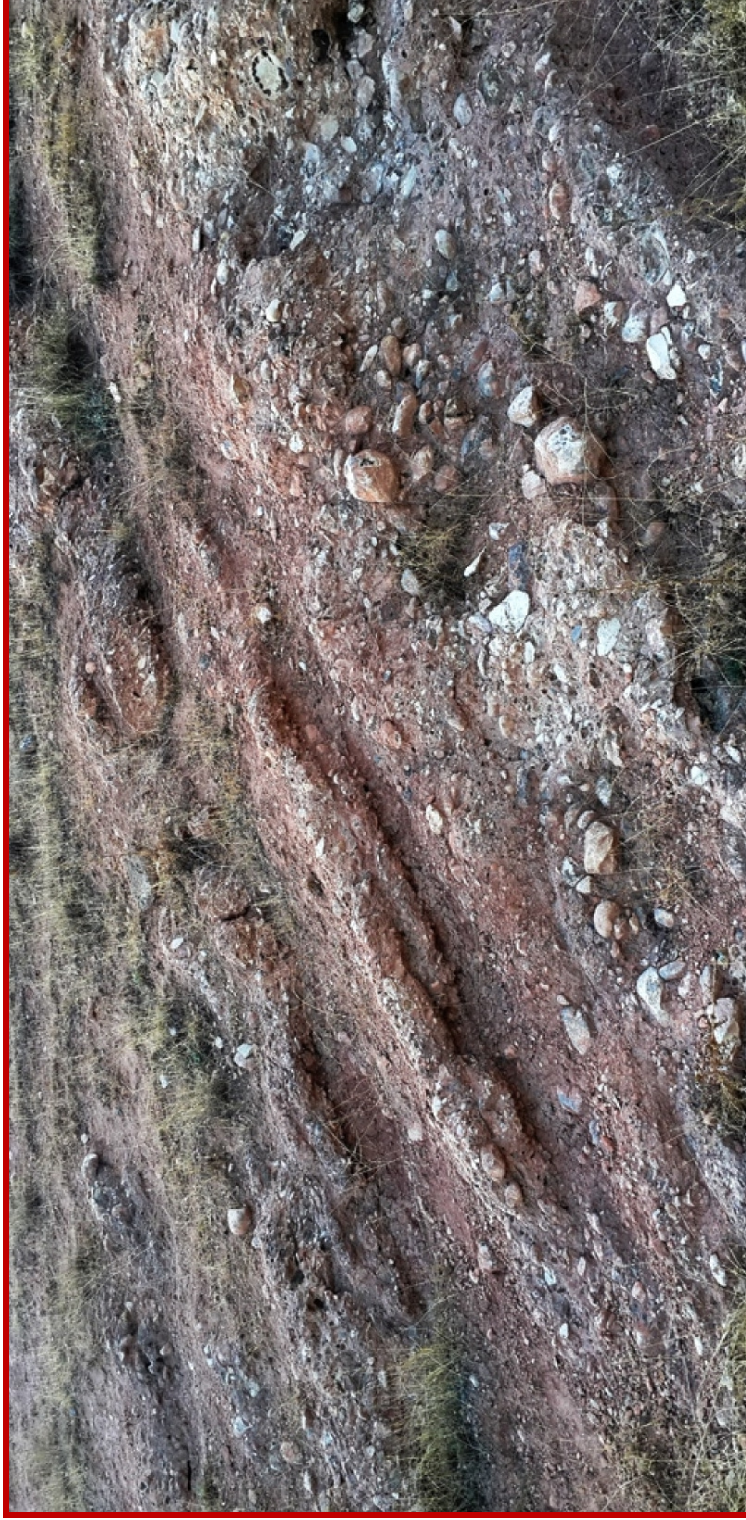


Figure 19. Close-up view of the boulder-block conglomerates comprising the Middle Miocene-Early Pliocene Şelmo Formation (approximately 900 m ESE of Ziyaret village located along the northern margin of the Altıntaş basin).

2.2.1. Neotectonic Units (or Modern Basin Fill)

2.2.1.1. Lahti Group (Q)

The Quaternary units in and adjacent to the Altıntaş basin were identified and reported by several researchers (Tolun, 1956; Ulu et al. 1991). However, a formal name (Lahti Formation) was first used for the Plio-Quaternary units in SE Anatolia by Yılmaz and Duran (1997). Recently the bottom of the Quaternary period was shifted backward up to 2.588 Ma before present so that it can include the previous Late Pliocene stage by international stratigraphy commission (2009). In this frame, early mentioned Late Pliocene units are included in the Early Quaternary period. Based on this time-table revision, all of Quaternary units exposing in the Altıntaş basin was collected under some name and it was shifted up to the grade of group in the present study (Appendix-A, Figure 5). The Lahti group or modern (neotectonic) basin fill is composed of two basic lithofacies assemblages; (1) coarse grained marginal facies, and (2) relatively finer-grained depocentral facies (Appendix-A and Figure 5). All lateral and vertical gradations are seen among these two categories of facies assemblages.

The marginal facies assemblage consists of fan-apron deposits, slope scree deposits, terrace deposits and renewed alluvial fan deposits. They are exposed well and concentrated mostly along the northern margin of Altıntaş basin (Appendix-A). They have been transported and accumulated at the east of northern mountainous area or faulted mountain front. Numerous sub-branches of the Fırat River emanating from the highest peaks of mountains flowed basinwards in down-slope direction, eroded the rocks, transported the clasts and accumulated them into fans when they enter into the gently sloping basin floor (Appendix-A, Figure 20). In time a long and margin-boundary faults-parallel zone or belt of unconsolidated sediments developed in terms of the coalescence of early-formed fans and the slope-scrree deposits accumulated under the control of gravity. Sediments comprising both the fan and fan-apron deposits range from a few cm to 1 m in size

or diameter. They are angular to sub-rounded in shape and derived directly from the underlying rocks of pre-Quaternary age. However, slope scree deposits are angular in shape, but have all other physical characteristics of the fan to fan-apron deposits. A series of renewed alluvial fans of dissimilar size also occur just on the relatively older fan-apron deposits along the northern margin of the Altıntaş basin (Appendix-A).

One of the major sub-branches of the Fırat River is the Karasu stream. This stream and its third-order sub-branches are located along the southern margin of the Altıntaş basin (Appendix-A). The Karasu stream drains the southern marginal side of the basin. Same kind of coarser facies assemblage also occurs along this margin. The renewed alluvial fans are more or less with respect to those along the northern margin which implies to the slower activity along the southern margin of the basin. The or diameter. They are angular to sub-rounded in shape and derived directly from the underlying rocks of pre-Quaternary age. However, slope scree deposits are angular in shape, but have all other physical characteristics of the fan to fan-apron deposits. A series of renewed alluvial fans of dissimilar size also occur just on the relatively older fan-apron deposits along the northern margin of the Altıntaş basin (Appendix-A).

The field photograph illustrating the deformed (tilted) Middle Miocene to Early Pliocene Şelmo Formation (nearly 900 m ESE of Ziyaret village located in the north of the Altıntaş basin).

One of the major sub-branches of the Fırat River is the Karasu stream. This stream and its third-order sub-branches are located along the southern margin of the Altıntaş basin (Appendix-A). The Karasu stream drains the southern marginal side of the basin. Same kind of coarser facies assemblage also occurs along this margin. The renewed alluvial fans are more or less with respect to those along the northern margin which implies to the slower activity along the southern margin of the basin. The Karasu stream is in the nature of meandering stream and the deposition in the form of point to mid-channel bars and flood plain clasts along this drainage system in the present (Figure 21). Some of these fluvial deposits have

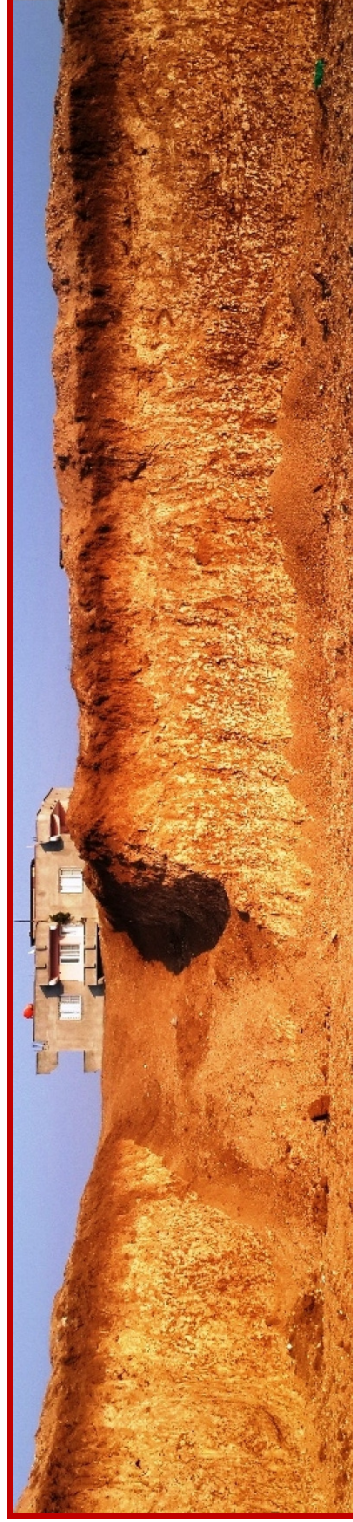


Figure 20. Close-up view of the nearly flat-lying Plio-Quaternary Lahti Formation (a few hundreds meters N of the Adyaman-Gaziantep Highway).

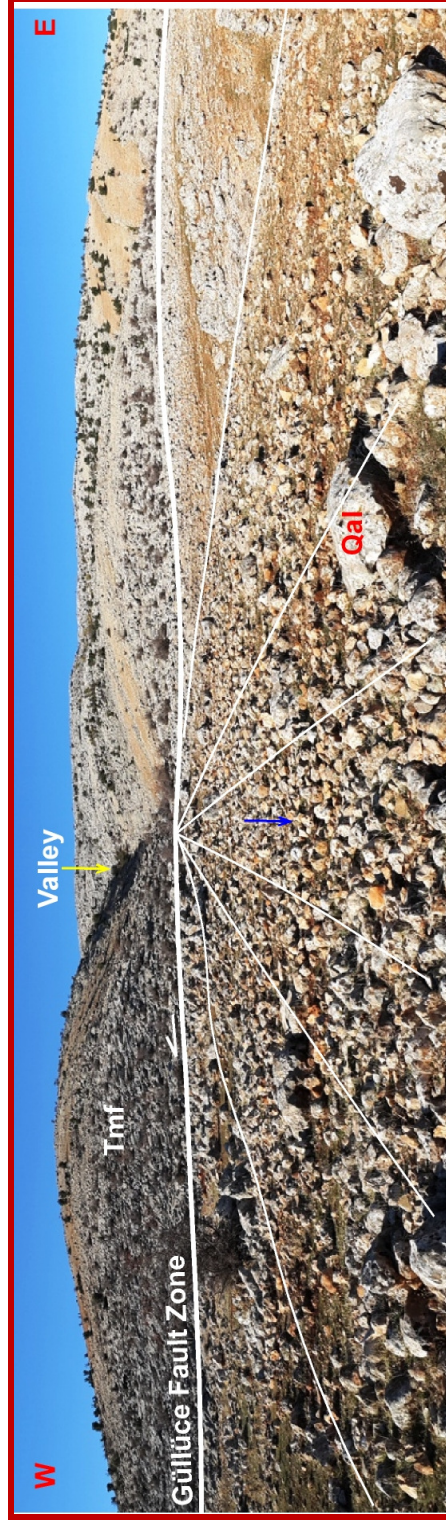


Figure 21. General view of the Quaternary alluvial sediments in the northern margin of the Altıntaş basin between Sarlı and Güllüce Villages (view towards N, nearly 1 km W of the Güllüce Village).

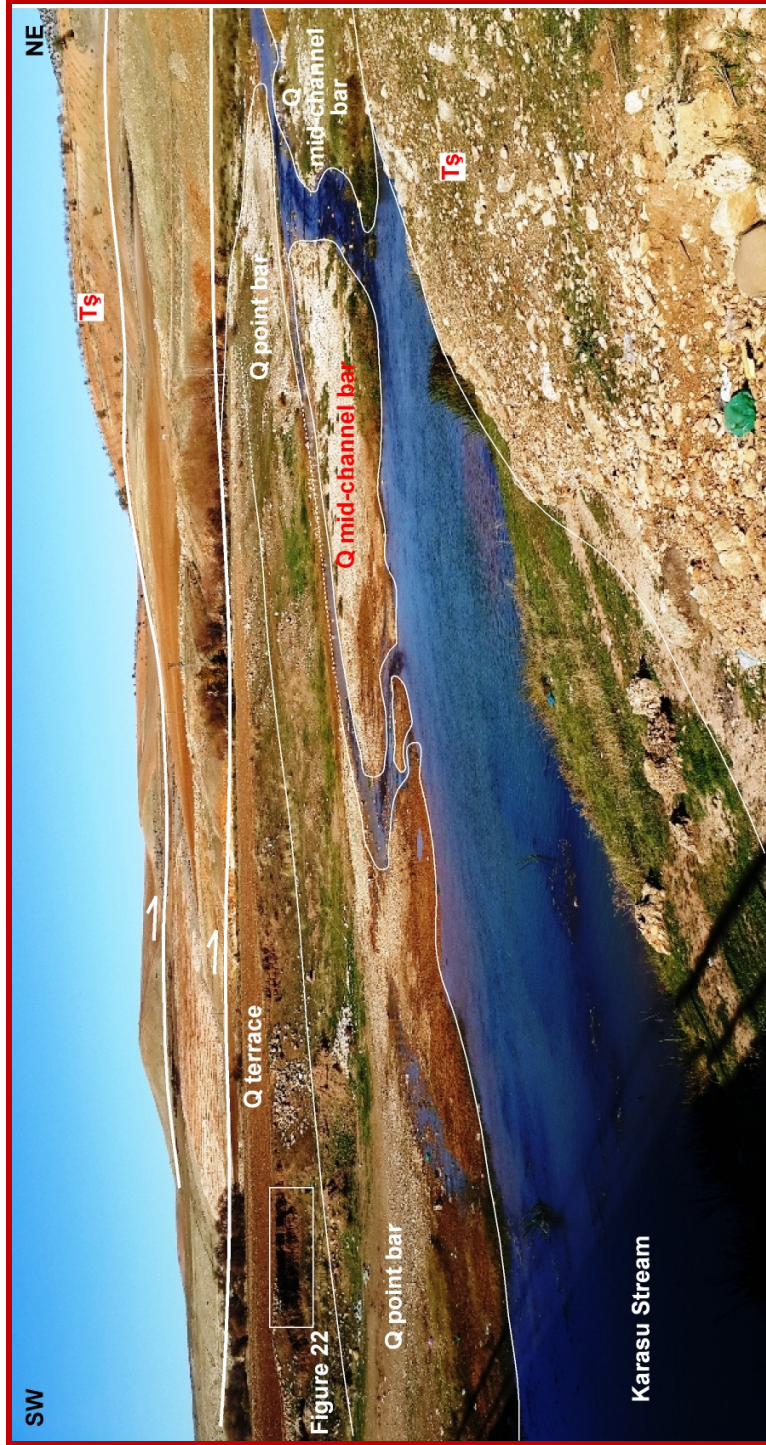


Figure 22. General view of the fluvial sediments (view towards, NW, between Dipçepni and Gümüşpınar Villages in SE margin of the Altıntaş basin).

been uplifted and left as terrace deposits at higher elevation above the present bed of the Karasu stream (Figure 22).

The second basic category of the Quaternary lithofacies is the relatively finer-grained depocentral facies assemblage (Figure 5). It occurs throughout the axial plain of the Altıntaş basin, and covers an area of approximately more than 100 km² (Appendix A). Indeed it is covered by a thinner usually several meters of loose brown to red soil to alluvial sediments. Therefore, its deeper part and internal structure are not seen. However, it exposes well inside the road cuts, mining pits and the deep foundation excavations of buildings (Figure 23). The axial plain deposits consist of gray, beige, light red, yellow and brown colored mudstone, claystone and organic material rich swamp deposits alternation with lenticular sand, pebble and calichy intercalations. The degree of consolidation increases with depth. The total thickness of both the Quaternary lithofacies assemblage could not be defined due to insufficient data. However, its apparent thickness was observed as 27 m in Araban-1 oil well. It is interpreted here that the average thickness of this rock assemblage is more than this.

In general, all of the Quaternary sediments are loose to semi-consolidated and nearly flat-lying except for the areas adjacent to the margin-boundary active faults. They overly the deformed (folded to tilted) pre-Quaternary rocks with an angular unconformity. This is a regional angular unconformity, because there is high-rate of uplift and widespread to high-rate of Late Pliocene erosion in not only in Turkey but also throughout the world (Ollier, 2006). Therefore, this regional unconformity of Late Pliocene age implies to a major inversion in the tectonic regime (Figure 5).



Figure 23. Terraced flat lying Quaternary sediments.

CHAPTER 3

STRUCTURAL GEOLOGY

This chapter deals with the definitions and analysis of the geological structures including beds, unconformities, folds, faults and some mesoscopic structures such as joints, crystal fibers, tension gashes, stylolites, sigmoidal veins, en echelon sigmoidal veins observed and examined in the study area. Based on tectonic periods during which they developed, these structures are divided into two categories: (1) Paleotectonic structures, and (2) Neotectonic structures.

The structures, that have reactivated or newly formed in the time slice of Miocene-Quaternary, will be described in detail. In addition to this, latest paleotectonic structures, which deformed the older basin infill and interrupted the previous stage development of the Altıntaş Basin, will also be explained in detail.

The dataset used in structural analysis and interpretations of neotectonic structures were collected mainly by field geological mapping at scale of 1/25,000. Some structural data collected by previous researchers have also been rectified and then used in this study. During the field work, attitudes of various planar and linear structures such as strike-dip, trend-plunge, rake, length, width, type, fill type if present, throw amount and their relationship with other structures were measured. Thereafter, the datasets were analyzed by using pole plots, strike amounts-dip amounts-dip directions and rakes by using the computer programmes designated as Tector, 5.42 (Angelier, 1990) and Stereonet 8.9.2 (Allmendinger et al., 2013; Cardozo and Allmendinger, 2013). They allowed us to be able to reveal the relationships between faults, folds, some mesoscopic structures and principle stress directions.

The program “Tector 5.42” processes the data based on four sub-programs. These are “Measure”, “Tensor”, “Diagra” and “Q-Basic”. They are the computer

softwares which give to the user the principal stress directions. The software “Q-Basic” presents the results of the processed data obtained from the fault planes by using stereographic projection method. During the processing of the slip-plane data, direct inversion method of Angelier (1990) has been used.

Stereonet 8.9.2 software allows the user to solve and do some structural analysis such as constructing rose diagrams, true dip/apparent dip calculations, stereographic projections of linear and planer structures and also some statistical analysis.

3.1. Altıntaş Basin

There are two configurations of the Altıntaş basin. These are the older (Middle Eocene-Early Pliocene) deformed configuration and the undeformed modern (neotectonic) configuration. Older Altıntaş basin developed through on both the pre-Middle Eocene –Late Cretaceous Arabian platform during the tectonic transportation of ophiolitic nappes in the Middle Eocene-Early Pliocene period. Therefore, outline of older Altıntaş basin is much more broad and intensely deformed. In contrast, the modern Altıntaş basin covers a relatively limited area on its older configuration. It began to developed in early Quaternary and still lasts to grow under the control of strike-slip tectonic regime.

The modern Altıntaş basin is a 6-9-km-wide and nearly 50-km-long E-W-trending depression located on the Araban Block of the SE Anatolian region (Figure 3). It is also included in the Strike-slip Neotectonic regime with reverse component (Figures 2). The Altıntaş basin is one of the major strike-slip structures comprising the SE Anatolia of Turkey. It is confined among some well developed strike-slip structures, the Gölbaşı basin to the northwest, the Keysun basin to the North east, the Yavuzeli basin to the south, and the Çöçelli and Karasu basins to the west (Figure 3).

The structures formed before the development of the modern Altıntaş basin are called here to be the paleotectonic structures. In contrast, the structures

reactivated or newly-formed during the development of the modern Altıntaş basin are named as the neotectonic structures.

3.2. Paleotectonic Structures

These are the beds, unconformities, some mesoscopic structures (tension gashes, fiber crystals, stylolites, conjugate shear fractures, en echelon sigmoidal veins), folds and thrust-reverse faults. They are described in detail below.

3.2.1. Beds

Older units exposed around and beneath the modern Altıntaş basin consist of the Middle Eocene Hoya Formation, the Middle Eocene-Middle Oligocene Gaziantep Formation, the Middle Oligocene-Early Miocene Fırat Formation, the Late Oligocene to Early Miocene Cingife Formation, the Early Miocene to Middle Miocene Yavuzeli basalts, and the Middle Miocene-Early Pliocene Şelmo Formation. All of these units are termed here as the pre-modern basin fill. Cingife Formation is characterized mostly by the well-bedded clastic sedimentary rocks (Appendix-A, Figures 7, 8, 9, 10, 11, 12 and 14). The dip amount of the Cingife Formation may reach 40° in places. However, in general, it is between 10 to 20°. The thicknesses of the beds commonly do not exceed 1 meter. They are exposed in the area a few kilometers N and NW of the Yavuzeli district along the southern and NW margin of the Altıntaş basin (Appendix-A).

The Şelmo Formation is also characterized by the medium to poorly-bedded clastic sedimentary rocks (Appendix-A, Figures 15, 16, 17, 20 and 21). Therefore, the bedding plane measurements are rare with respect to other formations. The dip amounts of bedding planes of the Şelmo Formation may exceed 33° along the northern margin of the Altıntaş basin (Appendix-A). However, they usually range between 02° to 15° (Appendix-A).

The Yavuzeli Volcanics are mostly lava flows in character. Therefore, they present layered structures in places (Appendix-A, Figures 13, 14 and 17). Their attributes (strike/dip amount/dip direction) could be measured along the northern margin of the Altıntaş basin. According to this, average dip amount is 25°.

3.2.2. Unconformities

Based on the occurrence ages, ten unconformities were identified and mapped during the field study. Seven of them are the angular unconformity, the rest three are the disconformities. The first and oldest angular unconformity occurs between the underlying Maastrichtian Koçali and Kardut Complexes and the overlying Maastrichtian-Early Paleocene Germav, Middle Eocene Hoya and the Middle Oligocene-Early Miocene Fırat Formations, respectively. The second angular unconformity separates the Germav Formation from the overlying Middle Eocene Hoya and the Middle Eocene-Middle Oligocene Gaziantep Formation, respectively. Both the first and second angular unconformities are exposed and observed well in the Çatboğazı area along the northern margin of the Altıntaş modern basin (Appendix-A). The rest five angular unconformities occur among the Middle Eocene Hoya, the Middle Eocene-Middle Oligocene Gaziantep, the Middle Oligocene-Early Miocene Fırat, the Early to Middle Miocene Yavuzeli, the Middle Miocene-Early Pliocene Şelmo Formation and the overlying modern basin fill (Quaternary Lahti Group), respectively. They are exposed and observed well along all of the margins of the Altıntaş modern basin. The longest angular unconformity occurs between the Quaternary Lahti group and the Middle Eocene Hoya Formation, while the youngest one separates the underlying Middle Miocene-Early Pliocene Şelmo Formation from the overlying and horizontally-bedded modern basin fill. This youngest angular unconformity corresponds to a definite time slice (latest Pliocene) during which a short-term of WNW-trending compressive tectonic regime occurred and then it was replaced by almost N-S-trending the strike-slip neotectonic regime at the beginning of Quaternary.

However, short-term local disconformities occurs among the Middle Oligocene to Early Miocene Fırat Formation and the Late Oligocene (?) to Early Miocene Cingife Formation, the Early to Middle Miocene Yavuzeli Volcanics and the Middle Miocene-Early Pliocene Şelmo Formation (Figure 5 and Appendix-A). These local disconformities seem to have formed owing to the rapid subsidence and the transgression of marine waters onto the early-eroded surfaces of relatively older rock units.

3.2.3. Mesoscopic Structures

During the field studies a series of both the mesoscopic and macroscopic features were identified. These are (1) Tension gashes, (2) Stylolites and (3) Shear fractures. Each of them is described below.

3.2.3.1. Tension gashes

Indeed, these are the open fractures filled by cements such as calcite, quartz, iron and some organic materials. There is a close relationship between the stress axes and the orientation of long axis of the tension gash (Ramsay and Huber, 1983; Eyal and Reches, 1983). Therefore, these features have a great importance in determination of the operation directions of stress that produced these structures (Figures 24) (Yürür and Chorowicz, 1998; Amrouch et al., 2010).

Tension gashes occur in various forms such as single gashes, en-echelon type gashes, single sigmoidal veins, en-echelon type sigmoidal veins, hybrid shear veins (Pinnate or feather joints) and the stepped veins (Figure 24). The set of single tension gashes occur as a result of coaxial deformation. They are independent from other counter parts in time and space (Figure 24). They were widely observed, measured and evaluated during this work (Figures 25, 26 and 27) (Appendix-A, Figures 24 to 30). The single tension gashes are usually regarded as the product of brittle deformation. The en-echelon type of tension gashes also

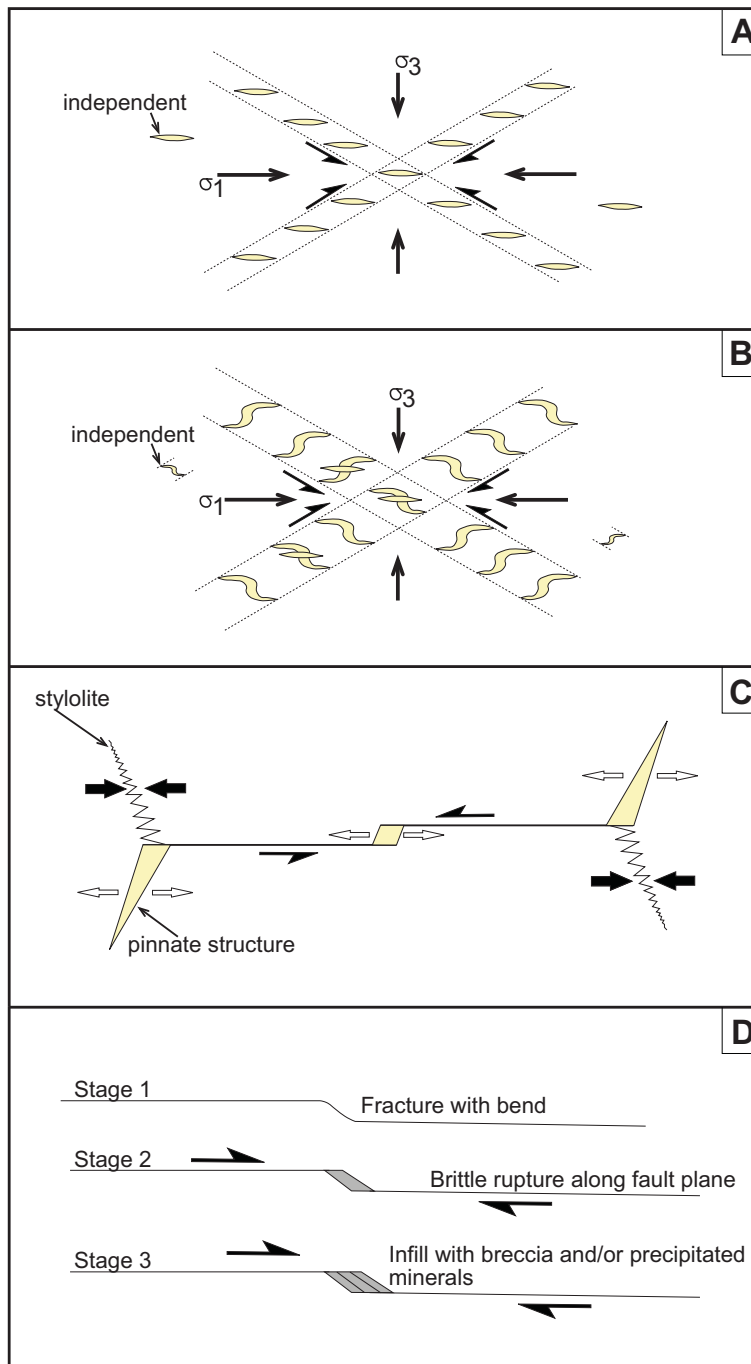


Figure 24. Types of Tension and hybrid (tension and shear) fractures. (“A”, “B”, “C” modified from www.files.ethz.ch/structuralgeology/JPB/files/English/4joints.pdf “ and “D” adapted from <https://structuredatabase.wordpress.com/brittle-shear-sense-indicators/>).



Figure 25. General view of an unfilled tension fractures nearly 1.5 km SE of Dağdağancık Village (Araban District).



Figure 26. Close-up view of a filled tension gash (~1750 m NE of Aşağı Mülk settlement).

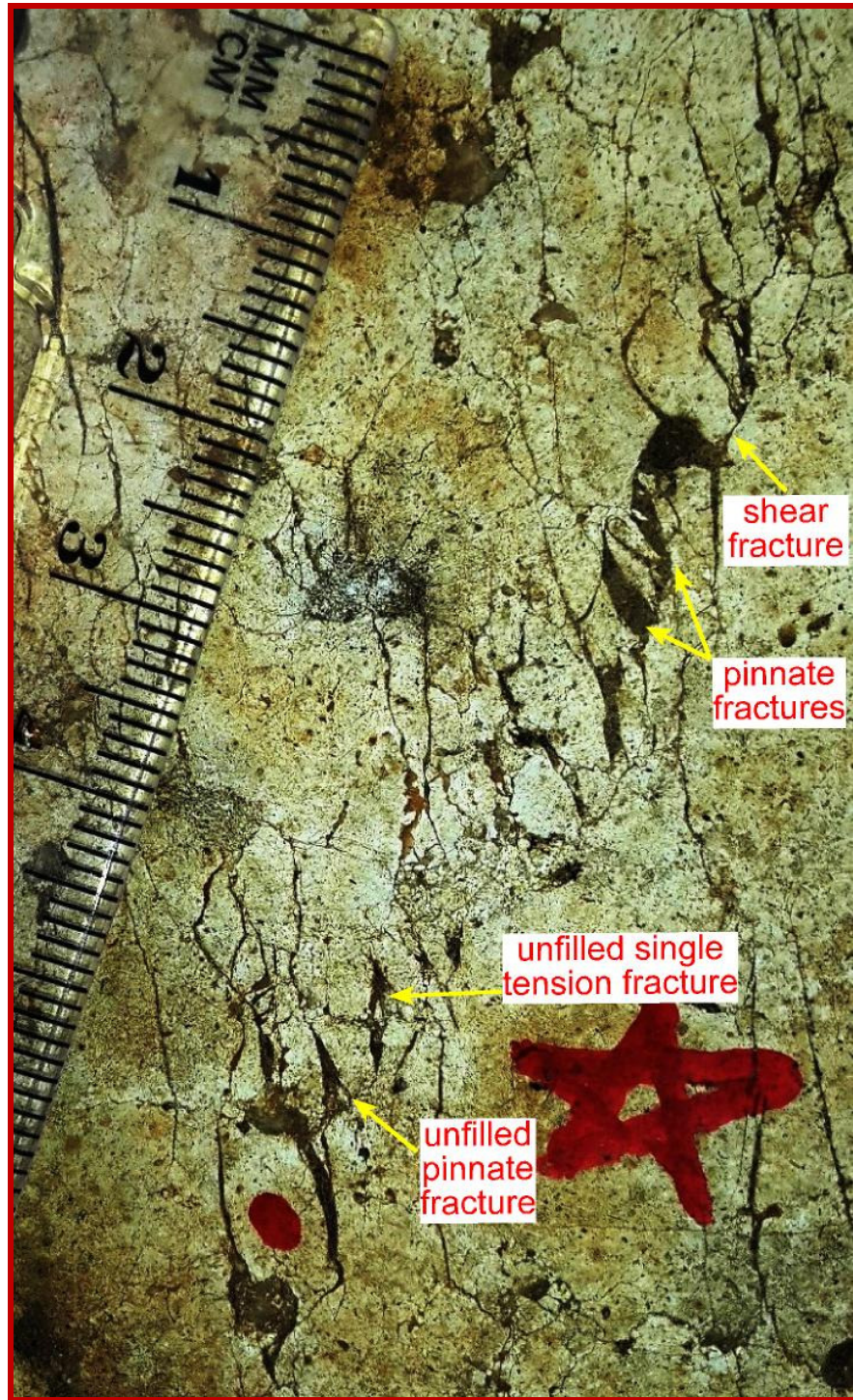


Figure 27. Close-up view of some mesoscopic tension and hybrid (combination of tension and shear features) fractures (~1750 m S of Akkuyu Village).

occurs as a result of coaxial deformation inside the shear fracture or zone (Figure 24B and 28). They are usually regarded as the product of brittle deformation. The single sigmoidal veins form as a result of non-coaxial deformation. Indeed, an early formed single tension gash is deformed into a sigmoidal shape due to the rotation in a shear zone (Figures 24A, B). However, their tip sections almost still retain their initial position (Dunne and Hancock, 1994; Allmendinger, 1999; Ramsay and Huber, 1987). Hence, these structures are reliable markers for paleostress analysis. They are usually regarded as the product of ductile deformation. The en-echelon sigmoidal veins are the arrays of veins with en-echelon geometry (Figure 24B). Their development history or mode is also same as those of the single sigmoidal vein. These are also reliable markers for local stress analysis. Because they give very reliable information about the sense of shear in the shear zone they developed (Figure 24B). The en-echelon sigmoidal veins are of three common types. These are the convergent, parallel and divergent types of en-echelon sigmoidal veins (Figure 28). The shear veins result from both the extension and shearing inside a shear zone (Figures 24C and D). They are two types such as the pinnate structure and the stepped veins (Figure 29). The pinnate structure is a kind of joint formed by the motion occurred in a direction opposite to the shear sense on the fault plane (Hancock, 1985; Hancock and Barka, 1987). The stepped veins are the features formed usually inside a shear fracture or zone with a mechanism similar to that of a pull-apart basin identified in the study area (Figure 24D). These are also widespread features.

One of the widespread mesoscopic features observed in the study area is the crystal fiber growth of CaCO_3 composition. They occur in a preferred orientation paralleling to the least principal stress axis during deformation (Figure 30).

During the field studies, a number of tension fractures have been observed in many stations such as (Appendix-A on ST-3, 4, 8, 11, 12, 16, 17, 18, 21, 22, 27). They have been differentiated from hybrid or pure shear fractures in order to

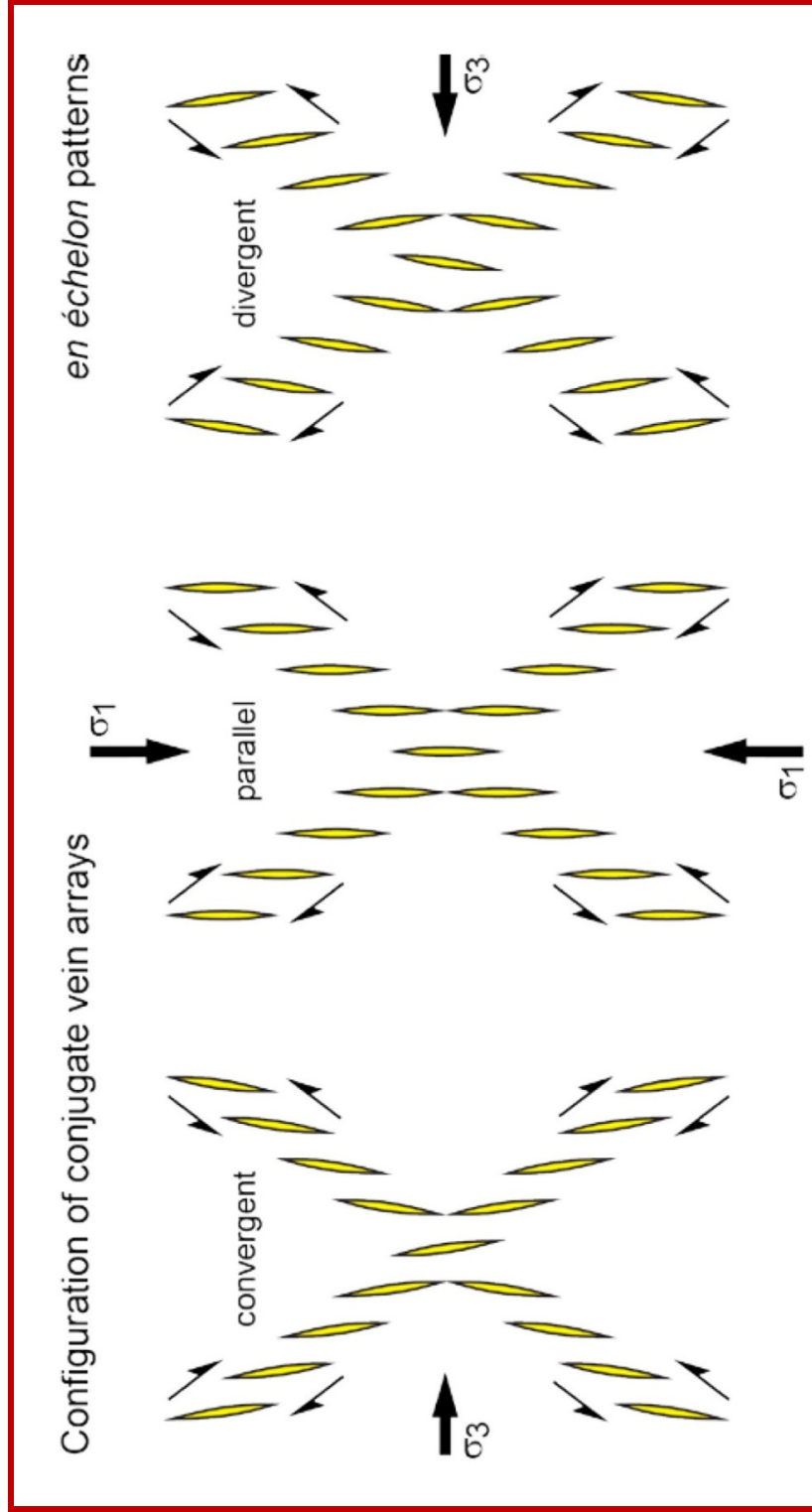


Figure 28. Types of conjugate en échelon tension gashes (Adapted from www.files.ethz.ch/structuralgeology/JPB/files/English/4joints.pdf).

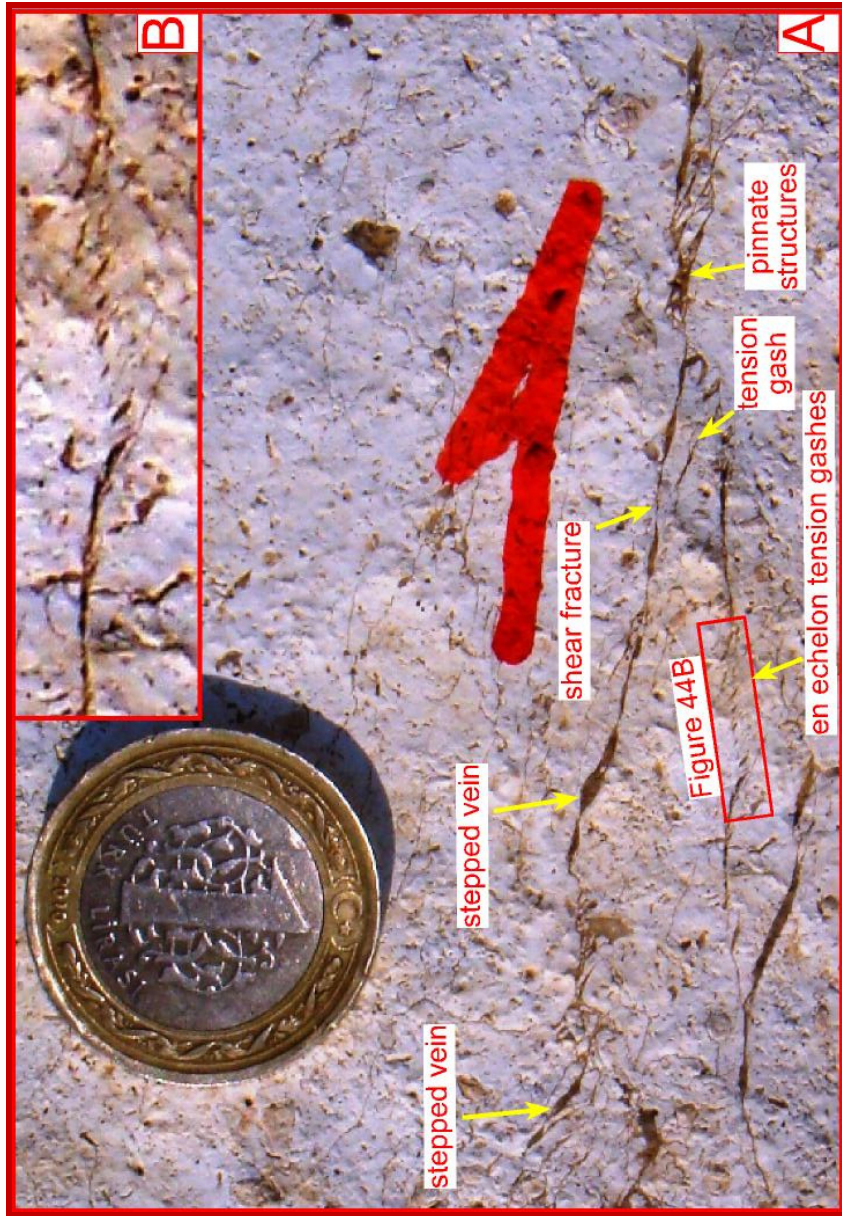


Figure 29. General view of some mesoscopic tension and hybrid (combination of tension and shear) fractures nearly inside the Dağdağancık Village (Araban-Gaziantep) located due South of the study area.

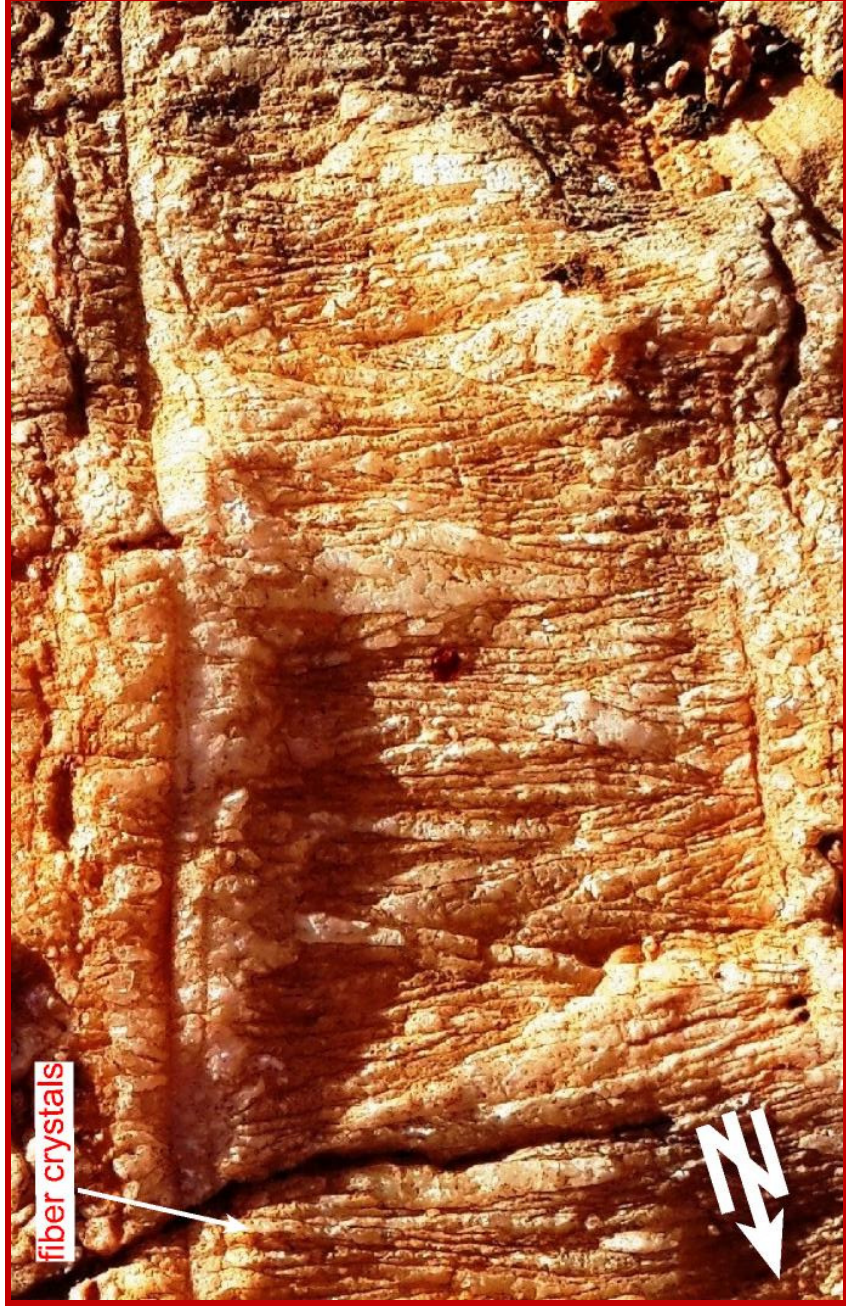


Figure 30. Close-up view of fiber crystals (Çatalbogazi area along northern margin of the Altınbaş basin).

avoid misevaluations in during the paleostress analysis (Figures 24, 25, 26, 27 and 29).

No direct aging could be assigned to the tectonic stylolites due to lack of data. However, to be able to use in the paleostress analysis, the structures were separated based on their relative chronology methods such as filled and unfilled tension gashes found a few meters away from each other (ST-4, 17 and 27 in Appendix-A). In these stations some of the filled and unfilled tension fractures display strong variations in their trends implying different stress states. Moreover, some of the active and partly filled (or reopened) tension fractures allow mild water seepages time to time (Appendix-A, ST-8). Based on these, the different groups of tension fractures have been assumed belonging to the different events. The phase separation of these structures were done by using this relationship. In addition to this, the other solutions obtained from various methods from the nearest stations were also used to separate the events. These events might have belong to significantly different events. This is because, there is at least one recorded regional angular unconformity between Quaternary Lahti Group and pre-Quaternary units inside the study area (Figure 5) and two different regional angular unconformities between (1) Early Pliocene and pre-Early Pliocene units, (2) between Pliocene and Quaternary units inside the basins around of the Altıntaş basin (Rojay et al. 2002; Boulton and Roberston, 2008; Yusufoglu, 2013; İmamoğlu, 1993; Çemen et al. 1990a, b) (Figure 3).

3.2.3.2. Stylolites

Stylolites are serrated sub-planar surfaces where mineral material is disoluted and removed away by pressure dissolution processes during deformation. Thus a decrease in total volume of the rock occurs (Railsback, 2003). They may be microscopic, mesoscopic and macroscopic in size. The stylolites include the residues of relatively insoluble materials such as pyrite, oxides, clays, and other silicates (Railsback, 2003). These are distinctive and pervasive structures that

resulted from water-assisted pressure solutions in rocks such as limestones and dolomites (Rutter, 1983; Passchier and Trouw, 1996). However, some stylolites are also observed in sandstones (Railsback, 2003) and igneous rocks (Golding and Conolly, 1962; Railsback, 2003). Orientations of stylolite surfaces and the associated features (spikes and teeth) mark the operation direction of the local maximum principal stress axis (Suppe, 1985; Stel and De Ruig, 1989; Dunne and Hancock, 1994; Petit and Mattauer, 1995; Koehn et al., 2007). This relationship makes them reliable paleostress indicators. The spikes occur parallel to the maximum principal stress axis (Figure 31).

The stylolites are subdivided into six types based on their geometry (Park and Scot, 1968). These are (1) simple or primitive wave-like type, (2) sutured type, (3) up-peak type (rectangular type), (4) down peak type (rectangular type), (5) sharp-peak type (tapered and pointed) and (6) seismogram type (Figure 32). During the field studies the most widespread type observed in the study area is simple or primitive wave-like type (Figure 33). Additionally, another type of stylolite (slickolite) has also been identified. The slickolite is a type of stylolite with teeth inclined $< 90^\circ$ to the plane of the stylolite (Figure 31) (Hancock, 1985).

Stylolites can also be classified into three categories such as the tectonic stylolites, the diagenetic stylolites (bedding-parallel stylolite) and object-dependent stylolites. The separation has been based on field observations of them in 3D (Figures 34 and 35). The diagenetic stylolites occur as a result of overburden pressure (Railsback, 2003). Some diagenetic or bedding-parallel stylolites were observed in both the Middle Eocene-Middle Oligocene chalky to clayey limestones of the Gaziantep Formation and the Middle Oligocene-Early Miocene massive limestones of the Firat Formation (Figure 34). They are differentiated from the tectonic stylolites during the field studies (Figure 35).

These structures were observed, measured and analyzed in five stations during the studies (Appendix-A, ST-6, 12, 17, 18, 23)

No direct aging could be assigned to the tectonic stylolites due to lack of data. However, to be able to use in the paleostress analysis, the structures were

separated based on their relative chronology methods such as abutting relationships. For example, many tectonic stylolites yielding NNE-trending compression axis end towards the tectonic stylolites yielding nearly E-W to NW-trending compression directions. On the otherhand, some tectonic stylolites yielding nearly E-W to NW-trending compression direction end towards the tectonic stylolites that give nearly NNE-trending compression directions (Figure 33). Based on these, first dominantly NNW-trending compression directions (event-1) was replaced by the nearly E-W to NW-trending compression direction (event-2). Later, nearly E-W to NW-trending compression direction (or event-2) has been replaced by the NNE-trending compression direction (or event-3). This is also evidenced by at least one recorded regional angular unconformity between Quaternary Lahti Group and pre-Quaternary units inside the study area (Figure 5) and two different regional angular unconformities between (1) Early Pliocene and pre-Early Pliocene units, (2) between Pliocene and Quaternary units inside the basins surrounding the Altıntaş basin (Rojay et al. 2002; Boulton and Roberston, 2008; Yusufoglu, 2013; İmamoğlu, 1993; Çemen et al. 1990a, b) (Figure 3). This is also supported by some other indicators observed in a particular station and its close vicinity such as folds, faults, tension gashes, conjugate shear fractures and cross-cutting slicken-lineations observed on the same fault planes in the nearest stations (Appendix-A). All these findings will be discussed in detail in the following sections inside this chapter.

3.1.3.3. Conjugate Shear Fractures

The Conjugate shear fractures develop as a result of compressive stresses (Figure 31) (Dunne and Hancock, 1994). The bisector of the acute angle of the conjugate shear fractures is parallel to the operation direction of the maximum principal stress axis (Dunne and Hancock, 1994). Therefore, these structures are reliable markers for the local stress analysis. The conjugate fracture are also widespread features observed in the study area (Figure 36).

Consequently, both the linear and planar parameters, such as the strike, dip amount to direction, length, width and fill type, of the above-mentioned mesoscopic features (tension gashes, stylolites and shear fractures) were measured during the field geological mapping and then they altogether were used in paleostress analysis (Figure 31).

No direct aging could be assigned to the conjugate shear fractures due to lack of data. In addition to this, no geological relative aging could be found during the field studies. The separation is only based on (1) other relatively well-constrained indicators such as tension gashes and slip plane data in the same station such as station-3 (ST-3) and (2) regional stress conjecture in the nearest stations.

Then, the relatively dated stylolites, tension gashes and conjugate shear fractures were assumed to develop in relation to some differing well-constrained deformation phases observed in surrounding basins of the Altıntaş basin (Figure 3). This is evidenced by the stratigraphic and structural data as discussed in detail the previous page.

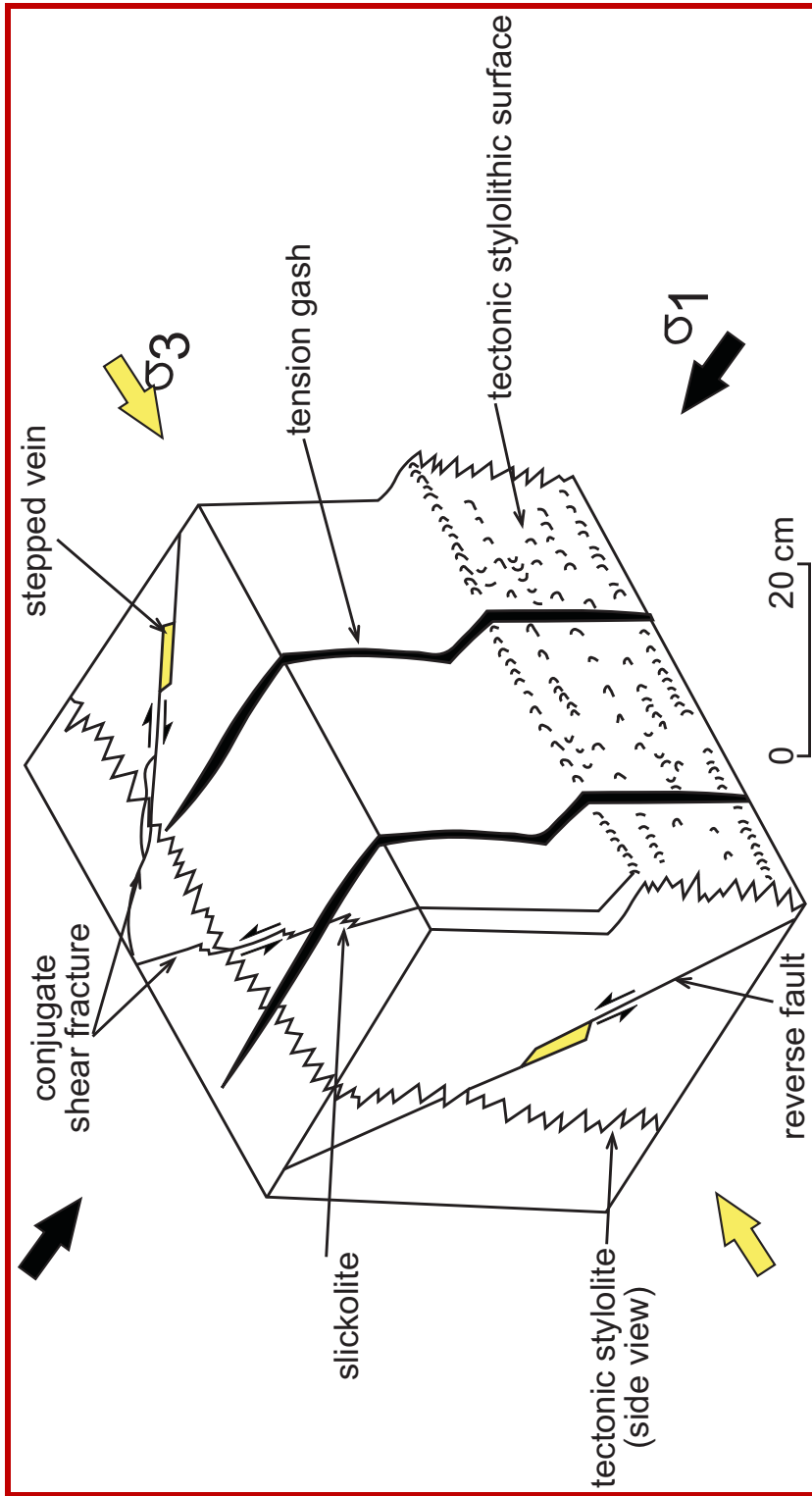


Figure 31. A block diagram the relationship between local stress and mesoscopic structures such as tension gashes, stylolites and shear fractures (modified from Eyal and Reches, 1983).

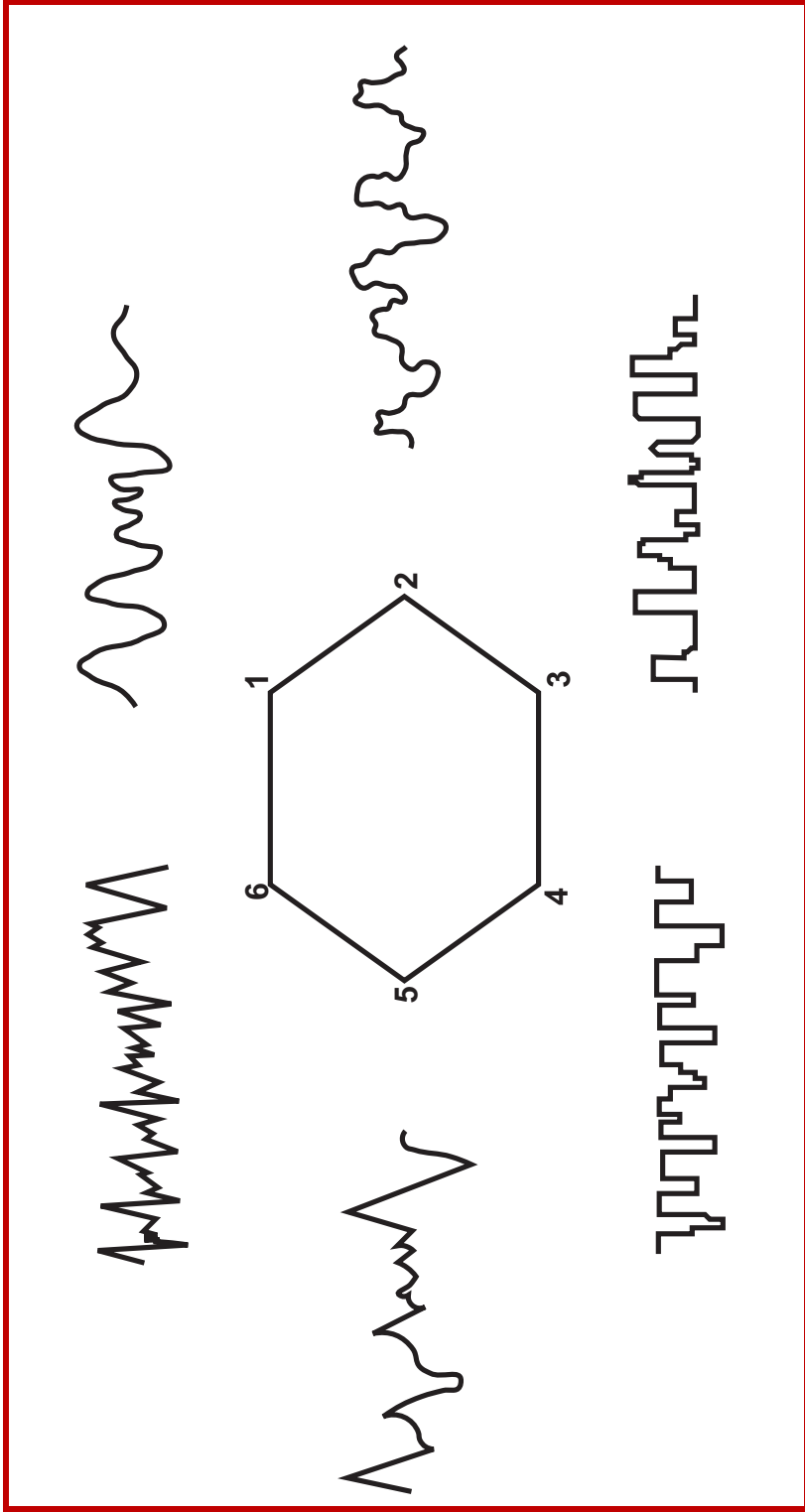


Figure 32. Classification of stylolites according to pure geometry. (1) Simple or primitive wave-like type, (2) Sutured type, (3) Up-peak type (rectangular type), (4) Down-peak type (rectangular type), (5) Sharp-peak type (tapered and pointed), (6) Seismogram type (Redrawn from Park and Scot, 1968).

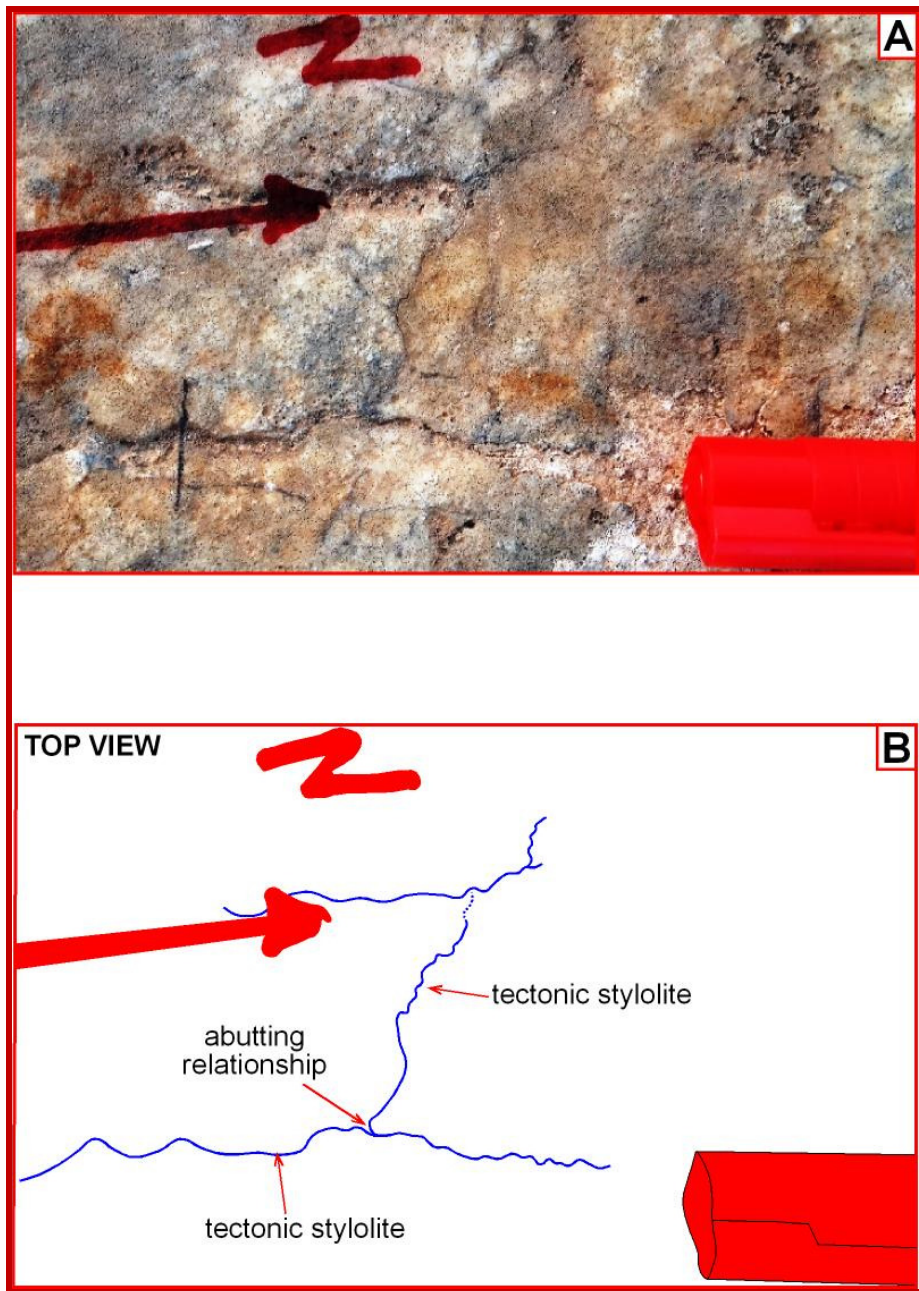


Figure 33. General view of two stylolite presenting abutting relationship nearly 1.5 km NE of Köklüce Village (Araban-Gaziantep).



Figure 34. General view of some bedding parallel (or diagenetic) stylolites nearly 1 km NE of Köklüce Village (Araban-Gaziantep).

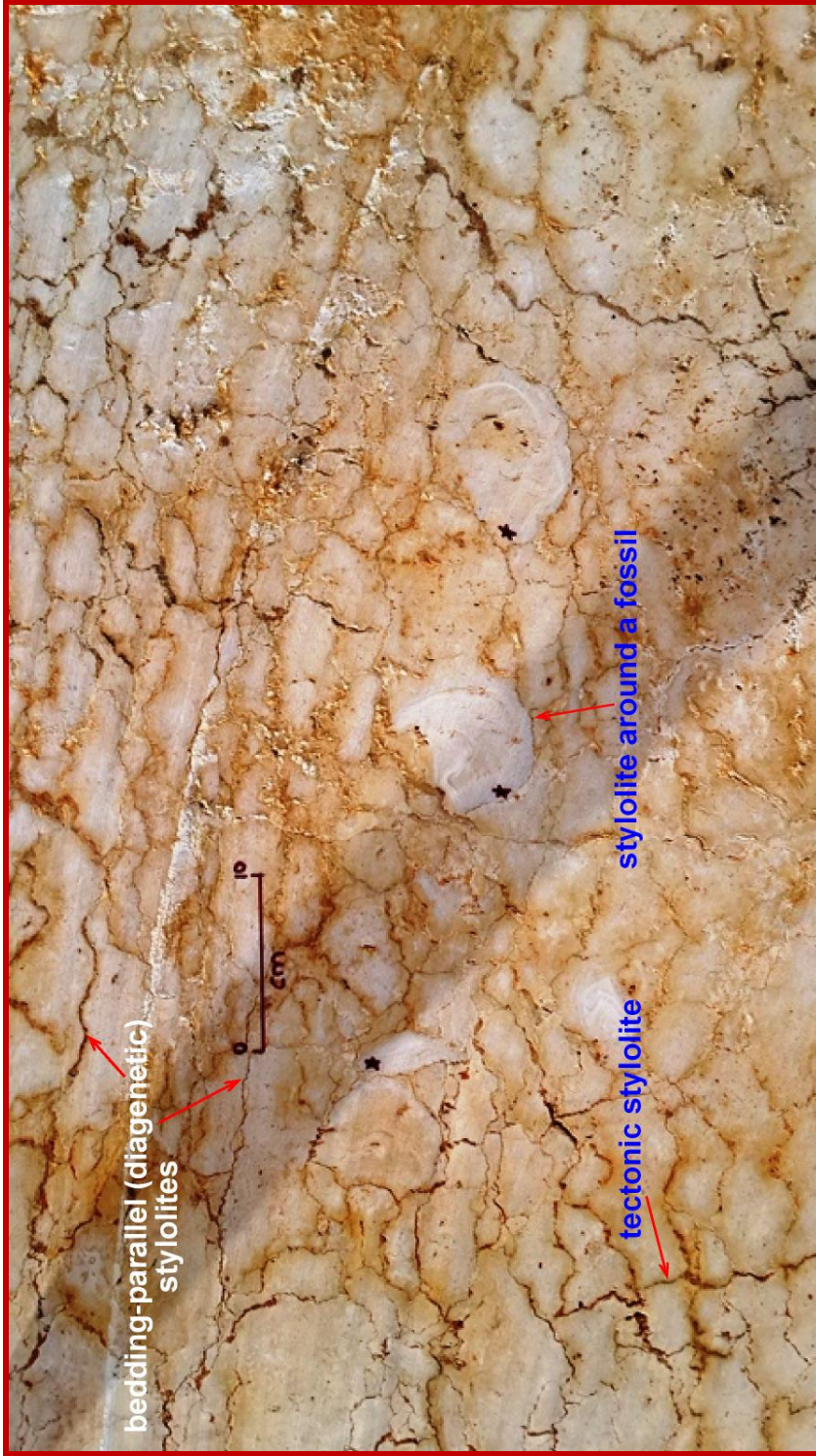


Figure 35. General view of tectonic, diagenetic and the stylonites developed around of nearly rounded objects located nearly several hundreds meters west of Köklüce Village (Araban-Gaziantep) (This photo has been taken from a vertical Wall of a stone quarry).

3.2.4. Macroscopic Structures

3.2.4.1. Folds

Attitudes (strike and dip amounts) of numerous beds belonging to the Middle Miocene-Early Miocene Midyat Group (the Hoya, Gaziantep and Firat Formations), the Latest Oligocene-Early Miocene Cingife Formation and the Middle Miocene-Early Pliocene Şelmo Formation were measured for the fold analysis during the field study. Additionally, same kind of data collected and reported in previous workers (Geophoto Services, Inc. Denver Colorado, 1958; Ayazoğlu, 1958; Tertemiz, 1958; Peksu, 1976; Çemen, 1987; Sonel and Sarbay, 1988; Ulu et al. 1991) have also been compiled, rectified and then inserted on our final geological map (Appendix-A). Later, all these compiled data were analyzed and evaluated. After the evaluation, the folds were classified into three categories based on the general trends of the fold axes. They are (1) E-W-trending Fold System, (2) NNE to NW-SE-trending Fold System and (3) NE-SW-trending Fold System. These Fold Systems are described in detail below:

3.2.4.1.1. E-W-Trending Fold System

Several fold sets in this system were identified, mapped and named during the field geological mapping. These are the E-W trending Tilkiler, Suvarlı and the Karadağ fold sets. Various fold sets are illustrated in blue lines on the structural map (Appendix-A and Figure 37)



Figure 36. Field photograph showing a conjugate shear fracture exposed in the Çatboğazi area along the northern margin of the Altıntaş basin.

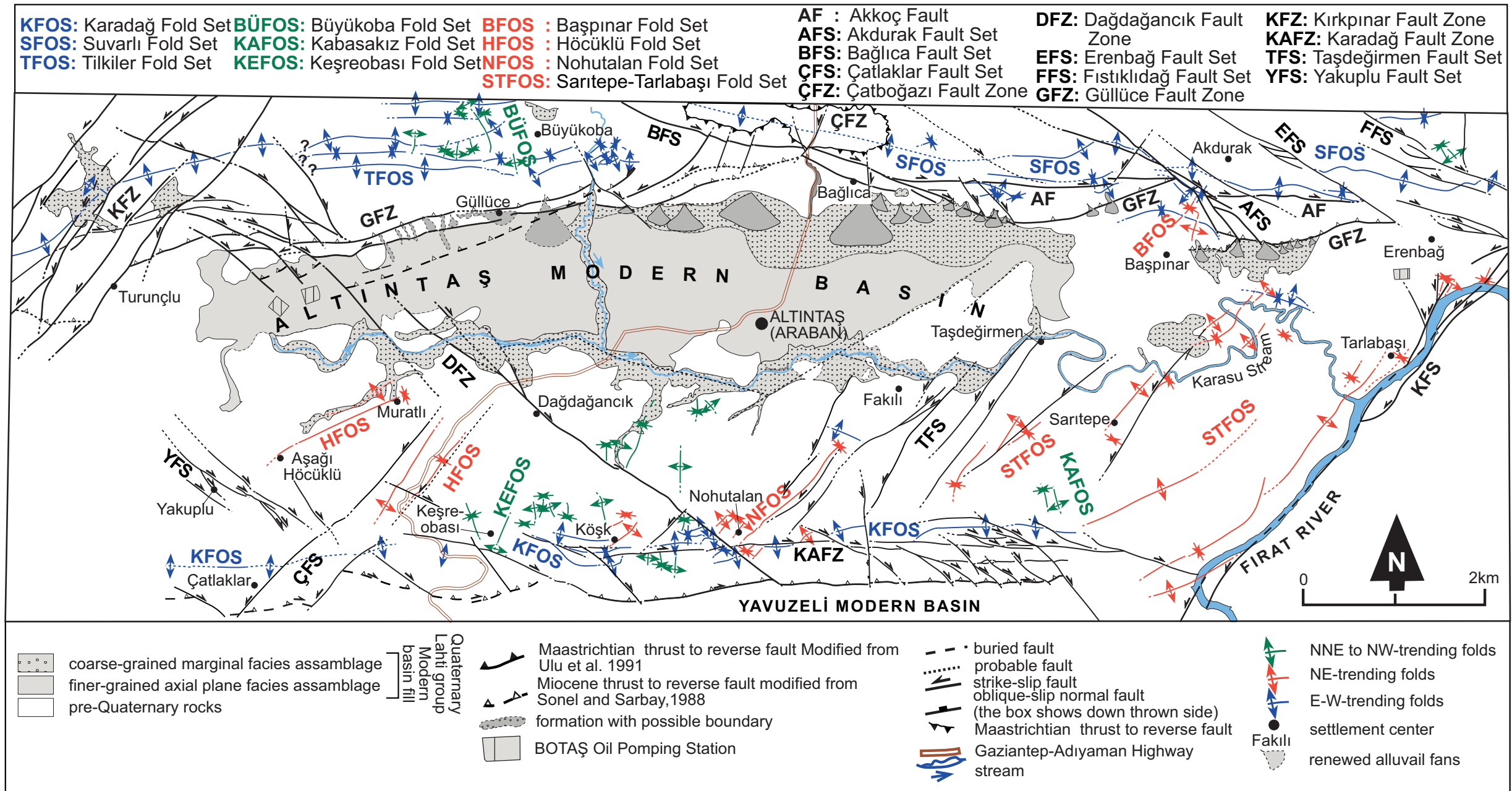


Figure 37. Simplified structure map of the study area.

3.2.4.1.1.1. Tilkiler Fold Set

This fold set is exposed well along the northwestern margin of the Aslantaş basin (Appendix-A, Figures 38, 39, 40 and 41). Some of the folds comprising the Tilkiler fold set were identified and reported by previous workers (Geophoto Services, Inc. Denver Colorado, 1958). Later (Peksu, 1976; Çemen, 1987; Yoldemir, 1987; Sonel and Sarbay, 1988; Ulu et al. 1991). Çemen (1987) has also named this fold set as a single fold (the Tilkiler Anticline) originated from the stresses operated in N-S direction.

The Tilkiler fold set is an about 2-5 km wide, 25 km long and E-W trending plastic zone of deformation located in the area between Çakallı village to the east and Çelikobası settlement to the west along the northern margin of the Altıntaş basin where it exists from the study area (Appendix-A). It consists of a series of parallel to sub-parallel anticlines and synclines with curved to curvi-linear axes. The wavelengths of folds range between 300 m and 2.5 km. However, the prominent wavelength is about 1 km. In general, folds are gentle based on the interlimb angle.

The Tilkiler Fold Set is cut and displaced in left-lateral (sinistral) direction by the fault segments comprising the Kırkpınar fault zone at the northwestern corner of the study area (Appendix-A). This sinistral offset and its amount are well-exposed in a locality outside the study area. It was measured to be 4.5 km by combining the maps presented in this study and earlier maps by (Ayazoğlu, 1958; Tertemiz, 1958).

The Tilkiler Fold Set developed widely within the Middle Eocene to Early Miocene Midyat Group, the Late Oligocene (?)–Early Miocene Cingife Formation and the Early Miocene stage 1 volcanics of the Yavuzeli Volcanics (Appendix-A). However, the youngest paleotectonic rock unit (the Middle Miocene–Early Pliocene Şelmo Formation) also seems to have been affected from this folding. This is also proved by the regional angular unconformity between the nearly horizontal modern basin fill (the Lahti group) and the underlying deformed (folded

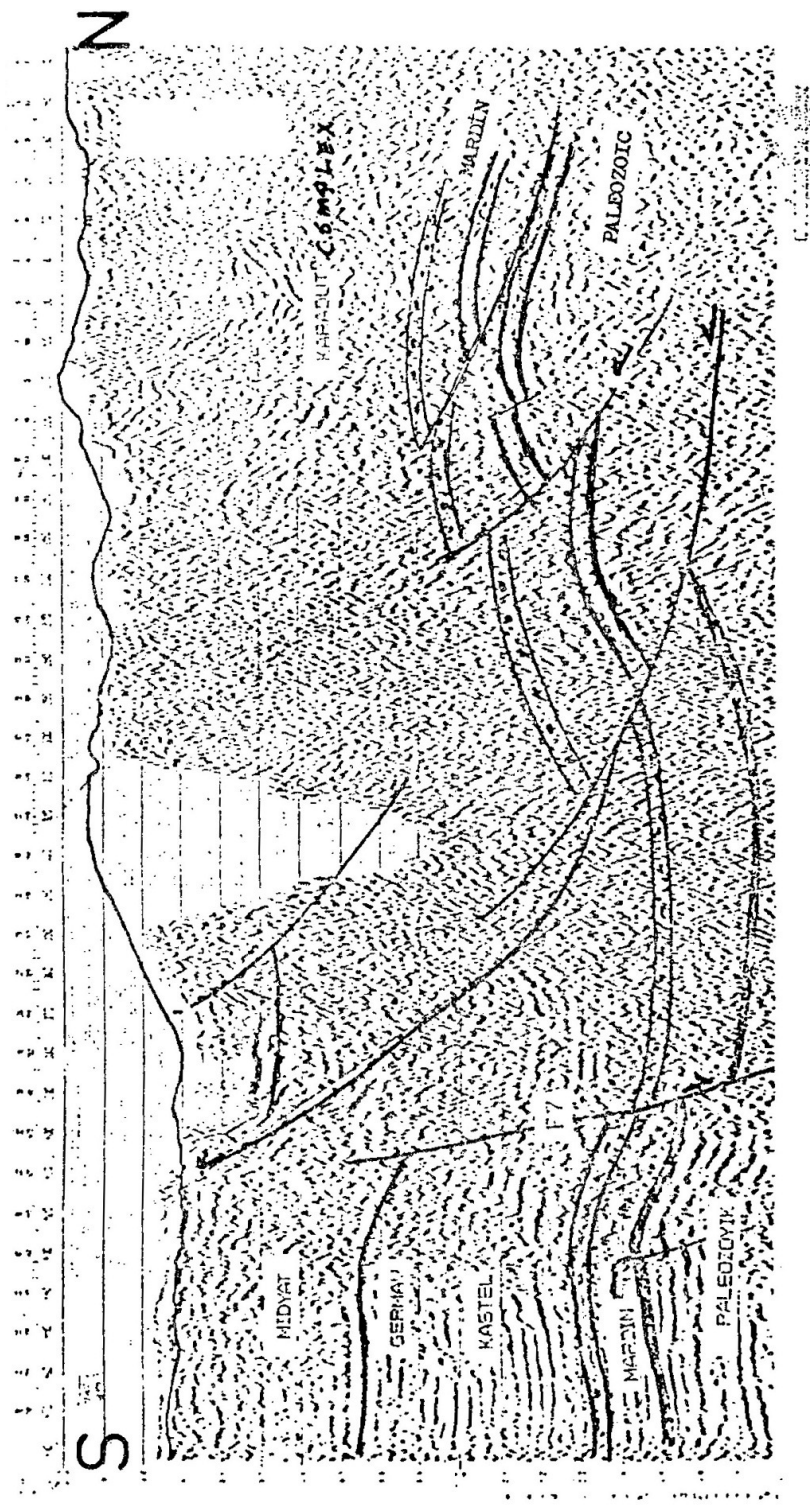


Figure 38. Unsimplified GAD-86-303 seismic section illustrating contact relationships among various rock units and the sub-surface structure of the Altıntaş basin (Adapted from Sonel and Sarbay, 1988).

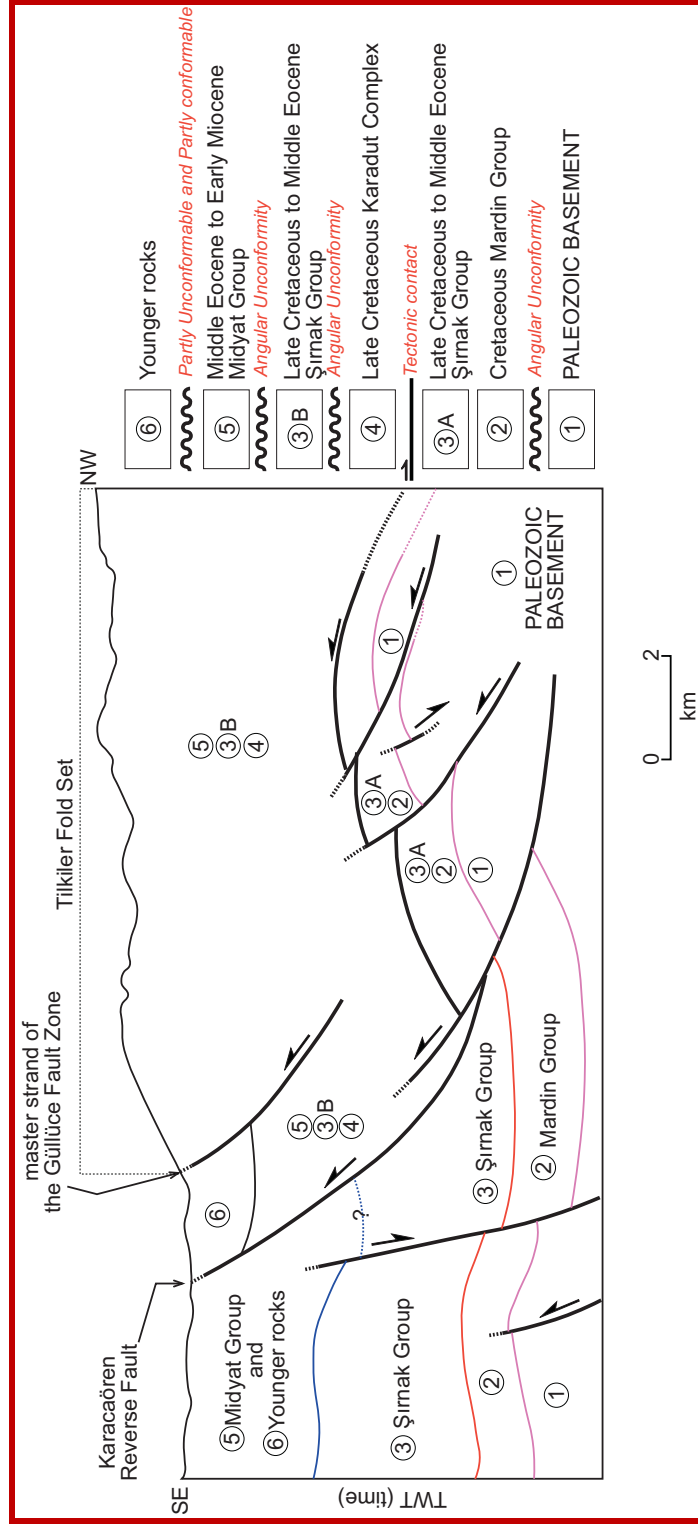


Figure 39. GAD-86-303 seismic section illustrating contact relationships among various rock units and the sub-surface structure of the Altıntaş basin (Modified from Sonel and Sarbay, 1988).

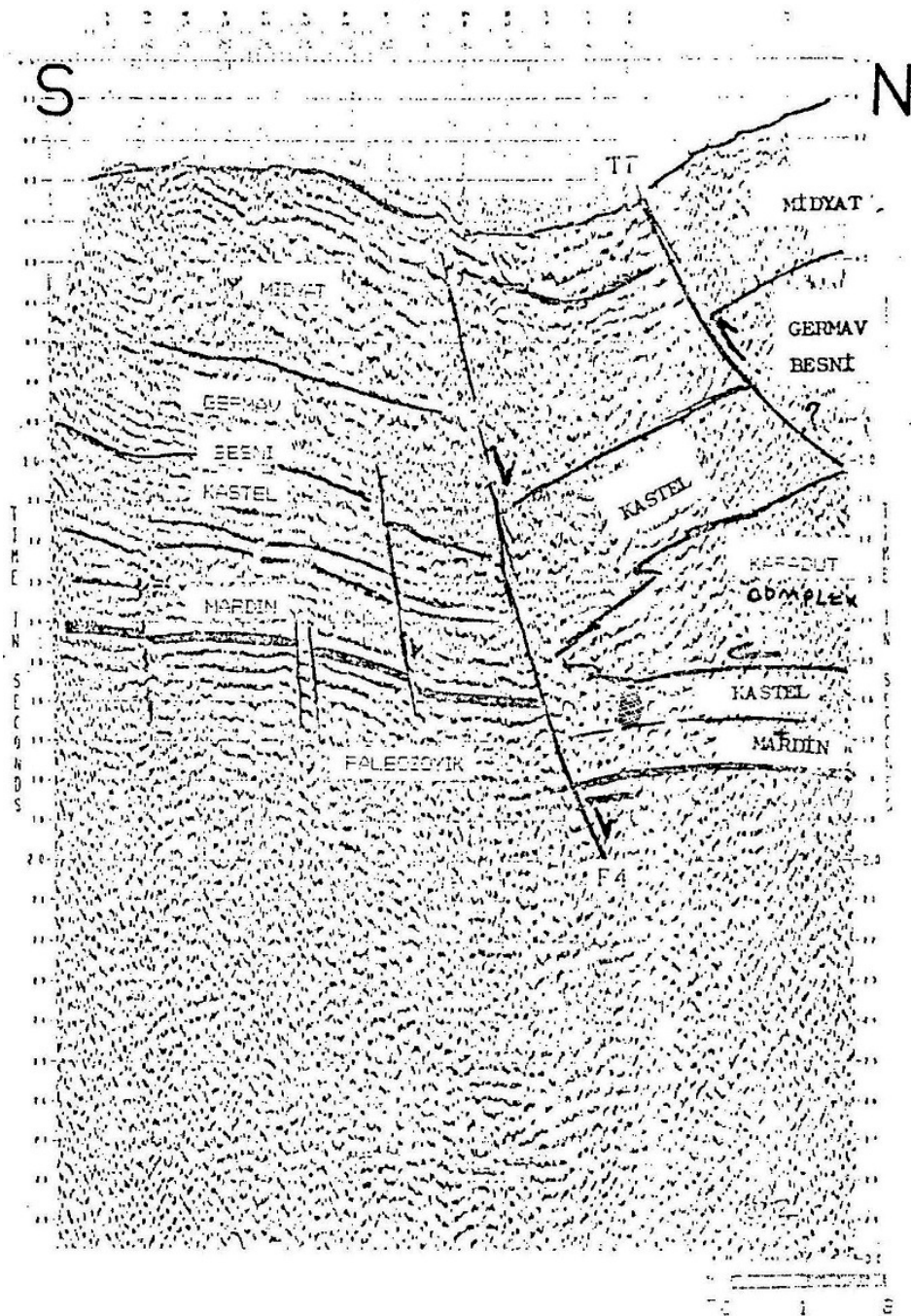


Figure 40. Unsimplified GAD-86-102 seismic section illustrating contact relationships among various rock units and the sub-surface structure of the Altıntaş basin. (Adapted from Sonel and Sarbay, 1988).

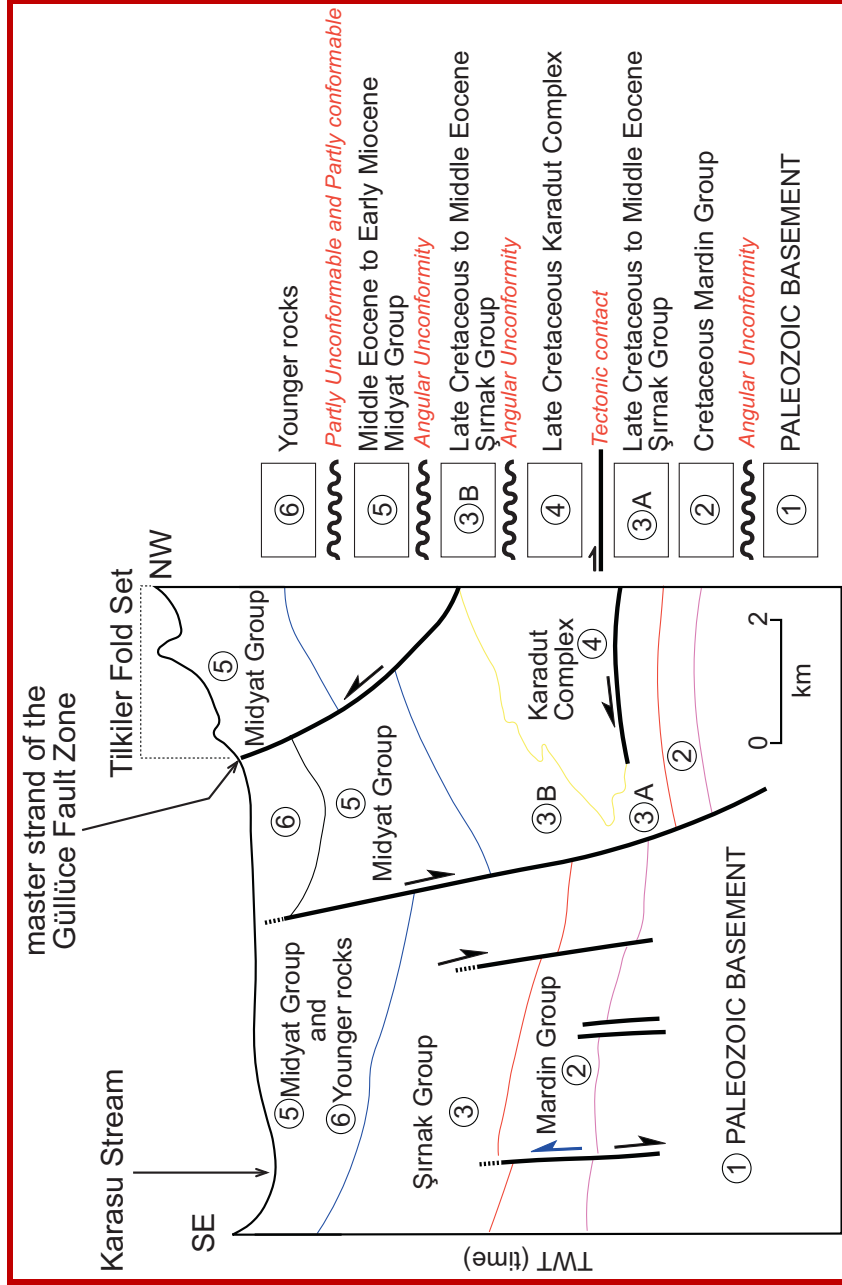


Figure 41. GAD-86-102 seismic section illustrating contact relationships among various rock units and the sub-surface structure of the Altıntaş basin. (Modified from Sonel and Sarbay, 1988).

and faulted) Şelmo Formation (Appendix-B). Consequently, except for several shorth-term stratigraphic gaps, the sedimentation is continues from Eocene to Early Pliocene. Therefore, the folding process seems to have occurred in the Late Pliocene.

3.2.4.1.1.2. Suvarlı Fold Set

This structure was first reported as the “Suvarlı Anticline” by previous workers (Peksu, 1976; Çemen, 1987; Yoldemir, 1987; Ulu et al. 1991). However, detailed field geological mapping carried out in the frame of the thesis study indicated that the “Suvarlı Anticline” is not a single structure. Instead, it consists of several anticlines and synclines with axes trending in approximately E-W direction.

The Suvarlı Fold Set is exposed well at the north-northeast corner of the study area (Appendix-A). It occurs in about 10 km wide, 50 km long and approximately E-W trending plastic zone of deformation. However, it continues to the north and east but outside the study area. The Suvarlı fold set consists of several parallel to sub-parallel, closely-spaced anticlines and synclines with curved to curvi-linear axes of en-echelon pattern. The wavelengths of folds range between a few hundreds meters to 2 km, however, the prominent wavelength is about 1.5 km. Folds are gentle based on the interlimb angle.

The Suvarlı fold set is cut and displaced up to 4.3 km in dextral direction by both the Akdurak and Erenbağ fault sets (Appendix-A). This is determined by the comparison of the tips of fold axes on both blocks of the fault set

The Middle Eocene-Early Miocene Midyat Group, the Middle Miocene Stage 2 Volcanics of the Yavuzeli Volcanics and the Middle Miocene-Early Pliocene Şelmo Formation have been deformed into a series of anticlines and synclines comprising the Suvarlı fold set (Appendices-A and B and Figure 42).



Figure 42. Field photograph illustrating an anticline comprising the Suvarlı Fold Set (view towards, SE, nearly 1.5 km SE of the Kesmetepe Village located nearly 5 km north of the Altıntaş basin).

The single unit, which has not been affected from folding is the Quaternary modern basin fill (the Lahti group) (Appendix-B). This reveals that the folding processes terminated in a time before Quaternary.

3.2.4.1.1.3. Karadağ Fold Set

This is the third set of folds comprising the E-W trending fold system. This structure was first identified by Geophoto Services, Inc. Denver Colorado (1958). Later on, it was studied in more detail by Çemen (1987). He subdivided the Karadağ fold set into 7 major and independent anticlines and the intervening synclines. Detailed field studies carried out during the present study clearly showed that so called “Karadağ Anticline” is not a single anticline, instead, it is more complicated structure including a series of very complex anticlines and synclines with varying trends and characters (Appendices-A and B).

The Karadağ Fold Set is about 10 km wide, 40 km long and ~E-W trending plastic zone of deformation located along the southern margin of the Altıntaş basin (Appendices-A and B). Based on the interlimb angles, folds comprising the Karadağ fold set are gentle in form (Figures 43, 44, 45, 46, 47, 48 and 49). The Karadağ Fold Set is cut and displaced by a fault zone and several single faults such as the Dağdağancık Fault Zone and Çukuryurt, Çatlaklar, Küçükkarakuyu faults (Appendices-A and B). Total offset amounts measured along these faults range from 0.4 km to 1.5 km.

All of the pre-Quaternary rock units have been deformed into a series anticlines and synclines comprising the Karadağ fold set. These deformed (folded and faulted) rock-stratigraphic units are overlain with an angular unconformity by the Quaternary modern basin fill. Both the mode of deformation and the angular unconformity reveal strongly the folding processes terminated in a time slice before early Quaternary. Based on the orientation of the fold axes, the Karadağ fold set seems to have formed by a N-S shortening. The sub-surface structures as

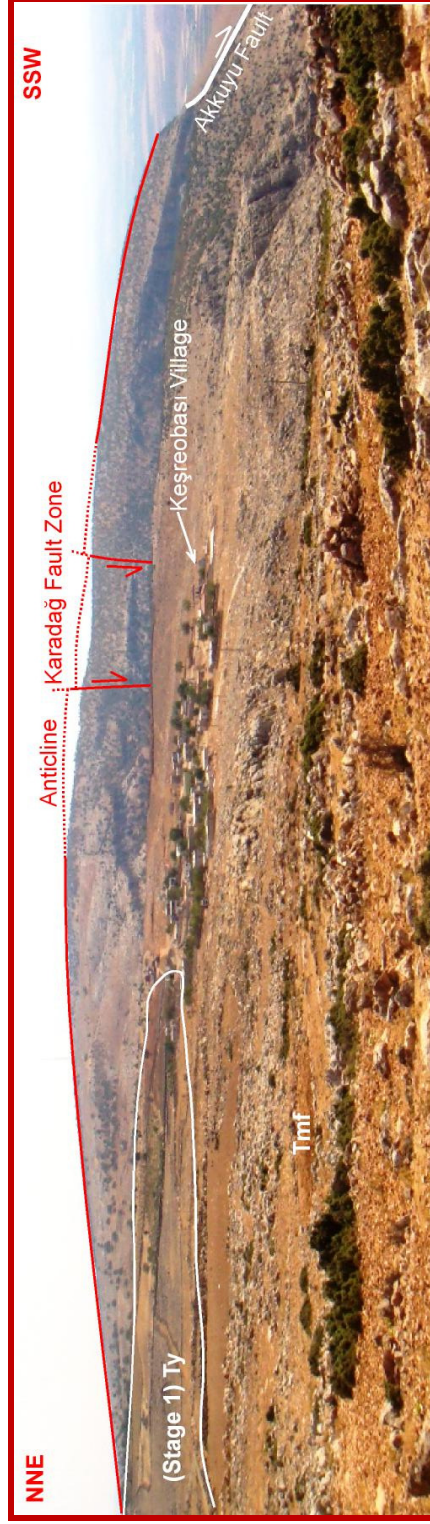


Figure 43. Field photograph illustrating an anticline comprising the Karadağ Fold Set (view towards ESE, nearly 1.5 km W of Keşreobası Village located southwestern margin of the Altıntaş basin).

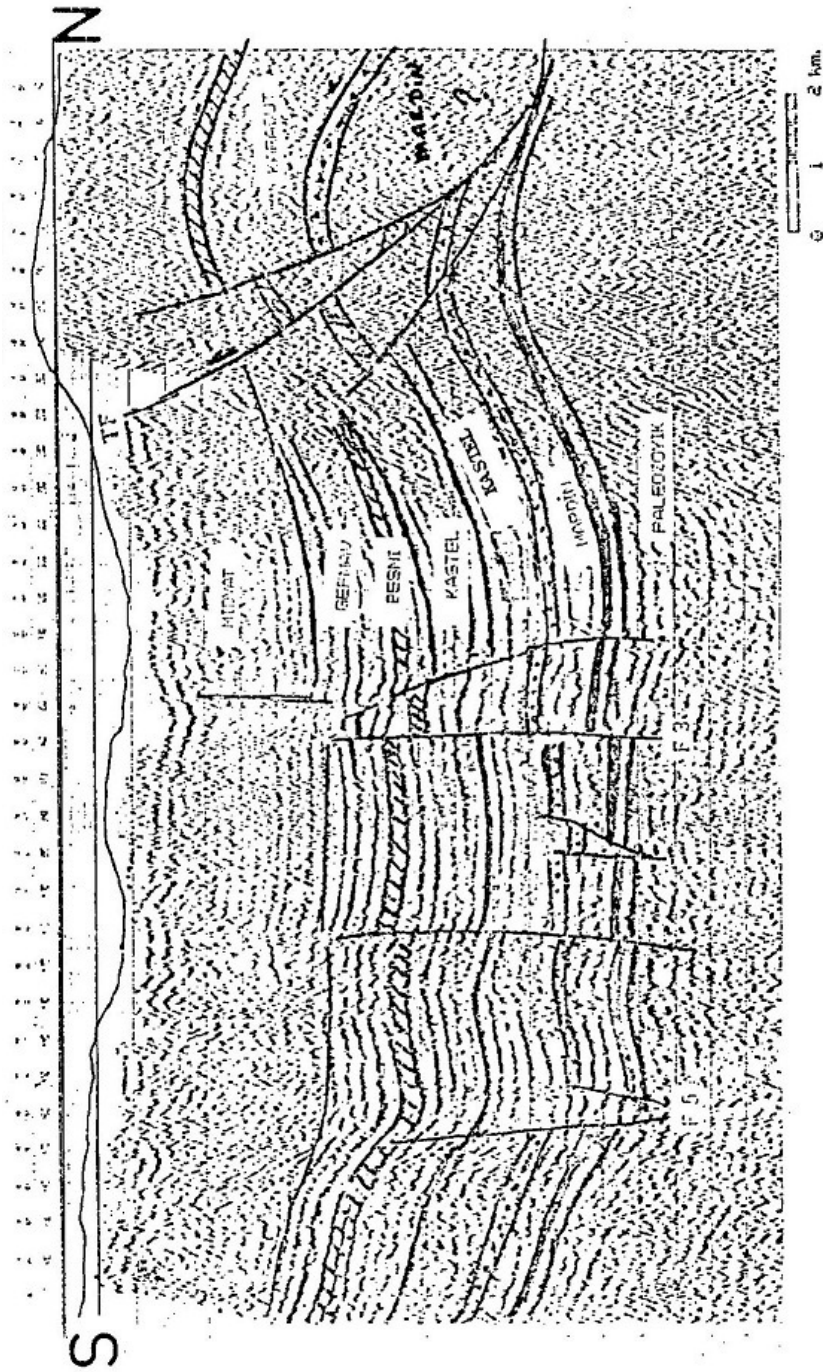


Figure 44. Unsimplified GAD-86-102 seismic section illustrating contact relationships among various rock units and the sub-surface structure of the Altıntaş basin. (Modified from Sonel and Sarbay, 1988).

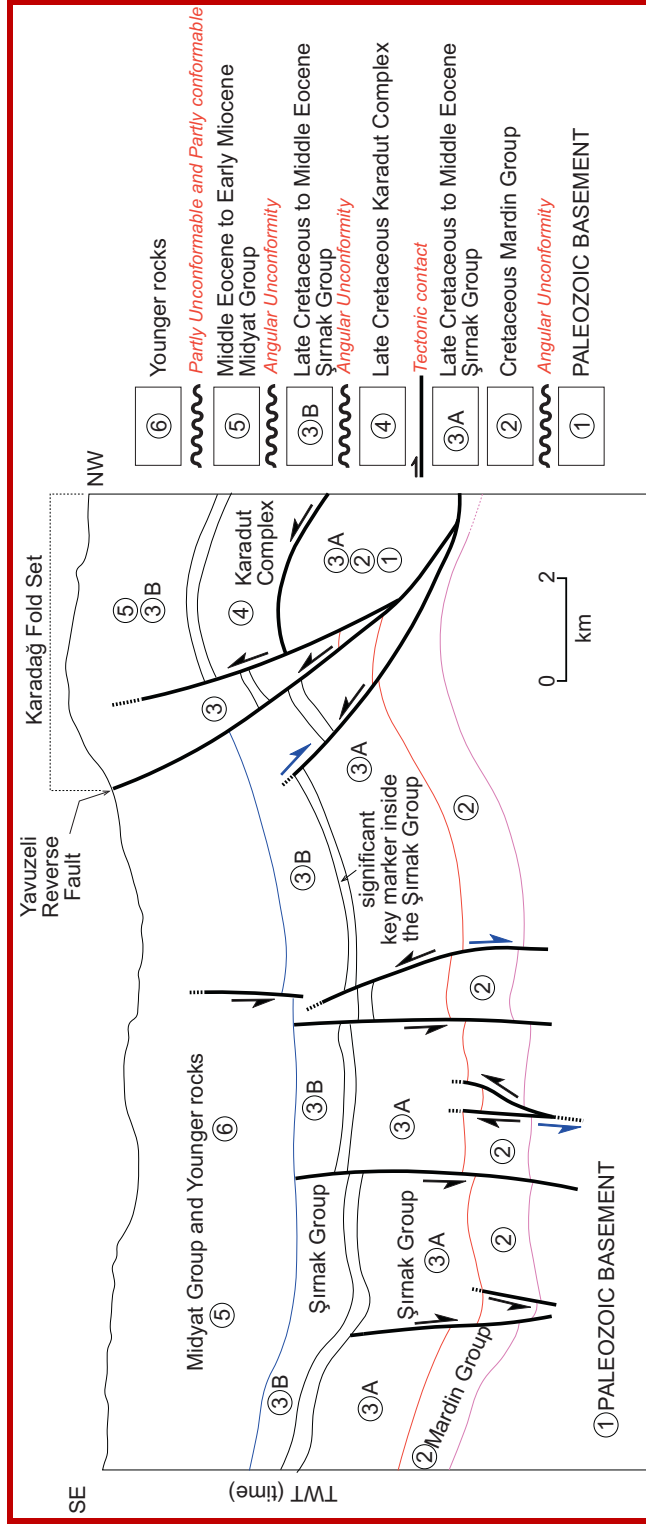


Figure 45. GAD-87-206 seismic section illustrating contact relationships among various rock units and the surface structure of the southwestern margin of the Altıntaş basin (Modified from Sonel and Sarbay, 1988).

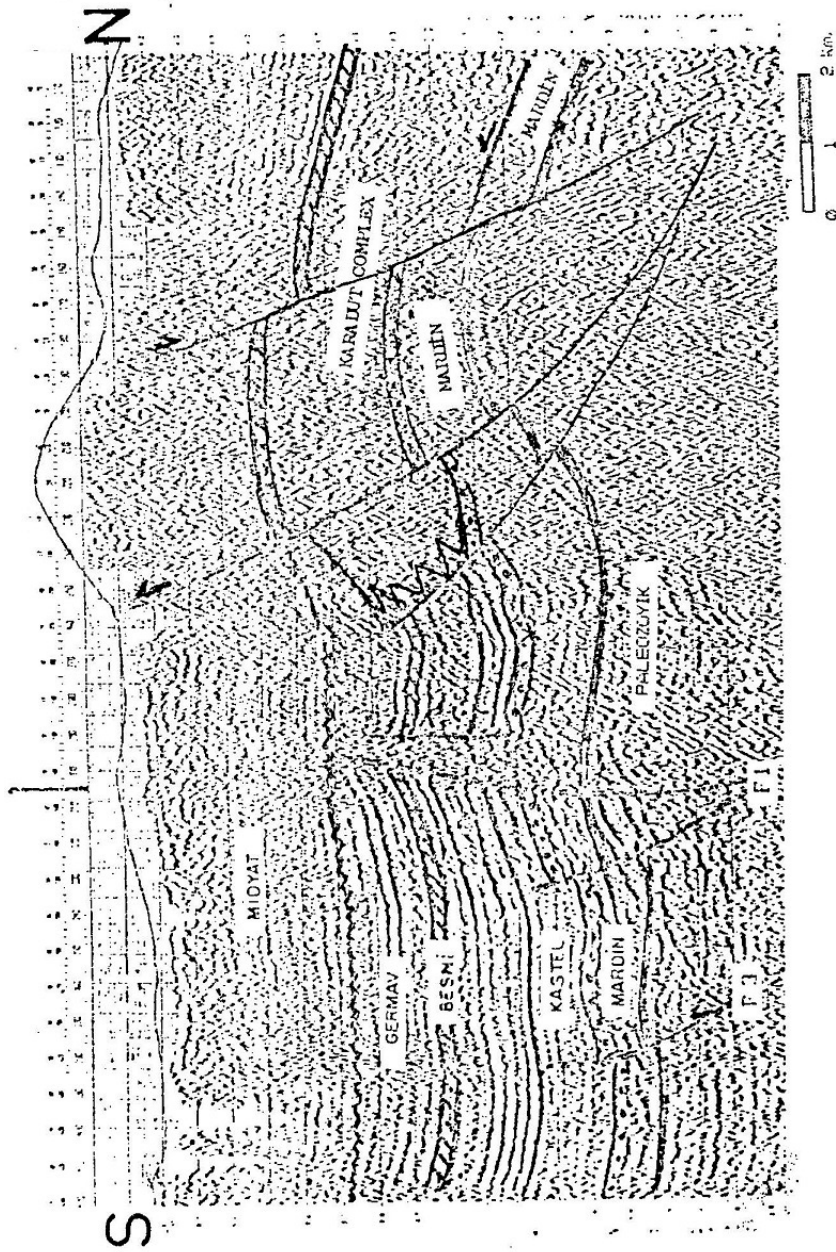


Figure 46. Unsimplified GAD-87-206 seismic section illustrating contact relationships among various rock units and the sub-surface structure of the southwestern margin of the Aluntaş basin (Adapted from Sonel and Sarbay, 1988).

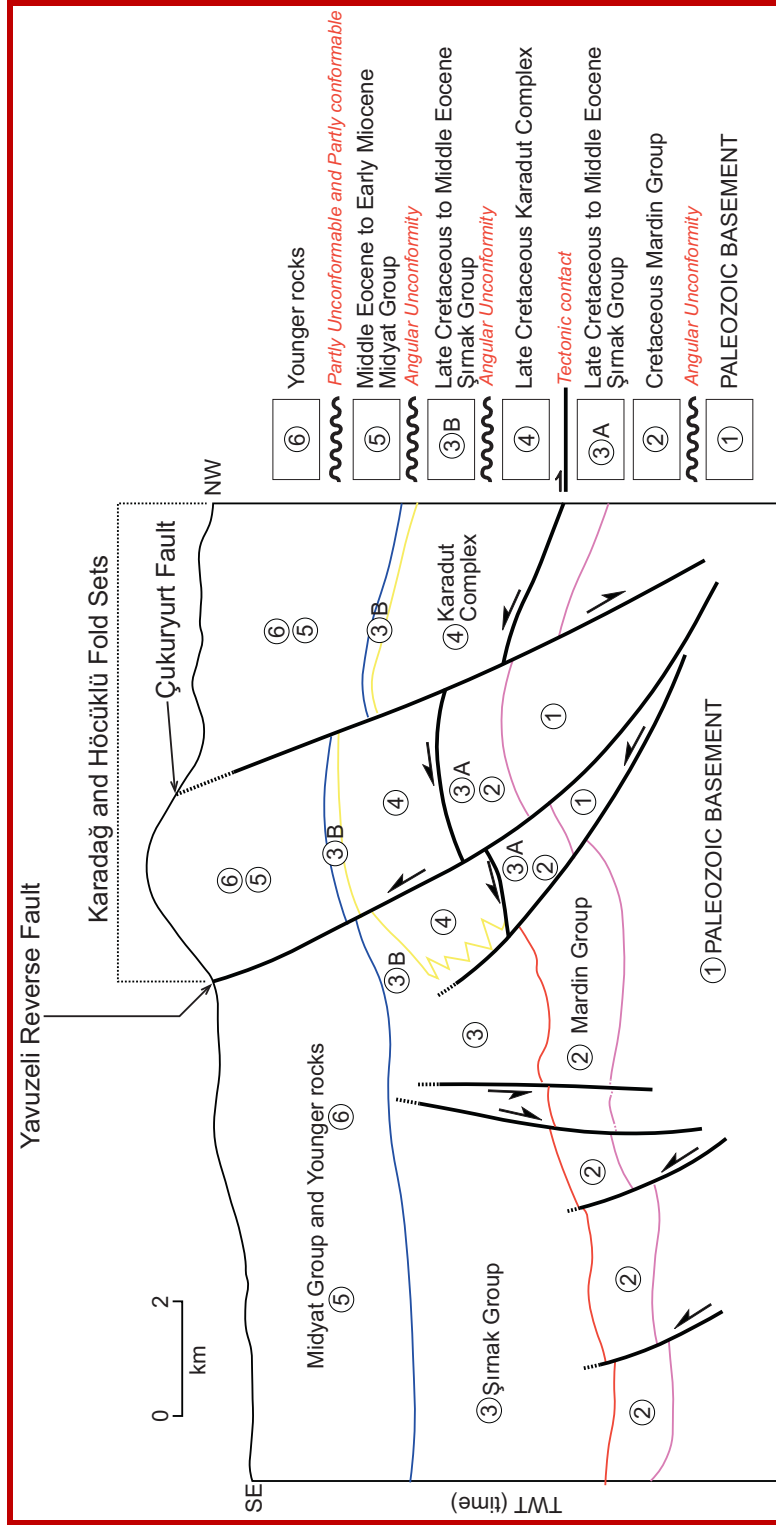


Figure 47. GAD-86-312 seismic section illustrating contact relationships among various rock units and the subsurface structure of the southwestern margin of the Altıntaş basin (Modified http://www.getfilings.com/sec-filings/120628/TRANSATLANTIC-PETROLEUM-LTD_8-K/d374244dex991.htm).

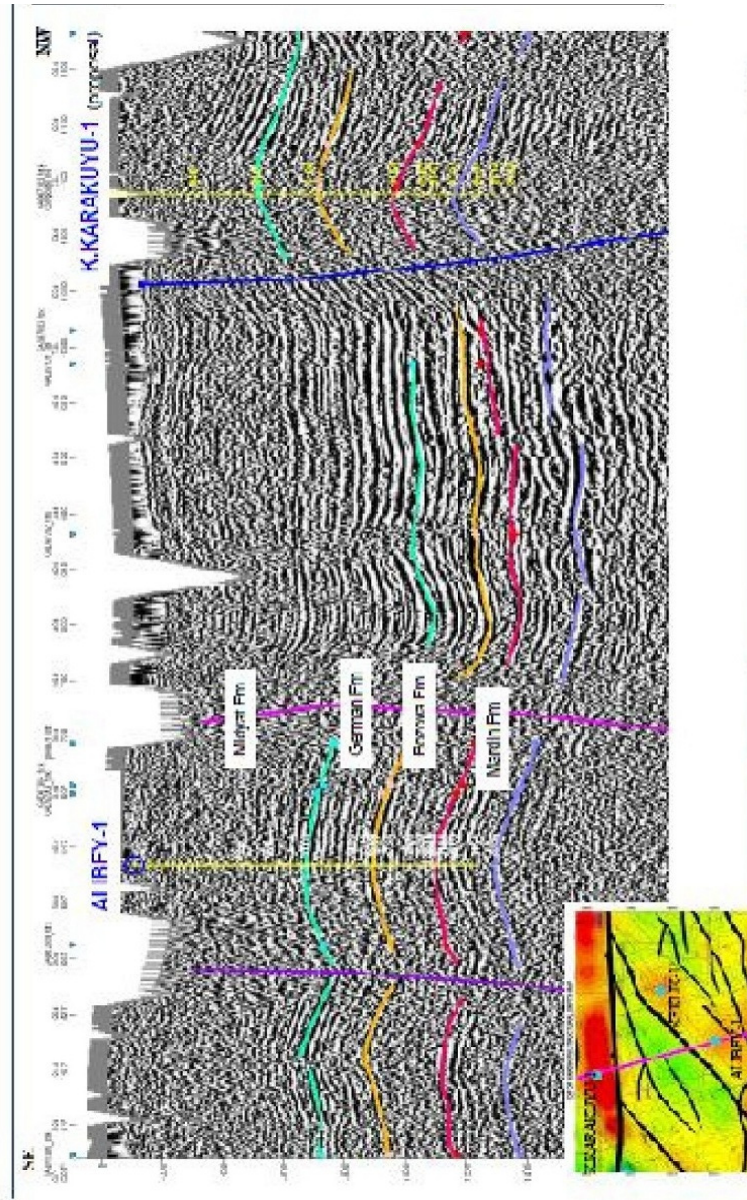


Figure 48. Unsimplified GAD-87-201 seismic section illustrating contact relationships among various rock units and the sub-surface structure of the southwestern margin of the Altınbaş basin (Modified [http://www.getfilings.com/sec-filings/120628/ TRANSATLANTIC-PETROLEUM-LTD_8-K/d374244dex991.htm](http://www.getfilings.com/sec-filings/120628/TRANSATLANTIC-PETROLEUM-LTD_8-K/d374244dex991.htm)).

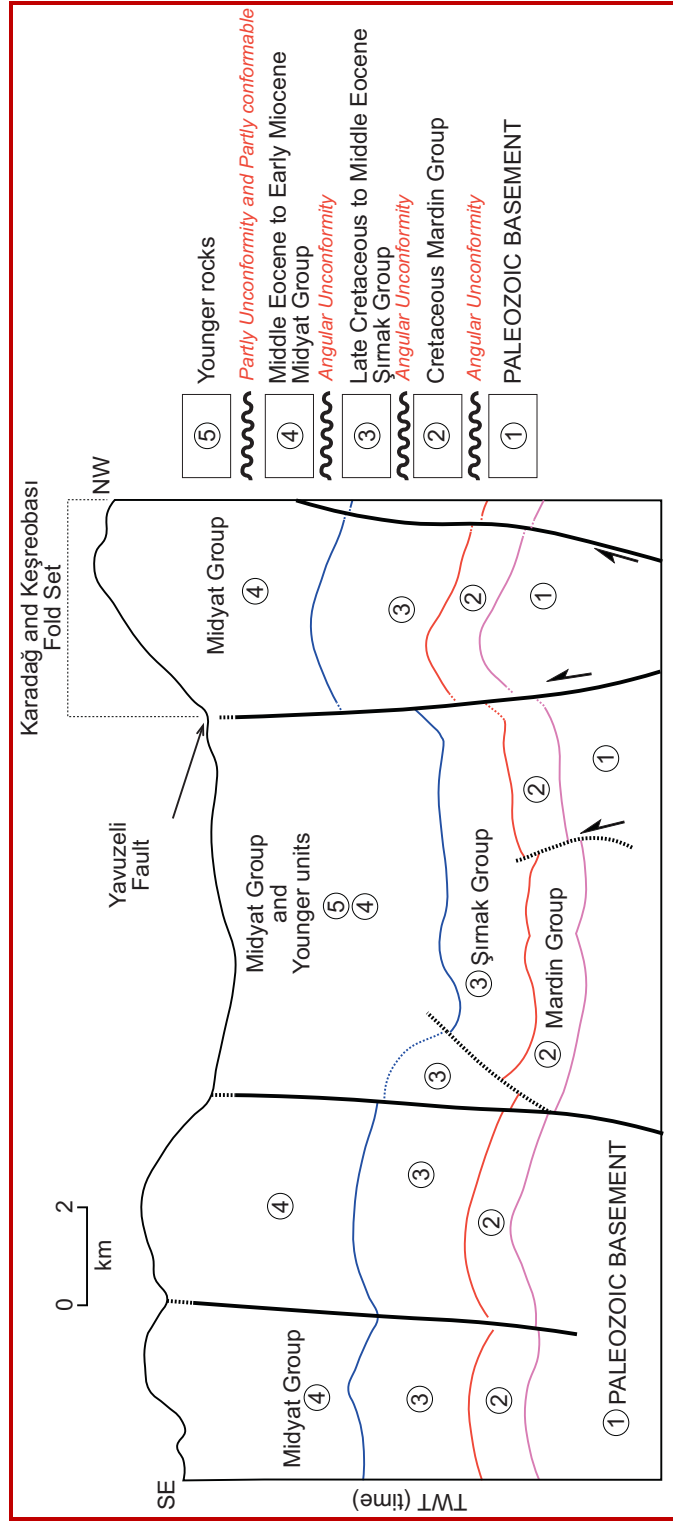


Figure 49. GAD-87-201 seismic section illustrating contact relationships among various rock units and the subsurface structure of the southwestern margin of the Altıntaş basin (Modified http://www.getfilings.com/sec-filings/120628/TRANSATLANTIC-PETROLEUM-LTD_8-K/d374244dex991.htm).

seen in seismic sections, it can also be said that this fold set may be a fault-propagation fold in origin (Figures 44, 45, 46, 47, 48 and 49).

3.2.4.1.2. NNE and NW-Trending Fold System

This fold system is not widespread with respect to the E-W-trending fold system (Appendix-A). It consists of three fold sets. They are the Keşreobası, Kabasakız and the Büyükoba fold sets. They occur in a relatively limited areas on both the southern and the northern margins of the Altıntaş basin (Appendix-A). The folds comprising the Keşreobası fold set were previously identified and reported by Geophoto Services, Inc. Denver Colorado (1958). However, they were identified and analysed well in the frame of our study. The Keşreobası fold set is an about 5 to 6 km wide, a few kilometers long and NNE- to NW-trending plastic zone of deformation exposed around the Keşreobası and Köşk settlements along the southwestern margin of the Altıntaş basin (Appendix-A and Figure 37). However, the prominent trend is ~N-S. The Keşreobası fold set consists of a series of anticlines and synclines with short wavelength, which ranges between 0.3 and 2 km, while it is 0.5-0.6 km as an average. Folds comprising the Keşreobası fold set are gentle in form based on the interlimb angle.

The Kabasakız fold set occurs in a local area south of Yukarıgözey settlement along the south-southeastern margin of the Altıntaş basin (Appendix-A and Figure 37). It is an about 1 km wide, a few kilometers long and NNW-trending plastic zone of deformation. It consists of a few anticlines and synclines with short wavelengths of 700 to 800 m. Folds comprising the Kabasakız fold set are gentle in form based on their interlimb angles.

The Büyükoba fold set is an about 4 km wide and NNW- to NNE-trending plastic zone of deformation exposed around Büyükoba Village along the northern margin of the Altıntaş basin. It consists of several anticlines and synclines with wavelengths of 500-600 m. Folds are gentle in form based on interlimb angles.

In general, all of folds comprising the Keşreobası, Kabasakız and the Büyükoba fold sets are relatively local, display short wavelength and gentle in form. They developed in the pre-modern basin fill such as the Midyat Group, the Cingife Formation and Şelmo Formations, i.e., these rock-stratigraphic units were deformed into also NNE- and NW-trending fold system (Appendix-A). These folds seem to have developed by an approximately E-W shortening based on the orientations of fold axes. However, their origins were also attributed to the normal faulting related rollover anticlines and the strike-slip related deformation (Çemen, 1987). This is observed in a few localities.

The field studies suggest that the smaller-scale E-W-trending folds are located inside the larger anticlines (or anticlinorium). The E-W-trending anticlinoriums are typically bounded by thrust to reverse faults as evidenced by the published and unpublished seismic sections (Figures 38, 39, 40, 41, 44, 45, 46, 47, 48 and 49 and Niyazi TOK, personal communication). However, these faults are not directly observed on the surface during the field studies. In addition, the anticlinoriums are typically asymmetrical folds verging towards south. Furthermore, the backlimb length to forelimb length ratios is high up to “5”. All these findings indicate that the E-W-trending anticlinoriums should have developed as fault-propagation fold. On the other hand, the extensive field data suggest that some of the smaller-scale folds inside the anticlinoriums seem to develop away from the major thrust to reverse faults (Appendix-A and Figure 37). This finding suggests that majority of the smaller-scale folds might have developed as classical buckle fold originated from the bed-parallel operation direction of major principal compressive stress. This is also supported by the existence of many tectonic stylolites and conjugate shear fractures observed inside the study area (Appendix-A, ST-3, 6, 10, 17, 18 and ST-23). Moreover, these findings are also supported by slip-plane analysis (Appendices A, ST-3, 5, 14, 15, 19, 28a). All these findings indicate that all of the E-W-trending folds should have developed due to nearly N-S-trending contractional deformation during or after the

Early Pliocene but prior to Quaternary time. This is because, these folds affect all of the units except Quaternary Lahti Group (Appendix-A)

3.2.4.1.3. NE-Trending Fold System

This is the another widespread and regional-scaled paleotectonic structure. It is widely exposed along the south and southeastern margins of the Altıntaş basin. This fold system also continues to the east and outside the study area (Çemen, 1987). The NE-trending fold system consists of four sets of folds. These are the Aşağıhöcükli, Nohutalan, Saritepe-Tarlabaşı and Başpınar fold sets (Appendix-A and Figure 37). Some of folds comprising these sets were previously identified and reported by Geophoto Services, Inc. Denver Colorado (1958) and Çemen (1987). However, the most of them were determined and analyzed in the frame of the present study.

The Aşağıhöcükli fold set is an about 5 km wide, 2-5 km long and NE-trending plastic zone of deformation exposed well around Aşağıhöcükli-Muratlı-Küçükarakuyu areas along the south western margin of the Altıntaş basin (Appendix-A and Figure 37). This set of folds consists of a series of anticlines and synclines of dissimilar wavelengths. The wavelengths range between nearly 700 m to 1700 m. Folds are gentle in form based on their interlimb angle.

The second fold set comprising the NE-trending fold system is exposed well around the Nohutalan settlement along the southern margin of the Altıntaş basin (Appendix-A and Figure 37). It is the Nohutalan fold set. It is an about 2 km wide, 2-6.5 km long and NE-trending plastic zone of deformation. The Nohutalan fold set consists of a series of anticlines and synclines with short wavelength, which ranges between 700m and 900 m. Based on their interlimb angle, folds are gentle in form.

The third set of folds included in the NE-trending fold system is the Saritepe-Tarlabaşı fold set. It is more widespread and larger with respect to other sets of folds. The Saritepe-Tarlabaşı fold set is an about 9 km wide, nearly 3.5 to

18 km long and NE-trending plastic zone of deformation exposed well in the Güzey, Aşağıgüzey, Sarıtepe-Elifköy and Çifteköy areas along the southeastern margin of the Altıntaş basin (Appendix-A and Figure 37). It consists of a series of anticlines and synclines of dissimilar wavelengths. It ranges between 0.3-5 km in length. Folds are gentle in form based on the interlimb angle (Figures 50, 51 and 52).

The fourth and last fold set included in the NE-trending fold system is the Başpınar fold set. It is an about 1 km wide, 1-1.5 km long and NNE-trending zone of deformation exposed well in a relatively local area to the northeast of Başpınar village along the northeastern margin of the Altıntaş basin (Appendix-A and Figure 37). Başpınar fold set consists of one anticline and one syncline. They are gentle fold in form based on the interlimb angle.

Consequently, all of the fold sets comprising the NE-trending fold system developed in the rock-stratigraphic units of the Middle Eocene-Early Pliocene age and deformed intensively them (Appendix-A). The intensively deformed pre-Quaternary older basin fill seems to have accumulated in the pre-modern Altıntaş basin under the control of a compressive tectonic regime accompanying to the sedimentation. This intensively deformed older basin fill is overlain with an angular unconformity by the nearly horizontal modern basin fill of the Quaternary age. This relationship indicates that the development age of all of the fold system is the Late Eocene-Early Pliocene period (?).

The NW to NNE and NE-trending fold systems are typically symmetrical upright folds based on field studies. In addition, the backlimb lengths to forelimb length ratios are nearly "1". Moreover, they commonly developed away from some major faults, although a few are restricted to them. Furthermore, they display systematic character (Appendix-A). When all these findings are combined all together, these folds might have developed as contraction-related classical buckle fold. This is also supported by the analysis of Phase-1 and Phase-2 tectonic stylolites, conjugate shear fractures and slip-plane data suggesting E-W to NE-trending maximum principal stress axis (Appendix-A). On the other hand, some

monoclinical folds are observable on seismic sections and seem related with some faults with normal component (Figures 44 and 45). The attitudes of these folds can not be directly assigned due to 2D interpretations. In any case, they characteristically do not reach to surface and might be related to the events older than Eocene time. This is also supported by early reported regional Paleocene-Middle Eocene extension and related normal faulting inside and outside of the study area (e.g. Kaymakçı et al. 2010) Therefore, it is interpreted here that the majority of the NW to NNE-trending and NE-trending fold systems exposing inside the study area might have developed as typical buckle fold in relation to E-W to NW-trending strike-slip faulting-related contractional deformation.

The careful examinations of the folds indicate that the fold axis of the E-W-trending folds are curvilinear in shape (Appendix-A). On the other hand, the fold axis of NW to NNE and NE-trending folds are more linear in shape. In addition, the N-S-trending bedding planes are quite continuous although nearly E-W-trending bedding planes are discontinuous when they meet particularly just in the north of the ST-26 and Akkuyu Village to the south (Appendix-A). These findings suggest that N-S-trending folds are younger than the E-W-trending large-scale folds (Appendix-A). The available data suggest that previously N-S-trending pure contractional deformation (Phase-1) was replaced by nearly E-W to NW-trending compression-related strike-slip regime (Phase-2). On the other hand, structural and geophysical data suggest that the present-day regime (Phase-3) is strike-slip and the compression direction is mainly NNE. This indicates that the present-day regime is quite different than the previous regime. Based on these, three major deformational phases are resolved based on the field studies. From older to younger, they are (1) nearly N-S-trending pure contractional tectonic regime (Phase-1), (2) nearly E-W to NW-trending compression-related strike-slip tectonic regime (Phase-2) and (3) nearly N-S-trending strike-slip tectonic regime (Phase-3).

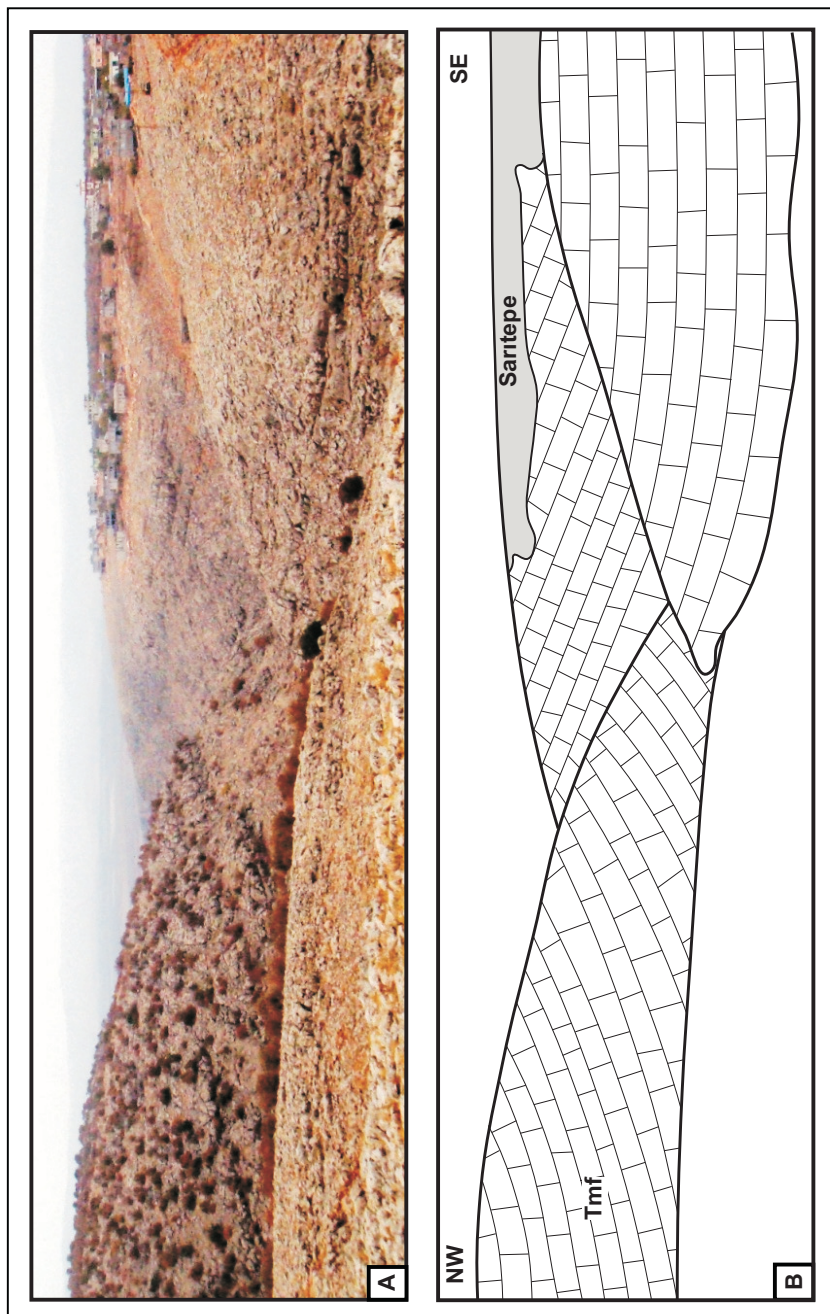


Figure 50. Field photograph illustrating an anticline exposed around Saritepe Village (view to NE)

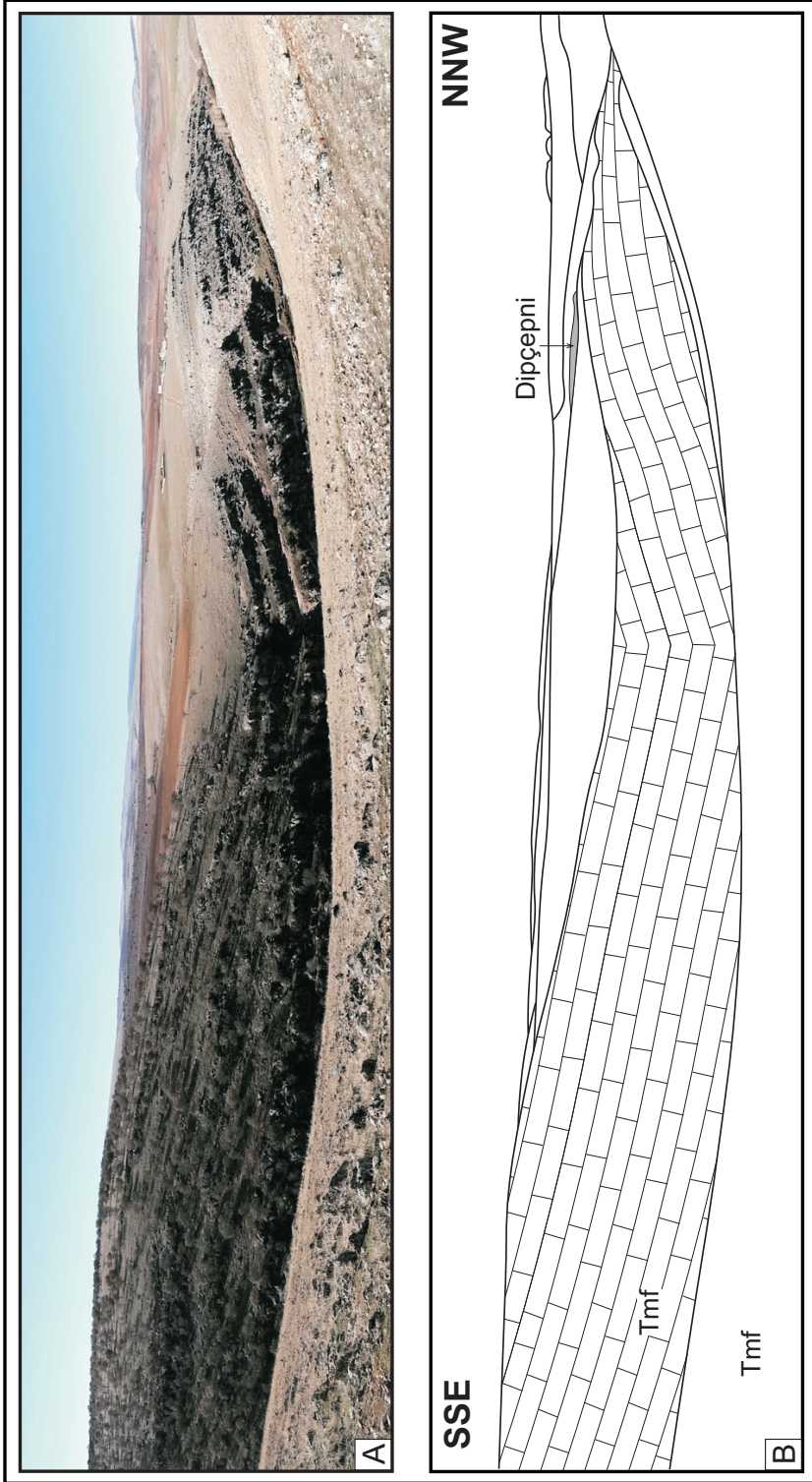


Figure 51. Field photograph illustrating an anticline and syncline included in the Santepe-Tarlabası fold set exposed around the Dipçepni village (view towards WSW).

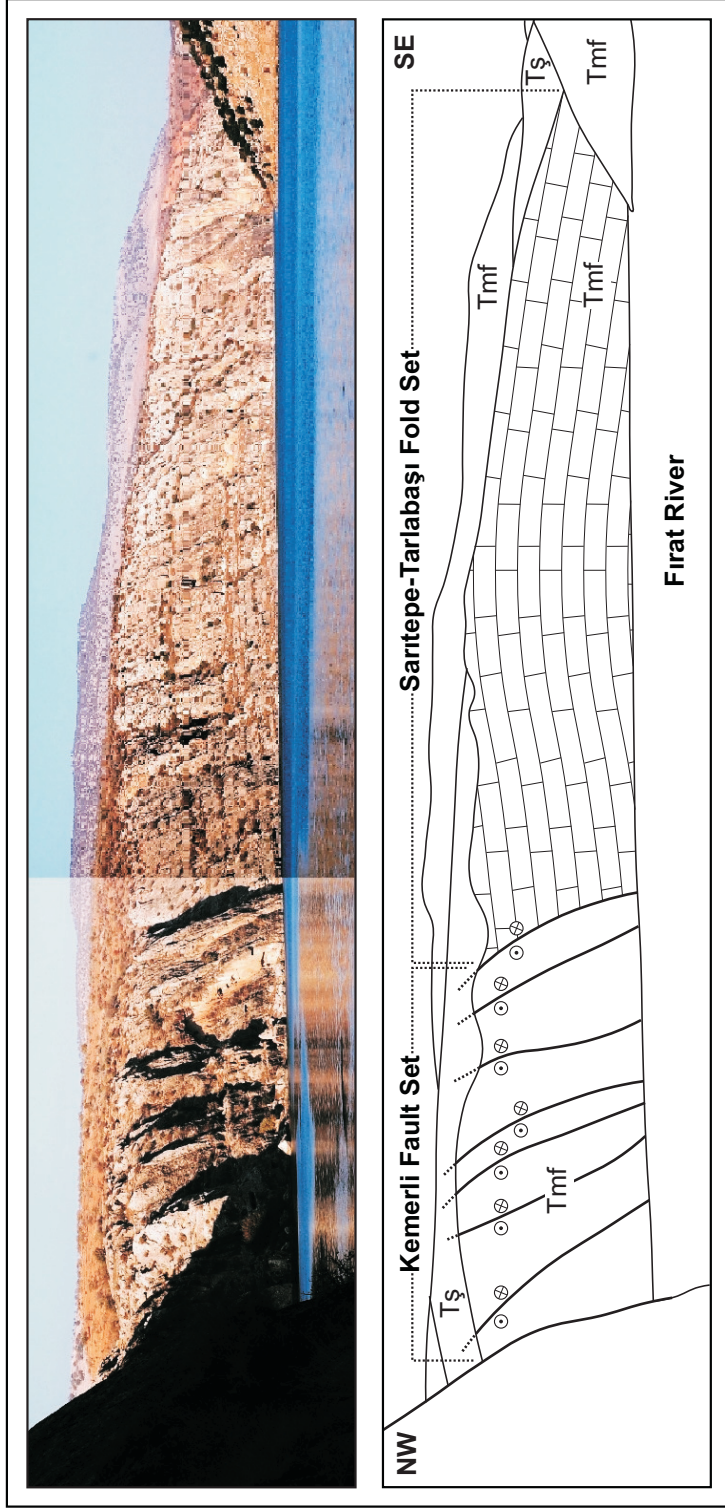


Figure 52. Field photograph illustrating a large scaled gentle anticline cut and reformed by the Kemerli fault set (1 km E of Çiftkeoz Village, view to NE)

3.2.4.2. Paleotectonic Faults

3.2.4.2.1. Çatboğazı Thrust Fault Zone

This is a low-angle thrust fault exposed well in a limited area (Çatboğazı area) in the study area along the northern margin of the Altıntaş modern basin (Appendix-A and Figure 37). Two nappe packages occur in a tectonic window (the Çatboğazı tectonic window). These are the Karadut Complex and Koçali Complex. They are separated by a low-angle thrust fault contact, namely Çatboğazı thrust fault zone made-up of a series of imbricate faults and intervening folds. Both underlying Karadut and overlying Koçali Complexes are the tectono-sedimentary chaotic mixtures of various blocks such as limestone, chert, radiolarite, spilit, volcanics, serpentinite and peridotite set in a sandy matrix. Ages of blocks range from Permian to Late Cretaceous. These chaotic rock assemblages are intensely deformed (folded, thrust to reverse faulted and sheared). Because they formed as the accretionary prism at the active margin of the northerly subducting southern branch of the Neotethys and then detached and obducted onto the Arabian Platform after a long tectonic transportation, the Karadut Complex overlies tectonically the Late Cretaceous Kastel Formation at the bottom. This relationship was determined by oil boreholes (cross-section B-B' in Appendix-A). However, it is overlain tectonically and with an angular unconformity by the Koçali Complex and the Late Cretaceous-Early Paleocene Germav Formation, respectively (Appendix-A and cross-section B-B' in Appendix-B). The tectonic contact (Çatboğazı thrust fault zone) is also overlain with an angular unconformity by the Late Cretaceous-Early Paleocene Germav Formation. Therefore, age of thrusting must be Late Cretaceous.

The Koçali Complex is overlain with an angular unconformity by the Late Cretaceous-Early Paleocene Germav, the Middle Eocene Hoya, Middle Eocene to Middle Oligocene Gaziantep and Middle Oligocene-Early Miocene Fırat

Formations, respectively (Appendix-A and cross-section B-B' in Appendix-B). Indeed, these two nappe packages and their cover of Late Cretaceous-Early Paleocene Germav Formation altogether are overlain with an angular unconformity by a thick sedimentary sequence and volcanics (the Hoya, Gaziantep, Fırat Cingife and Şelmo Formations and the intervening Yavuzeli volcanics). These formations and volcanics seem to be conformable, even though they are separated by some short-term erosional gaps (Local disconformities). These are also intensely deformed. Therefore, both nappe packages and their cover (Germav Formation) comprise the basement, while the deformed thick sedimentary sequence and volcanics form the fill of pre-modern Altıntaş basin (older Altıntaş basin, in the Altıntaş basin).

3.2.4.2.2. Karadağ Fault Zone

This is an approximately 1-1.5-km-wide, 30-km-long and E-W-trending zone of deformation dominated by dextral strike-slip fault with normal components (Appendix-A). The Karadağ Fault Zone is located between Küçükkarakuyu to the west and Fırat River to the east along the southern margin of the modern Altıntaş basin (Appendix-A). It consists of numerous parallel to sub-parallel, closely-spaced and nearly E-W-trending fault segments of dissimilar lengths (1-4 km). Fault segments comprising the Karadağ Fault Zone are cut and displaced by both the NW-trending dextral and NE-trending sinistral strike-slip neotectonic faults (Appendix-A). Additionally, paleostress analysis of slip-plane data measured at ST-19B, 25B, 26 and 28 reveal that the fault segment comprising the Karadağ fault zone operated as both normal and dextral strike-slip fault with normal component formed in paleotectonic periods (before Quaternary) (Appendix-A)

3.2.4.2.3. Erenbağ Fault Set

This is an about 0.4-km-wide, 8.2-km-long and NW-trending zone of deformation characterized by sinistral strike-slip faulting. It is located at the northeastern corner of the study area (Appendix-A).

3.3. Neotectonic Faults

These are the reactivated or newly formed structures during the Quaternary strike-slip neotectonic regime. Numerous strike-slip faults were identified, mapped and described in the frame of the PhD thesis. These faults are named here based on their trends and occurrence patterns of the fault segments. The most prominent faults were categorized into two fault zones and seven fault sets. These are from west to east Kırkpınar, Dağdağancık and Güllüce fault zones; Yakuplu, Çatlaklar, Taşdeğirmen, Bağlıca, Akdurak, Fıstıklıdağ, Kemerli fault sets and Yavuzeli fault respectively (Appendix-A and Figure 37). Each of these fault zones and sets are described below.

3.3.1. Yavuzeli Fault

This is the 33-km-long, northward steeply dipping (60° - 75°) and E-W-trending fault which operated as thrust to reverse fault during Phase-1, dextral strike-slip fault with normal component during phase-2 and partly thrust to reverse fault during the phase-3 or the neotectonic period. The Yavuzeli Fault is well exposed between the NE-trending Çukuryurt fault to the west and nearly 5 km east of Göçmez Village to the east along the southern margin of the modern Altıntaş basin (Appendix-A and Figure 54). It determines and controls the northern margin of the modern Altıntaş basin. The Yavuzeli fault originally formed as a thrust to reverse fault bounding the northern margin of the older Yavuzeli basin (Figures

44, 45, 46, 47, 48 and 49). Then this fault was reactivated as dextral strike-slip fault during the second phase (Appendix-A and Figure 54). This is also evidenced by subsurface seismic sections (Figures 44, 45, 46, 47, 48 and 49). This fault again reactivated as reverse fault later.

The Yavuzeli fault is cut, dissected into a number of segments of dissimilar length and displaced in both southwest and southeast directions by various segments of the NW-trending Dağdağancık Fault Zone, the NE-trending Çatlaklar and the Taşdeğirmen strike-slip fault set (Appendix-B).

3.3.2. Güllüce Fault Zone

This structure is another category of the early-formed but later reactivated faults. It is exposed well in the area between Mağaraköy to the west and Erenbağ Village to the east along the northern margin of the modern Altıntaş basin (Appendix-A and Figure 37). The Güllüce Fault Zone is an about 1 to 1.5-km-wide, 50-km-long and approximately ENE-trending zone of deformation characterized by the combination of northward steeply dipping reverse faults and the strike-slip faults with considerable amount of dip-displacement (Cross-sections A-A' and B-B' in Appendix-B). The Güllüce Fault Zone consists of various segments of dissimilar lengths (0.7 to 13 km). It is crossed, dissected into a number of fault segments and displaced in both lateral and vertical directions by the NW-trending dextral and NE-trending sinistral strike-slip fault sets such as the Karapınar, Dağdağancık, Bağlıca, and the Akdurak fault sets (Appendices-A and B).

The Güllüce fault zone also originally formed as the combination of a major thrust to reverse fault i.e. as a fold-thrust fault zone bounding and controlling the northern margin of the Altıntaş basin during the Middle Eocene-Early Pliocene paleotectonic period. However, it was reactivated again as strike-slip fault with normal component and later as partly reverse to thrust fault under



Figure 53. Field photograph illustrating the trace of northward steeply dipping Yavuzeli Fault and its south-facing steep scarp.

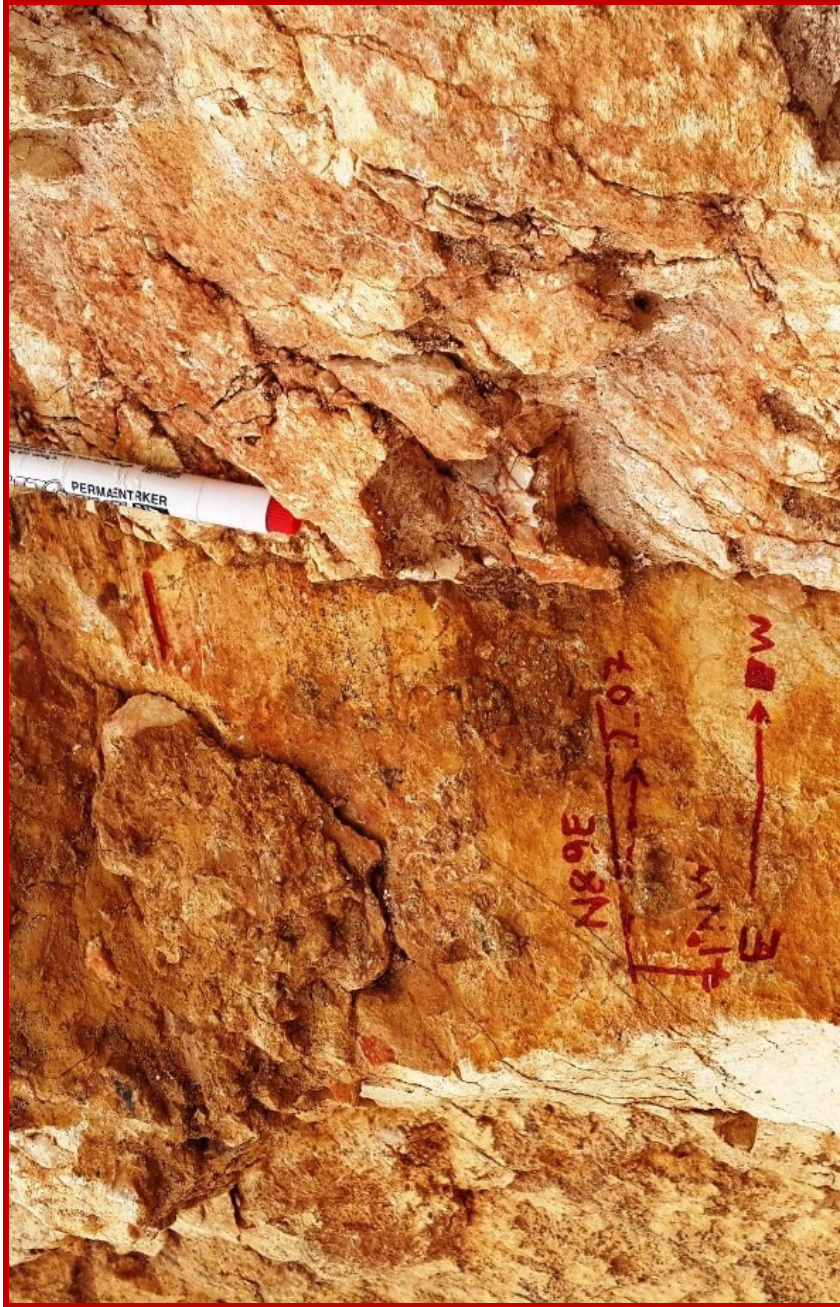


Figure 54. close-up view of the set of nearly horizontal slip-lines printed over the older set of steeply-plunging slip-lines (nearly 1750 m east of the Ballık Village).

the control of new strike-slip regime during the Quaternary neotectonic period. In the present, the Güllüce fault zone bounds and controls the northern margin of the modern Altıntaş basin (Appendices-A and B). Pre modern Altıntaş basin fill units such as the Hoya, Gaziantep, Fırat, Cingife and Şelmo formations and intervening

Yavuzeli volcanics are cut across, displaced in both vertical and lateral directions and tectonically juxtaposed with each other and also the Quaternary fill of the Altıntaş basin by the fault segments of the Güllüce fault zone (Appendix-A and cross-sections A-A' and B-B'in Appendix-B and Figures 55, 56, 57 and 58). Additionally, they display well-developed to preserved linear mountain front, triangular facet separated by a series of the transversal drainage system with deeply carved beds, sudden break in slope, crushed to brecciated strips of minor shear zones, fault-parallel alignment renewed alluvial fans and fault planes (Figures 55, 56 and 57) The Quaternary fill of the modern Altıntaş basin is also crossed across and displaced in both lateral and vertical directions (Figure 58). These indicate the neotectonic nature of the master fault of the Güllüce Fault Zone (Appendix-A).

Some presently active antecedent valleys which connect to Karasu stream and hence to Fırat River are present along the GFZ (Figure 59). One of them is the Ardıl stream (Appendix-A). The total amount of incision exceeds 130 m along this stream. At least 120 m of this incision took place inside Middle Oligocene to Early Miocene Fırat Formation while less than 10 m took place inside some Quaternary terraced sediments (Appendix-A). Moreover, the amount of uplift which possibly took place during this time is also reflected to some paleovalleys hanged in higher elevations along the GFZ (Figure 60). The measured amount of the uplift along these valleys exceeds 250 m in places. Although there is no direct age to these valleys, Demir et al. (2008) showed that the age of the Fırat River inside the study area is nearly 9 Ma and possibly contemporaneous with Karasu and Ardıl Streams. In addition to this, they also provided some evidences showing that much of the uplift along the Fırat River took place between nearly 9-5 Ma. The existence of

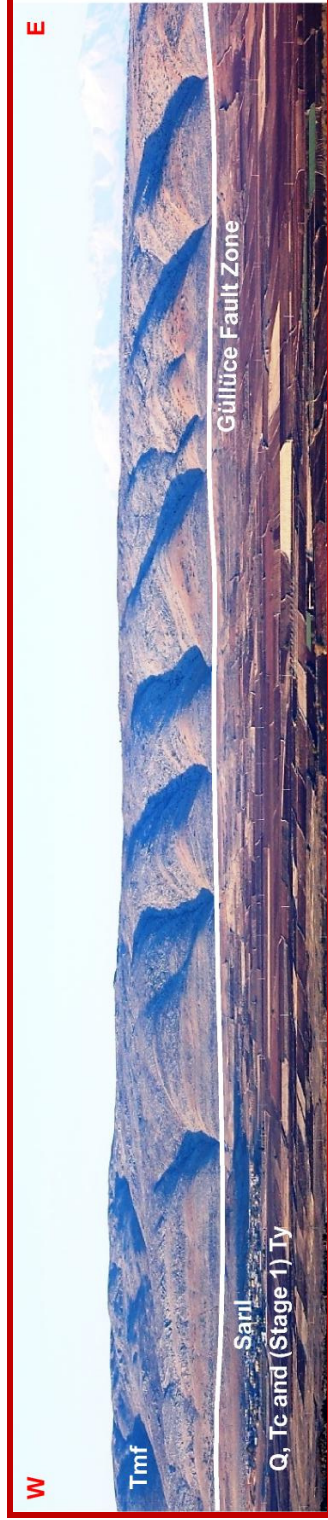


Figure 55. Field photograph illustrating various morphotectonic features produced by the master fault segment of the Güllüce Fault Zone (view towards north).

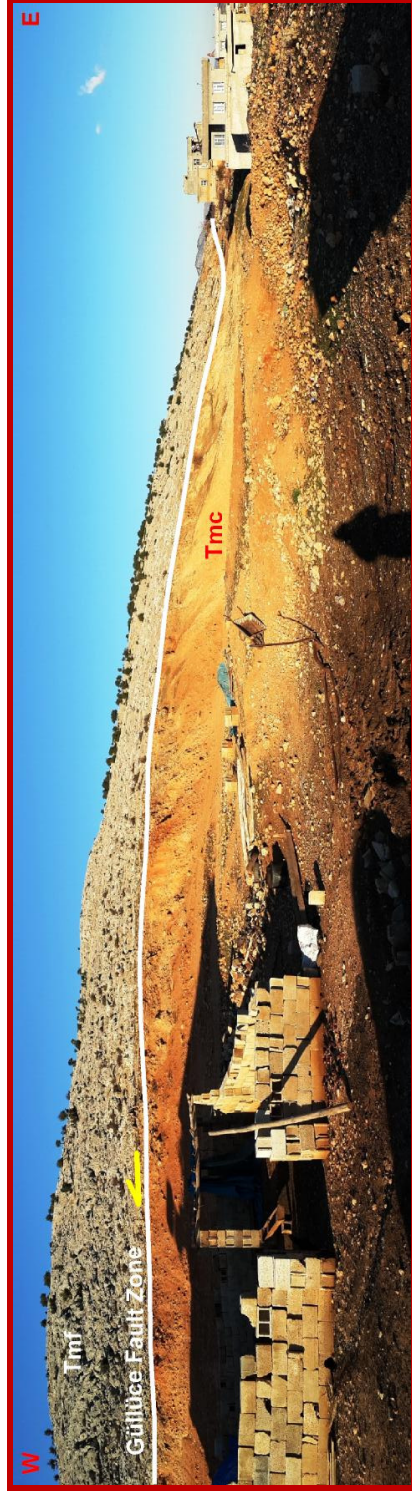


Figure 56. Field photograph illustrating the faulted contact between the Firat Formation and the Cingife Formations exposed across near the Güllüce Village (view towards north).

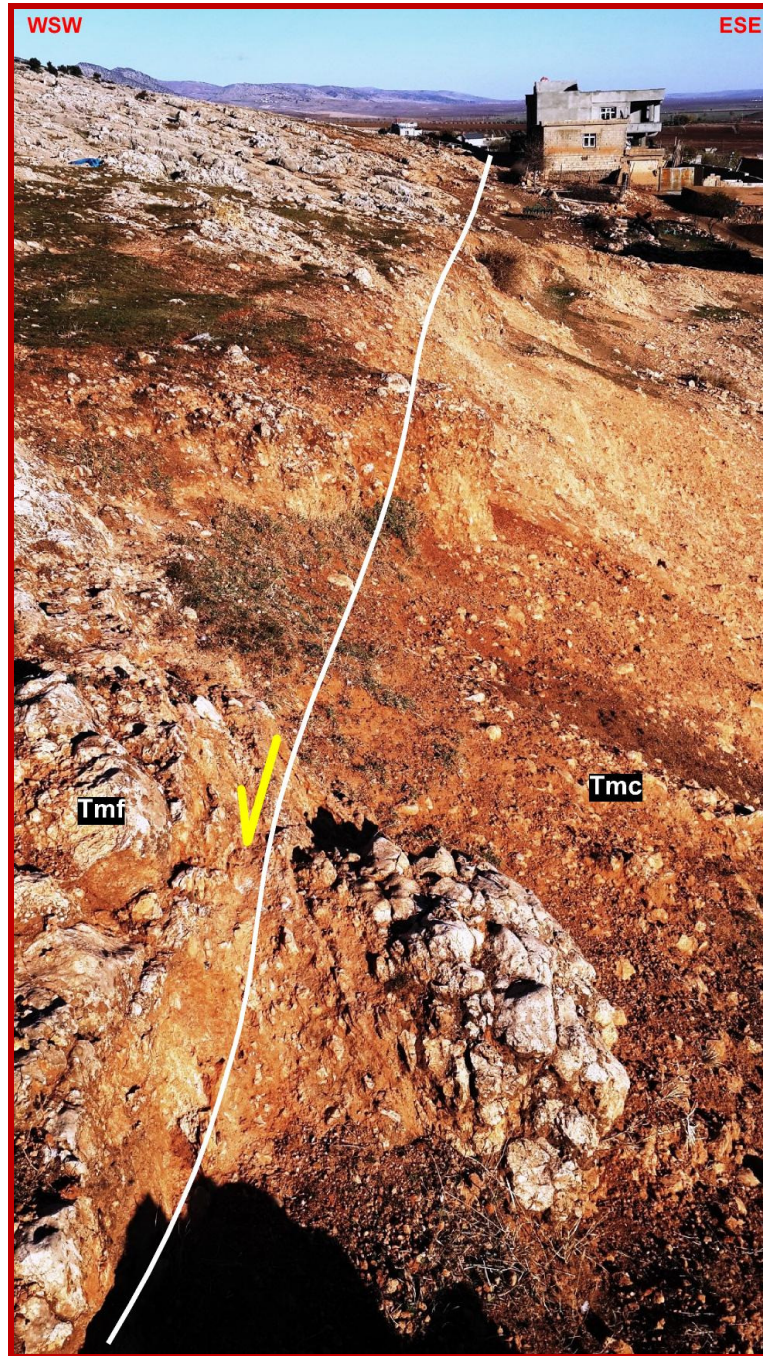


Figure 57. Field photograph illustrating Close-up view of the Güllüce Fault Zone that cuts both Fırat and Cingife Formations and displaced them in vertical direction (view towards ENE).



Figure 58. Close-up view of the Güllüce master fault which cuts across the Quaternary basin fill and displaced it in both lateral and vertical directions (nearly 1 km WSW of the Köklüce Village).

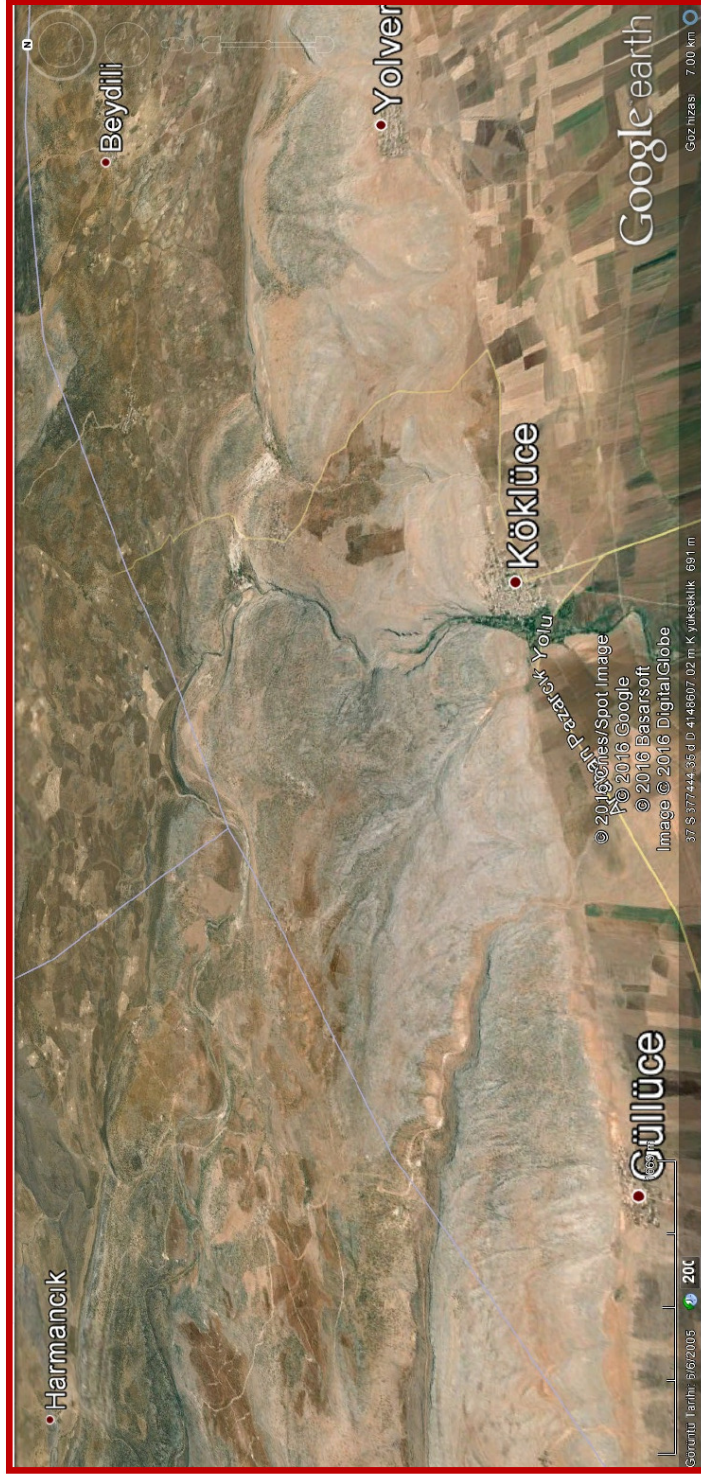


Figure 59. A Google earth image showing the antecedent Ardlı stream which existed before the uplift of the Kızıldağ Mountain.

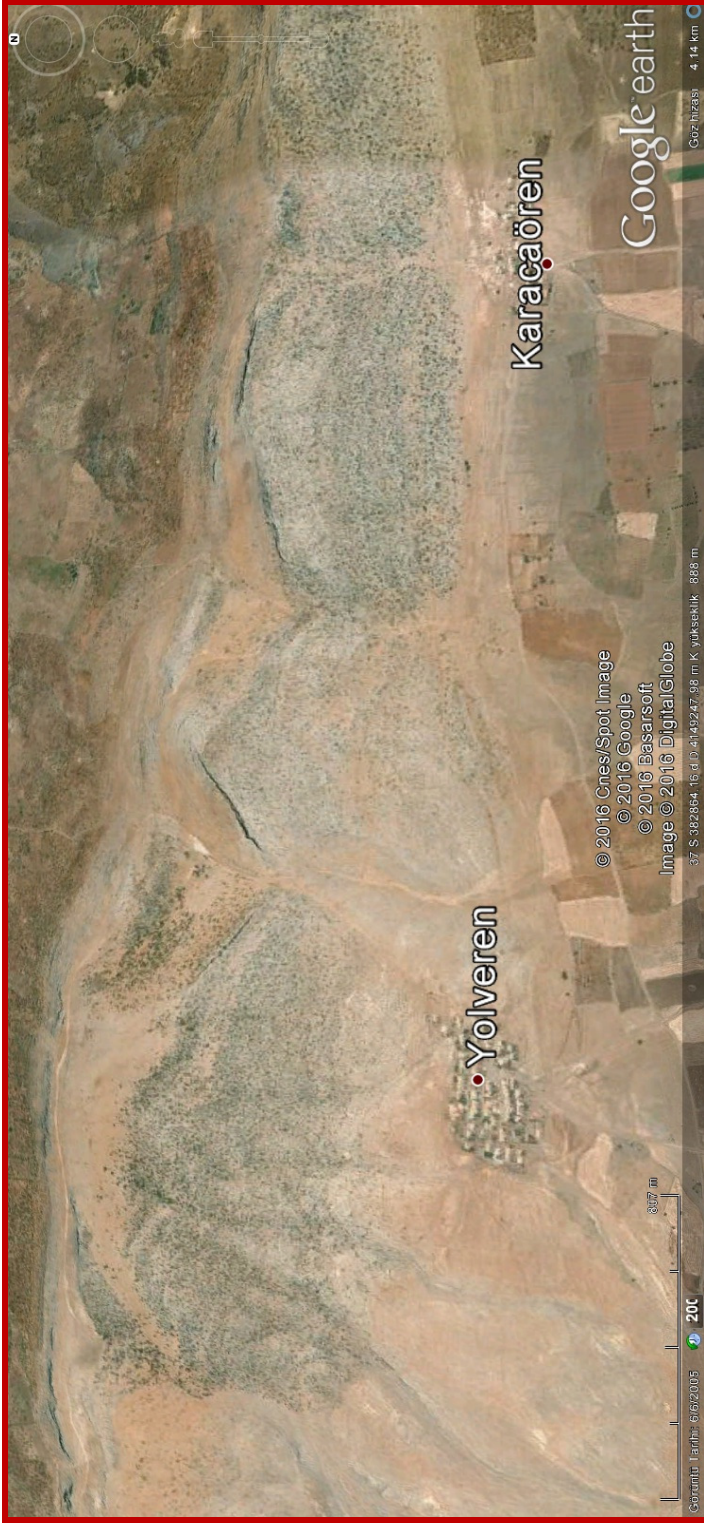


Figure 60. A Google earth image showing some paleovalleys which were active before the uplift of the Kızıldağ Mountain.

thrust to reverse character which does not fit the present day character of the GFZ and majority of the incision that restricted to pre-Quaternary sediments imply that GFZ is a paleotectonic structure which at least partly reactivated during the neotectonic period based on some field observations.

The Güllüce fault zone is cut across and displaced in left-lateral (up to 2.5 km) and right lateral (more than 8 km) directions by the NE-trending Turunçlu fault segment of the Kırkpınar Fault Zone and NW-trending Dağdağancık, Bağlıca and Akdurak fault sets, respectively (Z-Z', P-P', R-R', X-X', X-Y and D-D' in Appendix-A and Figure 37).

3.3.3. Kırkpınar Fault Zone

This is an about 5-km-wide, 14.4-km-long and NE-trending zone of deformation characterized by sinistral strike-slip faulting. The Kırkpınar fault zone, which is also East Anatolian Fault System-parallel structure occurs and is exposed well at the northwestern corner of the study area. It consists of three fault sets such as the Sadakalar, Ganıdağ and Turunçlu fault sets (Appendix-A and Figure 37). The linear mountain front, sudden break in slope, steeply-sloping fault scarps, tectonic juxtaposition of older rocks with the Quaternary basin fill, well-preserved fault slickensides and structural markers of the offset features are the most common morphotectonic and fault-plane related criteria used for the recognition of faults in the field (Appendix-A and Figures 59, 60, 61 and 62). The paleostress analysis of the slip-plane data measured at station-1 (ST-1) indicates that the Tutunçlu fault set is a sinistral strike-slip fault produced by the maximum principal stress operated in N-S-direction (ST-1 in Appendix-A). The Dağdağancık fault zone is a conjugate to the NE-trending Kırkpınar fault zone, in contrast, it cuts and displaces both the ENE-trending Güllüce and E-W-trending Karadağ fault zone (Appendix-A and Figure 37). The reverse fault included in the Güllüce fault set is cut and displaced more than 1.9 km in dextral direction by fault segments at the western tip of the modern Altıntaş basin (P-P' in Appendix-A and Figure 37).

Steeply sloping fault scarps, sudden break in slope, tectonic juxtaposition of the older rocks with the Quaternary fill, well preserved fault slickensides and the structural offset markers indicate that the Kırkpınar fault zone is sinistral strike-slip fault zone (Figures 37, 61, 62, 63 and 64 Appendix-A). This is proved once more by the paleostress analysis of slip-plane data measured at station-1 (ST-1 in Appendix-A).

3.3.4. Dağdağancık Fault Zone

This structure was first named as the “Dağdağancık Fault” and reported by Ulu et al. (1991). However, detailed field geological mapping carried out in the present study indicate that this structure is a zone of deformation. Dağdağancık fault is an about 0.2-4 km-wide, 30-km-long and NW-trending zone of deformation characterized by dextral strike-slip faulting. It is located in the area between Oğullar village to the NW and and the Şenlikçe village to the SE (Appendix-A and Figure 37). Dağdağancık fault zone consists of numerous parallel to sub-parallel, closely to medium spaced (0.1 to 1.5 km) and WNW-to NW-trending fault segments. The Dağdağancık fault segments cut across both the northwestern and southwestern margins of the Altıntaş basin (Appendix-A and Figure 37). Additionally, the Middle Eocene-Early Miocene Midyat Group, the Late Oligocene (?) to Early Miocene Cingife Formation and Early Miocene volcanics and the Quaternary fill of the Altıntaş basin are crossed, displaced in lateral and vertical directions, and steeply sloping fault scarps, sudden break in slope, tectonic juxtaposition of the older rocks with the Quaternary fill, well preserved fault slickensides and the structural offset markers indicate that the Dağdağancık fault zone is a dextral strike-slip fault zone (Figures 37, 65, 66 Appendix-A). This is proved once more by the paleostress analysis of slip-plane data measured at station-21 (ST-21 in Appendix-A).

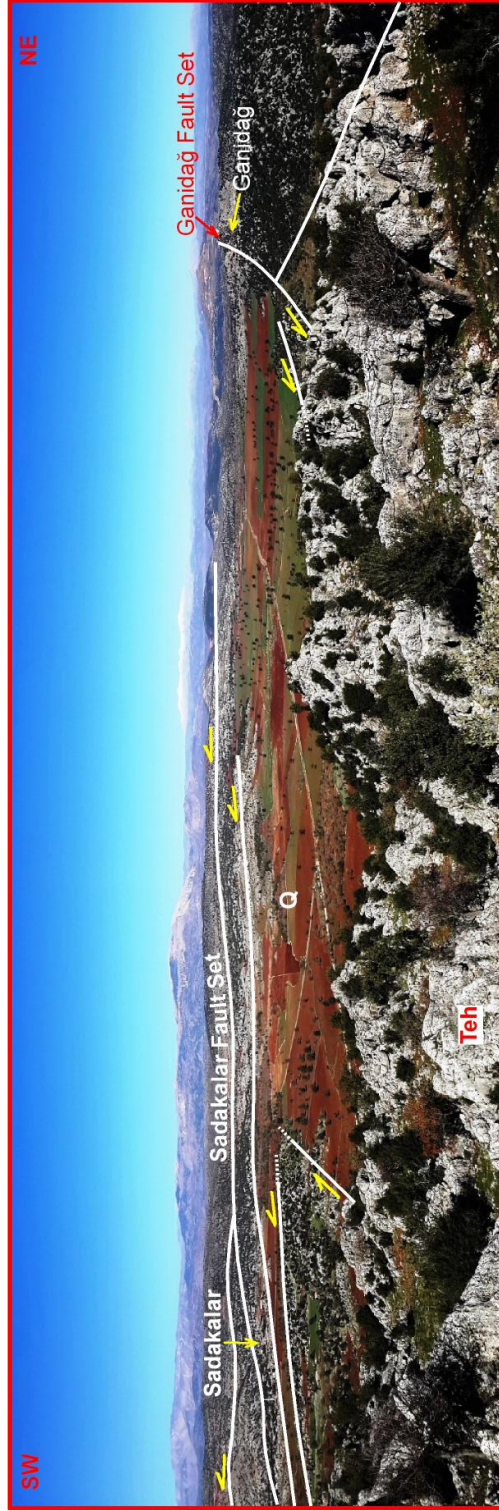


Figure 61. Field photograph illustrating both the Sadakalar and Ganidağ Fault Sets comprising the Kirkpınar Fault Zone.



Figure 62. Close-up view of the fault plane of the fault segment included in the Ganidağ Fault Set (nearly 300 m SW of the Ganidağ Village, view towards NE).



Figure 63. Field photograph illustrating the linear mountain, steep fault scarp and the sudden break in slope due to motion on the Turunçlu Fault Set. (nearly 1 km SW of the Hörüklü Village).



Figure 64. Close-up view of the Turunçlu Fault Set (nearly 300 m of Hörüklü Village, view to N).

The Karasu Stream significantly incised the Quaternary Lahti Group (maximum of nearly 60 m) near the trace of the Dağdağancık Fault zone on the up thrown block to the west while almost no incision took place on the down thrown block just to the east. This finding implies that the Dağdağancık Fault Zone is a neotectonic structures as supported by the clear morphological evidences discussed earlier along the trace of it.

3.3.5. Yakuplu Fault Set

Numerous fault segments occur in the area between Yakuplu-Yeniyurt villages to the west and the Fırat River to the east along the northern margin of the modern Yavuzeli basin (Appendix-A and Figure 37). These faults are altogether termed here as the Yakuplu fault set. The fault segments comprising the Yakuplu fault set show a very broad and areal distribution in about 3-6-km-wide and 37-km-long area. These fault segments are 1-4-km-long, NW-trending dextral strike-slip faults in nature. The pre-modern basin fill of Middle Eocene-Early Miocene age, the E-W-trending Yavuzeli reverse fault and the Karadağ fault zone are altogether cut and displaced at least 2.5 km in dextral directions (Appendix-A and Figure 37). Additionally, some of the segments of the Yakuplu fault set display well-preserved slickensides with over-printed sets of slip lines. Their paleostress analysis indicates at least two phases of deformation recorded on the slickensides (slip-planes) of the NW-trending strike-slip fault segments. These are the WNW operated strike-slip phase of deformation and the approximately N-S operated (ST-25 and 28 in Appendix-A). Based on the paleostress analysis, the Yakuplu fault set seems to have reactivated older structures. For this reason, it was interpreted to be the combination of both the reactivated older and newly formed neotectonic faults.

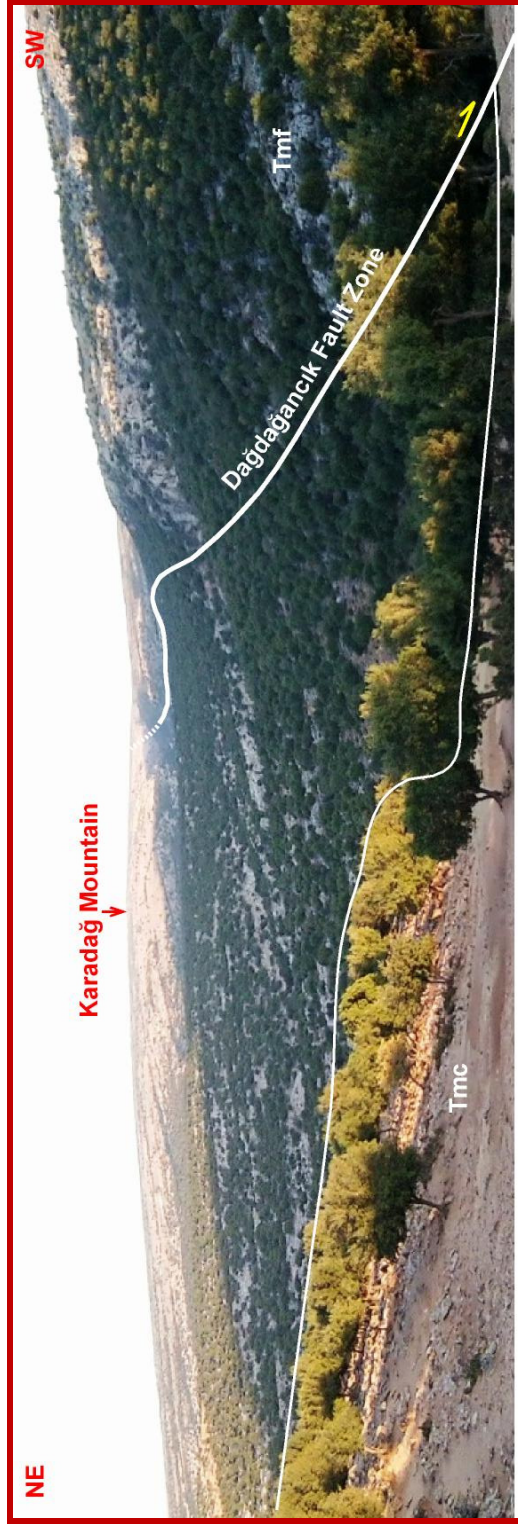


Figure 65. Field photograph illustrating the Dağdağancık section of the Dağdağancık Fault Zone (nearly 1 km SE of the Dağdağancık Village, view to SE).



Figure 66. Close-up view of the Dağdağancık Fault Zone (nearly 300 m of Hörüklü Village, view to N, nearly 1 km SE of the Dağdağancık Village, view to SE).

3.3.6. Çatlaklar Fault Set

This is an about 5-km-wide, 15-km-long and NE-trending zone of deformation characterized by three sinistral strike-slip faults. The Çatlaklar fault set is located at the southwest corner of the study area (Appendix-A). The faults comprising the Çatlaklar fault set are the 14-km-long Çukuryurt, the 10.7-km-long Çatlaklar and the 10.5-km-long Küçükkarakuyu sinistral strike-slip faults (Appendix-A and Figure 37). The pre-modern basin fills of Middle Oligocene-Early Miocene age and the modern Altıntaş basin fill are cut and displaced in lateral and vertical directions (Appendix-A and Figure 37). Additionally, E-W-trending older structures such as the Karadağ fault zone, the Karadağ fold set and Yavuzeli reverse fault displaced up to 1.7 km in dextral direction (V-V' in Appendix-A and Figure 37). These cross-cutting relationships reveal strongly that the Çatlaklar fault set is younger than the offset ones, i.e. it is a neotectonic structure. This is also proved by the paleostress analysis of slip-plane data recorded in both the Cingife formation and the Yavuzeli volcanics (ST-25 and 28 in Appendix-A and Figure 37).

3.3.7. Taşdeğirmen Fault Set

This is an about 9-km-wide, 13-km-long and NE-trending zone of deformation characterized by strike-slip faulting. The Taşdeğirmen fault set determines and controls the ESE margin of the modern Altıntaş basin. It consists of numerous, parallel to sub-parallel, closely to medium-spaced (0.3- 2 km), 1-12-km-long and NNE- to NE-trending sinistral strike-slip fault segments. The Middle Oligocene to Early Miocene Fırat Formation, the Early-Middle Miocene Yavuzeli volcanics and Quaternary fill of the modern Altıntaş basin are cut, displaced in both vertical and lateral directions, and tectonically juxtaposed to each other (Appendix-A). Additionally, both the E-W-trending Karadağ fault zone and the

Yavuzeli reverse fault are also cut and displaced in sinistral direction. The steeply sloping fault scarps sudden break in slope, linear mountain front, fault-controlled drainage systems such as Karasu stream and the tectonic juxtaposition of the older rocks with the Quaternary modern basin fill are common features produced fault segments of the Taşdeğirmen fault set (Figures 37, 67 and Appendix-A). Some fault segments display well-preserved slickensides in places (ST-14, 15 and 19 in Appendix-A, Figures 68 and 69). Paleostress analysis of slip-plane data measured at these stations clearly illustrate that this fault segments are steeply dipping (75° - 87°) sinistral strike-slip faults with minor amount of dip-slip component. The diagram also indicate that these faults formed by the almost N-S operating stress system in the Paleotectonic periods and reactivated during the uaternary neotectonic period (diagrams at ST-14, 15 and 19 in Appendix-A).

The Karasu Stream has incised along its bed rock just on the trace of the Taşdeğirmen Fault Set (Figure 70). The amount of incision increases from west to east. It is observable inside the Middle Oligocene to Early Miocene Fırat Formation, Early Miocene Stage 2 units of the Yavuzeli Volcanics and Quaternary Lahti Group along the fault set (Figure 70). The amount of incision on the Quaternary Lahti Group reaches approximately 15 m just north of the Fakılı Village. On the other hand, almost no incision has taken place away from its trace in the west. This finding also implies that the Taşdeğirmen Fault Set is a neotectonic structures.

3.3.9. Akdurak Fault Set

This structure was first recognized, mapped and reported as a lineament by Geophoto Services Inc. Denver Colorado, (1958). However, some structures was studied in detail and named as a fault set (Akdurak fault set) in the present study. The Akdurak fault set is an about 1-2.5-km-wide, 11.2-km-long and NW-trending zone of deformation characterized by dextral strike-slip faulting. It is located to the west of Akdurak village along the NNE margin of the modern Altıntaş basin

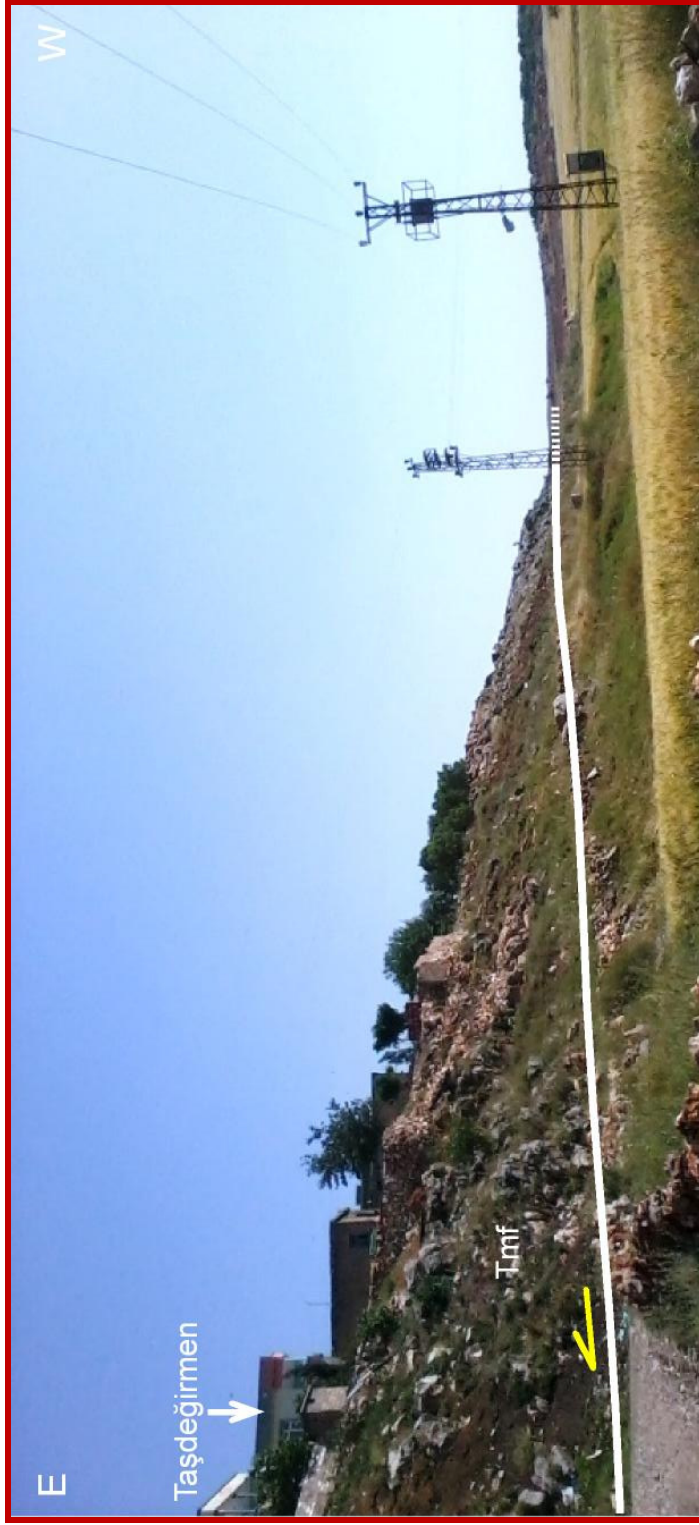


Figure 67. Field photograph illustrating the trace and the scarp of the Taşdeğirmen Fault Set (Taşdeğirmen Village, view to S).



Figure 68. Close-up view slip-plane (fault slickenside) with overprinting relationship. (nearly 1750 m east of the Ballik Village).



Figure 69. Close-up view of another slip-plane (fault slickenside) with overprinting relationship. (nearly 1750 m east of the Ballık Village).

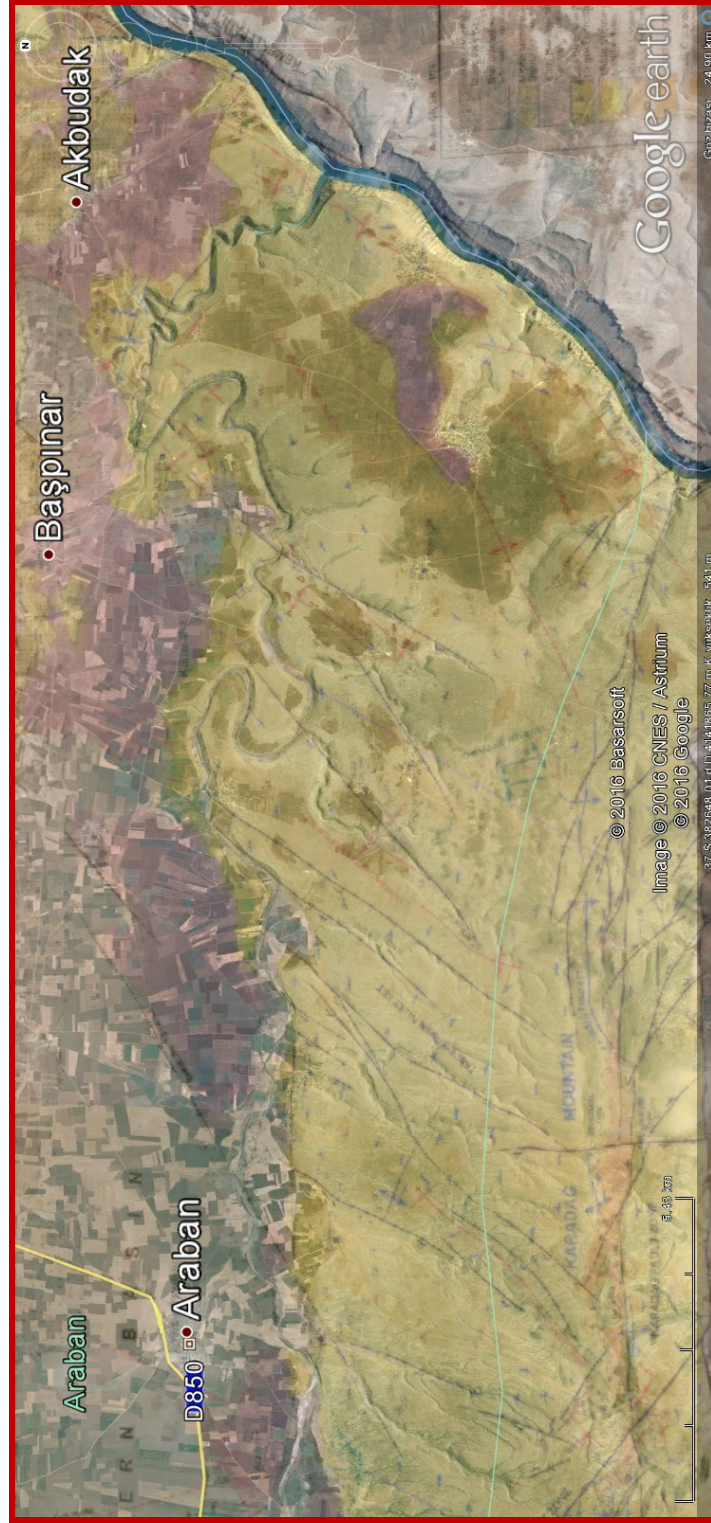


Figure 70. A Google earth image overlain by the geology map along the Taşdeğirmen Fault Set. (see Appendix-A for the legend of the geology map).

(Appendix-A and Figure 37). The Akdurak fault set consists of a number of fault segments of dissimilar length (1-5 km) and trends. Both the pre-Quaternary and the Quaternary fills of the modern Altıntaş basin are crossed and displaced in both lateral (more than 3.7 km) and vertical (up to 60 m) directions (D-D' in Appendix-A and Figure 37) and tectonically juxtaposed to each other by the Akdurak fault set. Additionally, two diagnostic structures such as the Akkoç fault and the Karacaören reverse fault are also cut and displaced a bit more than 1.4 km and 4 km, respectively in dextral direction by the Akdurak fault set (X-Y and X-X' in Appendix-A and Figure 37).

3.3.8. Bağlıca Fault Set

This structure was previously recognized, mapped and interpreted as a single fault of dissimilar nature and names such as a lineament, southward dipping normal fault and northward dipping Harmancık reverse fault (Geophoto Services Inc. Denver Colorado, 1958, Peksu, 1976, Çemen, 1987; Yoldemir, 1987). Indeed, this structure is an about 0.1-1.5-km-wide, 35-km-long and NW-trending zone of deformation characterized by dextral strike-slip faulting. It is here renamed as the Bağlıca fault set. The Bağlıca fault set is located between 3.5 km NW of Akçalar village (outside of the study area) to the northwest and Yukarıkaravaiz village to the SE. Its 19-km-long southern section (the Çakallı-Yukarıkaravaiz section) is included in the study area (Appendix-A). It determines and controls the N-NE margin of the Altıntaş basin. The Bağlıca fault set consists of one relatively long and some short, parallel to sub-parallel fault segments (Appendix-A). The Late Cretaceous Koçali and Karadut Complexes, the Maastrichtian-Early Paleocene Germav, the Middle Eocene Hoya, the Middle Eocene-Middle Oligocene Gaziantep, Middle Oligocene-Early Miocene Fırat Formations, the Middle Miocene Yavuzeli volcanics, the Middle Miocene-Early Pliocene Şelmo Formation and Quaternary fill of the modern Altıntaş basin are cut, displaced in both lateral and vertical directions, and tectonically juxtaposed with each other

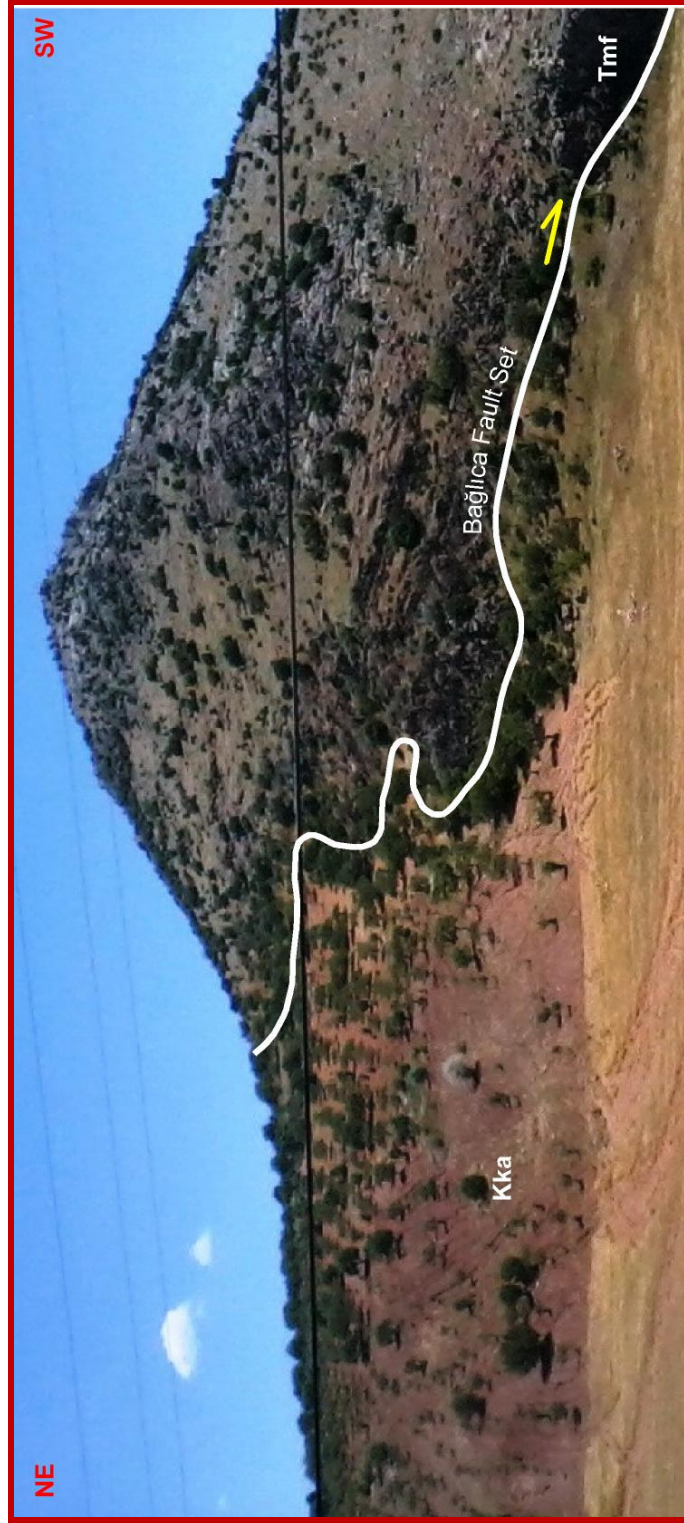


Figure 71. Field photograph illustrating the tectonic contact (Bağlıca master fault). Between the Karadut Complex and the Çatbogazi area, view towards SE).

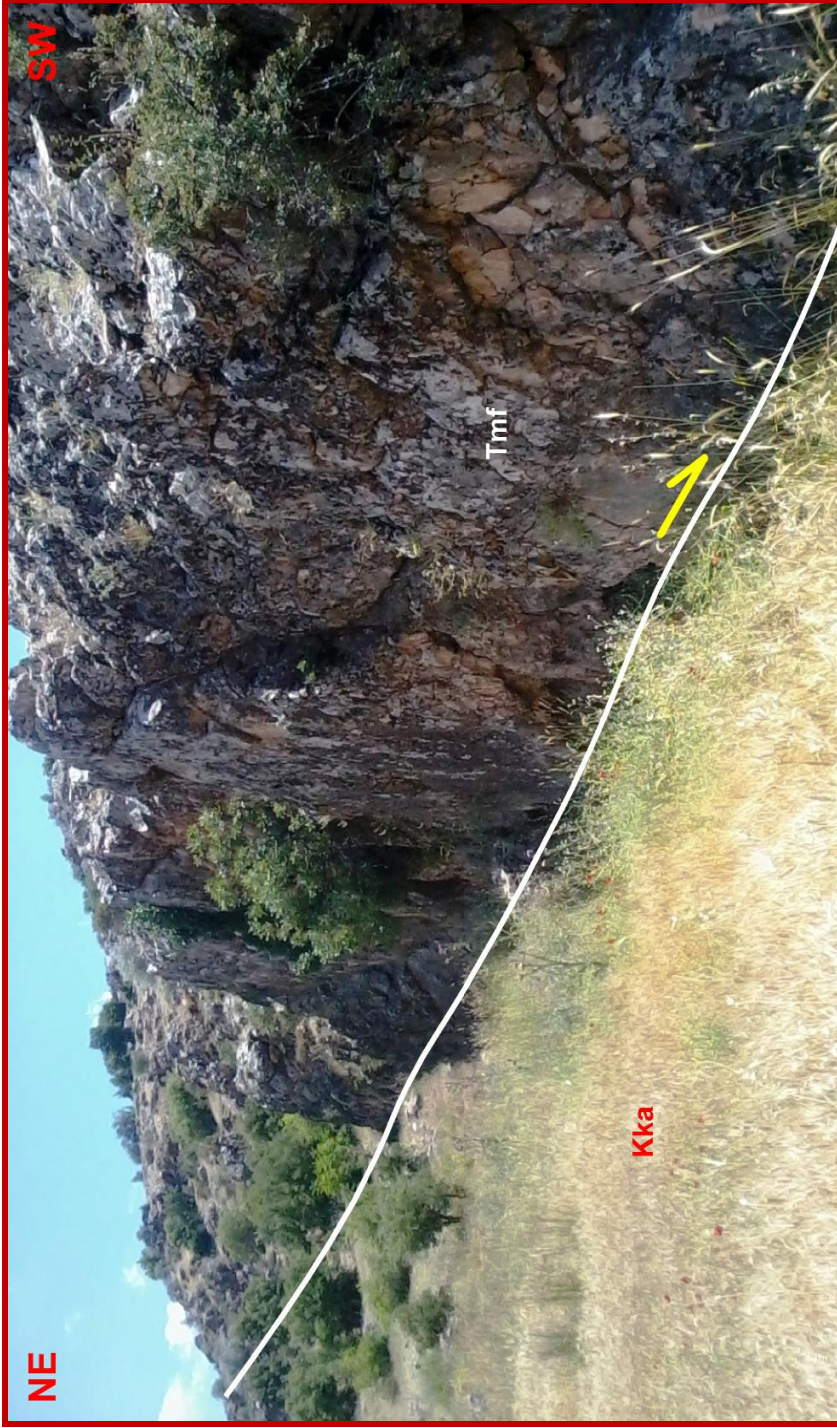


Figure 72. Close-up view of the fault plane of the Bağlica master fault in Çatboğazı area (view towards SE).

(Appendix-A and Figures 71 and 72). In the same way, some other older structures, such as the Güllüce fault zone, are also cut and displaced more than 8 km in dextral directions (R-R' in Appendix-A).

The linear fault trace, steeply-sloping fault scarps, well-preserved slickensides, offset structural markers such as the offset formation boundaries and offset reverse faults, fault-parallel aligned newly formed alluvial fans and the tectonic juxtaposition of older rock units with the Quaternary fill of the modern Altıntaş basin altogether indicate that the Bağlıca fault set is a neotectonic structure in the nature of dextral strike-slip fault.

The fault-controlled drainage system with deeply beds, tectonic juxtaposition of older rocks with younger ones (Figure 73), dextrally offset structural markers (the offset formation boundary, fold axis and the older faults traces), and fault plane (Figures 73 and 74), preserved in places, more than 1 km dextral-strike-slip offset on the Akkoç Fault which operated during Phase-2 all together indicate that the Akdurak fault set is a neotectonic structure in the nature of dextral strike-slip fault.

3.3.10. Fıstıklıdağ Fault Set

This structure was first mapped and named in the present study. Indeed, the Fıstıklıdağ fault set is 0.4-1.1-km-wide, more than 10-km-long NW-trending zone of deformation characterized by dextral strike-slip faulting. It is located to nearly 1 km east of Suvarlı 2 and Suvarlı 4 oil wells along the NE corner of the study area (Appendix-A and Figure 37). Only the 8-km-long part of the Fıstıklıdağ fault set is included in the study area. It consists of several parallel to sub-parallel, closely-spaced fault segment of dissimilar length (1.2-8 km). The Middle Eocene to Middle Oligocene Gaziantep Formation and the Middle Oligocene-Early Miocene Fırat Formation are cut, displaced in both vertical and lateral directions, and tectonically juxtaposed to each other by fault segments comprising the Fıstıklıdağ fault set.



Figure 73. Field photograph illustrating the Akkoç Fault and Akdurak F.S. Note that the pre modern basin fill is cut and displaced and tectonically juxtaposed to each other by the Akdurak Fault Set. (nearly 2.5 km SW of Akdurak Fault Village, view towards east).



Figure 74. Close-up view of the fault plane of the Akdurak master fault nearly in 2.5 km SW of Akdurak Fault Village (view towards east).

Sub-vertical fault scarps and well-preserved fault planes altogether indicate the existence of the Fault. Although no clear slickenline which show the character of the fault set could be found during the field studies, some folds belonging to originally almost E-W-trending en-echelon type Suvarlı fold set has been rotated in clockwise direction along this fault set (Appendix-A and Figure 37). This implies that this fault is a dextral strike-slip fault with neotectonic character. This character has been also supported by some dextral offsets observed in the Firat River outside of the study area.

3.3.11. Kemerli Fault Set

This structure was first mapped and named as the “Kemerli fault” by (Çemen, 1987). Indeed, it is an about 60 m to 1.2-km-wide, 40-km-long and NE-trending zone of deformation characterized by the sinistral strike-slip faulting. It is located along the bed of the Firat river at the ESE corner of the study area (Appendix-A). Only the 18-km-long part of the Kemerli fault set is included in the study area. It consists of several parallel to sub-parallel, closely-spaced fault segment of dissimilar length (2-13 km). The Middle Oligocene-Early Miocene Firat Formation, the Early Miocene-Middle Miocene Yavuzeli volcanics and the Middle Miocene-Early Pliocene Şelmo Formation are cut, displaced in both vertical and lateral directions, and tectonically juxtaposed to each other by fault segments comprising the Kemerli fault set. The fault-controlled drainage system (the Firat River), the sub-vertical fault scarps and well-preserved slickenlines with nearly horizontal slip-lines altogether indicate the existence and the sinistral-strike-slip nature of the Kemerli fault set (Figures 75 and 76). Some fault segments of the Kemerli fault set display preserved slickenside (ST-13 in Appendix-A). Paleostress analysis of slip-plane data measured at ST-13 also indicates that the Kemerli fault set is a sinistral strike-slip structure produced by the N-S-operating strike-slip stress-regime (at ST-13 in Appendix-A) i.e. it is a neotectonic and even an active neotectonic structure. The active character of this fault has been proved



Figure 75. General view of the Kemerli Fault Set's scarp and plane (nearly 1 km east of the Çiftekoz Village, view towards S).



Figure 76. Close-up view of the fault slickenside of the the Kemerli Fault Set (nearly 1 km east of the Çifteköy Village, view towards SW).

by an ancient offset water storage tank constructed and used by Roman-Byzantine period ruled between 395 A.D. and 636 A.D. (Prof. Dr. Attila Engine and Assistant Prof Dr. Abdulkadir GÜZEL, personal communication). No clear offset marker could be observed in the study area. In contrast, 0.5 km sinistral offset was reported for the so-called “Kemerli fault” by Çemen, (1987) outside of the study area. During the field studies, some cross-cutting relationships have been observed in many places. Some of these relationships have allowed separating the events. The examples are common in both the north and south of the study area (Appendix A and Figure 37). For example, E-W-trending large-scale fold system and nearly E-W-trending thrust to reverse faults such as Güllüce Fault Zone to the north and Yavuzeli Fault to the south roughly suggest N-S-trending pure contractional deformation. These folds and faults affect the rocks of Early Pliocene and older rocks, but do not affect the Quaternary units. This suggests that the N-S-trending contractional deformation might have ended pre-Quaternary times. On the other hand, nearly E-W-trending some fold sets (such as Suvarlı Fold Set to the northeast) are cut and sinistrally displaced by the Erenbağı Fault Set to the northeast (Appendix-A, K-K’). This type of faulting mechanism roughly requires nearly E-W to NW-trending maximum principal stress axis but strike-slip style of deformation. This state of stress commonly evidenced by many structures observed in many stations inside the study area (Appendix-A). This is also supported by the existence of compression-related N-S-trending and NE-trending folds. All these structures that developed during the second event affect the rocks of Early Pliocene and older rocks, but do not affect the Quaternary units. This suggests that this nearly WNW-trending compression-related strike-slip deformation might have ended pre-Quaternary times as well as N-S-trending pure contractional phase. Additionally, the field observations also suggest that nearly N-S-trending contractional deformation is followed by the nearly WNW-trending compression-related strike-slip tectonic regime. Moreover, the field data suggest that some of these earlier structures are typically deformed by the youngest NE-trending sinistral, the NW-trending dextral and nearly N-S-trending oblique-slip

faults. This youngest state of stress is commonly evidenced by the slip-plane data collected above active Kemerli Fault Set to the east and earthquake focal mechanism solutions inside and outside of the study area (Appendix-A). Briefly, three major deformational phases are resolved based on the field studies. From older to younger, they are (1) nearly N-S-trending pure contractional tectonic regime, (2) nearly WNW-trending compression related strike-slip tectonic regime and (3) nearly N-S-trending strike-slip tectonic regime.

CHAPTER 4

DEVELOPMENT HISTORY OF THE ALTINTAŞ BASIN

In this chapter, the previously collected data is evaluated and interpreted to present tectonic development history of the Altıntaş basin. To fulfill this, first the events will be separated briefly, then the model will be discussed in detail.

Based on the Paleocene-Eocene plate tectonic configuration of the southeastern Anatolia, the study area is located on the passive continental margin of the northerly-subducting Arabian plate. Field-based new stratigraphic and structural data presented in aforementioned chapters and the international literature information allowed us to reveal and interpret the multiphase development history of the Altıntaş basin since Middle Eocene. The Altıntaş basin is a superimposed basin based on the two different basin fills separated from one another by an intervening angular unconformity. These are: (1) older and deformed (folded and faulted) basin fill, (2) younger and non-deformed (nearly flat-lying) basin fill or modern basin fill. The older basin fill is composed of mainly Middle Eocene thick-bedded marine limestones, Middle Eocene to Middle Oligocene Chalky and Clayey marine limestones, Middle Oligocene to Early Miocene thick-bedded marine limestone, the Late Oligocene (?)–Early Miocene marine to terrestrial detrital rocks, rare carbonates, Early-Middle Miocene volcanic rocks and the Middle Miocene–Early Pliocene fluvio-lacustrine sedimentary sequence. This package overlies the older rocks with a regional angular unconformity. On the other hand, the younger or modern basin fill (Lahti Group) consists of finer-grained axial and the coarse-grained marginal lithofacies assemblages. The modern basin fill also overlies the older basin fill with a regional angular unconformity.

The evaluation of the folds, thrust to revers faults, regional angular unconformity between Quaternary and pre-Quaternary units, strike-slip faults, nearly N-S-trending oblique-slip normal faults and focal mechanism solutions of the earthquakes both inside and outside of the study area indicate that there are more than one phase between Middle Eocene to recent geological time inside the Altıntaş basin. This is also supported by some mesoscopic structures. These were discussed earlier in detail. Based on the above-mentioned structural and stratigraphic data, the study area seems to have experienced at least three main phases of tectonic deformations since Middle Eocene. These are: (1) prominent NNW-trending Middle Eocene-Early Pliocene real contraction phase, (2) the prominent WNW to E-W-trending Pliocene strike-slip phase, and (3) the prominent NNE-trending Quaternary strike-slip phase or neotectonic phase (Figures 77, 78 and 79). These phases are discussed below in detail.

4.1. Middle Eocene-Early Pliocene Real Contractional Phase (phase-1)

Under the control of this phase, first of all the Middle Eocene Early Miocene Midyat Group rocks (Middle Eocene Hoya, Middle Eocene-Middle Oligocene Gaziantep and Middle Oligocene-Early Miocene Firat Formations) were deposited in a lowland area in a relatively shallow sea environment of Arabian carbonate platform located in the southern section of the southern Neo-Tethys Ocean. Later on, the deposition of the upper levels of the Middle Oligocene-Early Miocene Firat Formation was accompanied by the deposition of the prominent detrital facies of the Late Oligocene-Early Miocene Cingife Formation of both shallow-marine to terrestrial nature. This sedimentation was interrupted by the eruption of the stage-1 levels of the Yavuzeli Volcanics in a local area. However, at a regional scale, the deposition of the Cingife Formation continued by the alternation of basaltic lavas and sedimentary beds resulting in a thick pile of volcano-sedimentary sequence, which comprises the main bulk of the Cingife Formation. Onwards, the volcanic activity became prominent, interrupted

the sedimentation in places, and reached up to more than 300 m thick basaltic lava piles so-called “the Stage 1 and Stage 2 levels of Yavuzeli Volcanics” during Early Miocene-Middle Miocene time (21.24 ± 2.04 to 12.1 ± 0.4 Ma) as evidenced by some radiometric age data (Çemen, 1987; Tatar et al., 2004). Both the sedimentation and volcanic activity continued coevally until Late Serravallian. This coeval sedimentation and volcanic eruption were succeeded by the deposition of prominent coarse-grained boulder block conglomerates of the Şelmo Formation during Middle Miocene-Early Pliocene. Lastly, all these units accumulated under the control of the prominent NNW-operating real compressive tectonic regime were deformed into an approximately E-W-trending fold-thrust fault zone shaping the older configuration (foreland basin) of the pre-modern Altıntaş basin, i.e. the Middle Eocene-Early Miocene Midyat Group (Hoya, Gaziantep and partly Firat Formations) deposited in the southern section of a passive margin belonging to the southern Neo-Tethys Ocean, while partly Firat, Cingife and Şelmo Formations, and the Yavuzeli Volcanics were accumulating in a foreland basin. During the same time interval, a number of mesoscopic and macroscopic structures have developed. Among significant macroscopic structures the E-W-trending Tilkiler, Suvarlı and Karadağ Fold Sets, and the Güllüce and Yavuzeli thrust to reverse fault zones and thrust to reverse faults. This type of intensive deformation may be related to the continent-continent collision between the Eurasian and the Arabian Plates in the time slice between the end of Serravallian and Early Pliocene (Şengör et al., 1985; Yiğitbaş and Yılmaz, 1996a, b; Huesing et al., 2009; Kuşçu et al., 2010; Kaymakçı et al., 2010; Hisarlı et al., 2016) and related formation of the Arabian Block during the Early Pliocene (Çemen et al. 1990b). All the events seem to be related with some global-scale tectonic processes such as (1) the Afar Mantle Plume upwelling along ATJ to the south, (2) the complex subduction processes to the north (Potter and Szatmar, 2009; Faccenna et al., 2013 and some references therein), the extension along the Red Sea, Gulf of Aden and Ethiopia (or as a whole along the Afar Triple Junction-ATJ) (Hempton, 1987; Bayer et al., 1998; Ghebreab, 1998; Garfunkel and Beyth, 2006; Trifonov et al., 2011), (3) cessation

of the plate motions following Serravalian continental collision between Eurasian Plate to the north and Arabian Plate to the south, (4) locking of the Dead Sea Transform Fault System (Quennel, 1958; Hempton, 1987; Koçyiğit et al., 1999, Koçyiğit et al., 2000; Trifonov et al., 2011 and some references therein), and (5) formation of the Araban block which was separated from the northwestern margin of the Arabian Plate at the end of this phase of deformation. Consequently the deformed area was uplifted, eroded and dissected into smaller blocks. This has resulted in a relatively small but more than one basins originated from the fragmentation of the Arabian foreland area by some structural highs such Altıntaş and Yavuzeli ramp basins. Similar evidences of this phase are common along the western margin of the Arabian Plate (Hempton, 1987; Çemen et al., 1990a, b; Kaymakçı et al., 2010; Zanchi et al., 2002; Niyazi, TOK, personal communication). Briefly, first of all, the pre-modern Altıntaş basin succession began to be deposited in a passive marginal basin, and then its sedimentation and intensive deformation continued inside the foreland basin during this phase of deformation.

4.2. Pliocene Strike-slip Phase (Phase-2)

Starting from the Early Pliocene (?), a significant changeover or inversion occurred in the first phase of tectonic regime operating in approximately N-S direction within the study area (Figure 78). It is an approximately NW to E-W operating strike-slip tectonic regime. It is named here as the Phase-2. No any sedimentary unit accumulated under the control of this new tectonic regime could be identified in the study area. This is most probably related to: (1) the time span is not long enough to produce new significant sedimentation, (2) the units, which possibly have deposited during this time span, but they are most probably covered by the Quaternary Lahti Group, and (3) the units, which deposited during this time interval, might have been eroded and removed away just before the deposition of Quaternary basin fill. In contrast, the existence of units accumulated under the

control of this new phase was reported from the Pazarcık area 15 km west and outside the Altıntaş basin (İmamoğlu, 1993). In the Pazarcık area, the bottom and top boundaries of the Pliocene units are bounded by angular unconformities (İmamoğlu, 1993). Therefore, the existence of the Phase-2 is obvious, and it corresponds to most probably Pliocene time span. The phase-2 is characterized by a series of folds with approximately NW-trending and N-S-trending axes such as Başpınar, Sarıtepe-Tarlabası, Nohutalan, Höcükü; the Büyükoba, Keşreobası and the Kabasakız fold sets; the NW-trending sinistral (e.g. the Erenbağ fault set) and the NE-trending dextral strike-slip faults and the E-W-trending dextral strike-slip faults with normal components such as the Karadağ fault zone, some faults inside the Güllüce Fault Zone and the Akkoç fault s(Appendix-A, Figures 37 and 78).

The earlier maximum principal stress operating in approximately N-S direction (NNW to NNE) was switched on a new maximum principal stress operating in an approximately E-W direction (WNW to WSW) through time along the northwestern margin of the Arabian Plate. This is clearly evidenced by (a) the stresses analysis; (b) the prominent N-S- to NNE-trending folds developed in the Middle Miocene-Early Pliocene Şelmo Formation and older rocks, and (c) some sinistral displacements along NW-trending faults such as the Erenbağı Fault Set (K-K' in Appendix-A). This inversion in the stress operation direction can be attributed to the complex geometry of the northwestern margin of the Arabian Plate. Additionally, the stress state and related deformation of the Phase-1 caused almost E-W-trending elongation and related gradual increase in the stress magnitudes along the complex edges of the Araban block. Due to these events, possibly the lateral stress magnitudes exceeded the previous maximum principal stresses, and so, a new stress field was established in approximately E-W direction. Following this replacement, some pre-existing structures were reactivated and/ or new structures developed inside the study area (Appendix-A). During the phase-2 period, the pre-modern Altıntaş basin succession was deformed once again by the strike-slip tectonic regime.

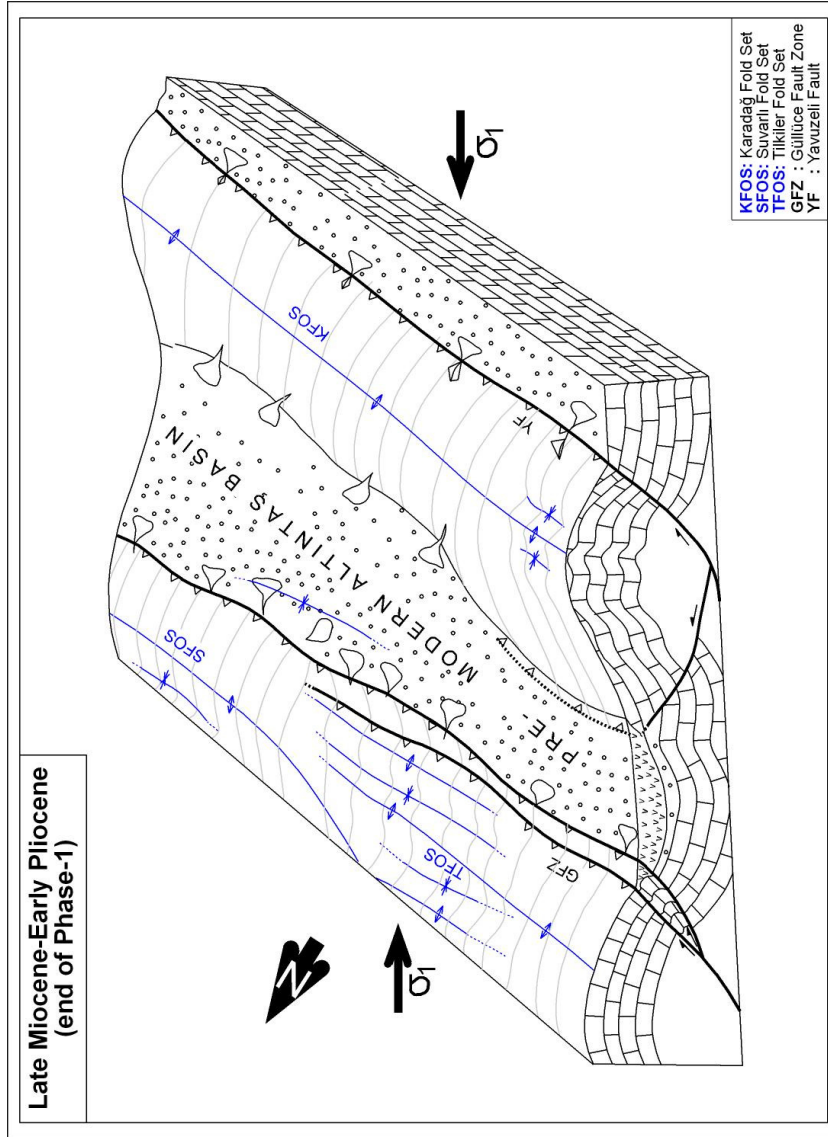


Figure 77. Sketch block diagram depicting development history of the pre-modern Altıntaş basin during Late Miocene (?)–Early Pliocene.

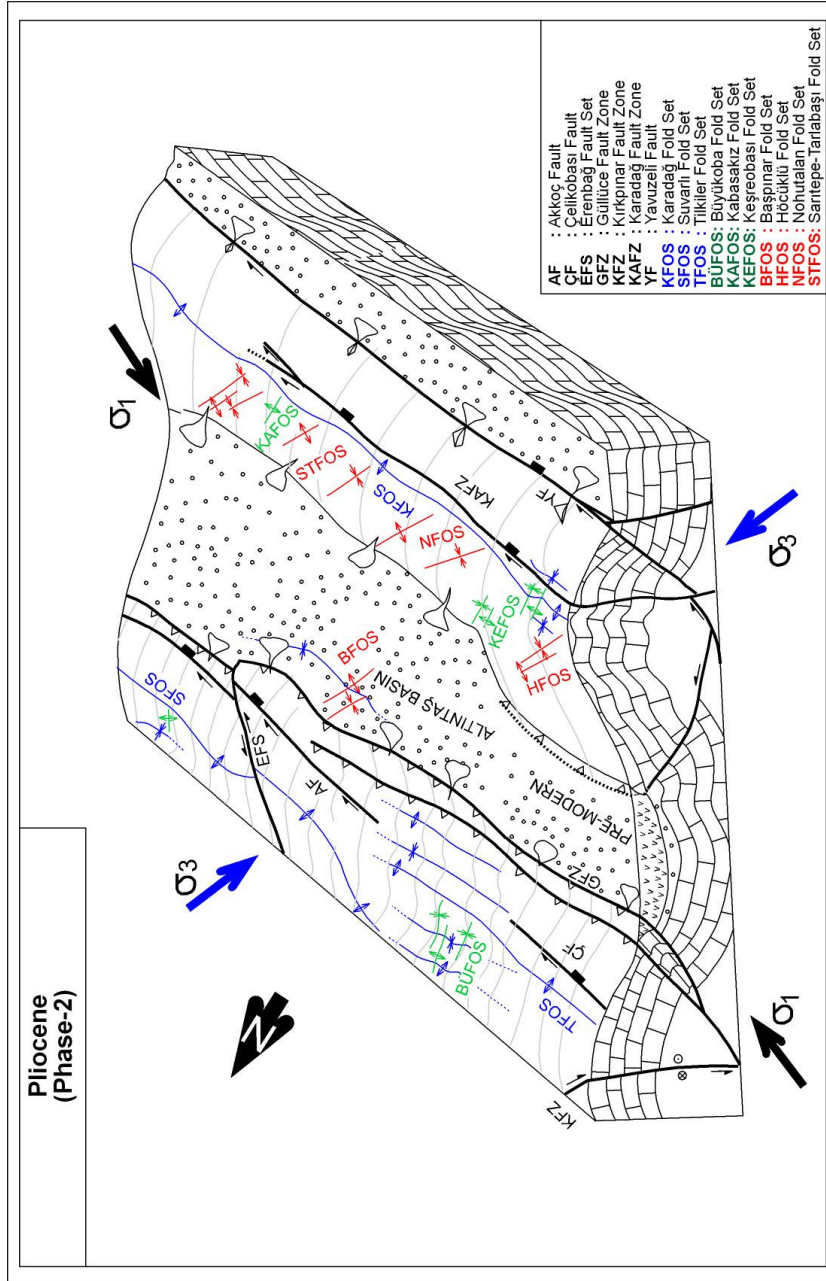


Figure 78. Sketch block diagram depicting development history of the pre-modern Altıntaş basin during Pliocene.

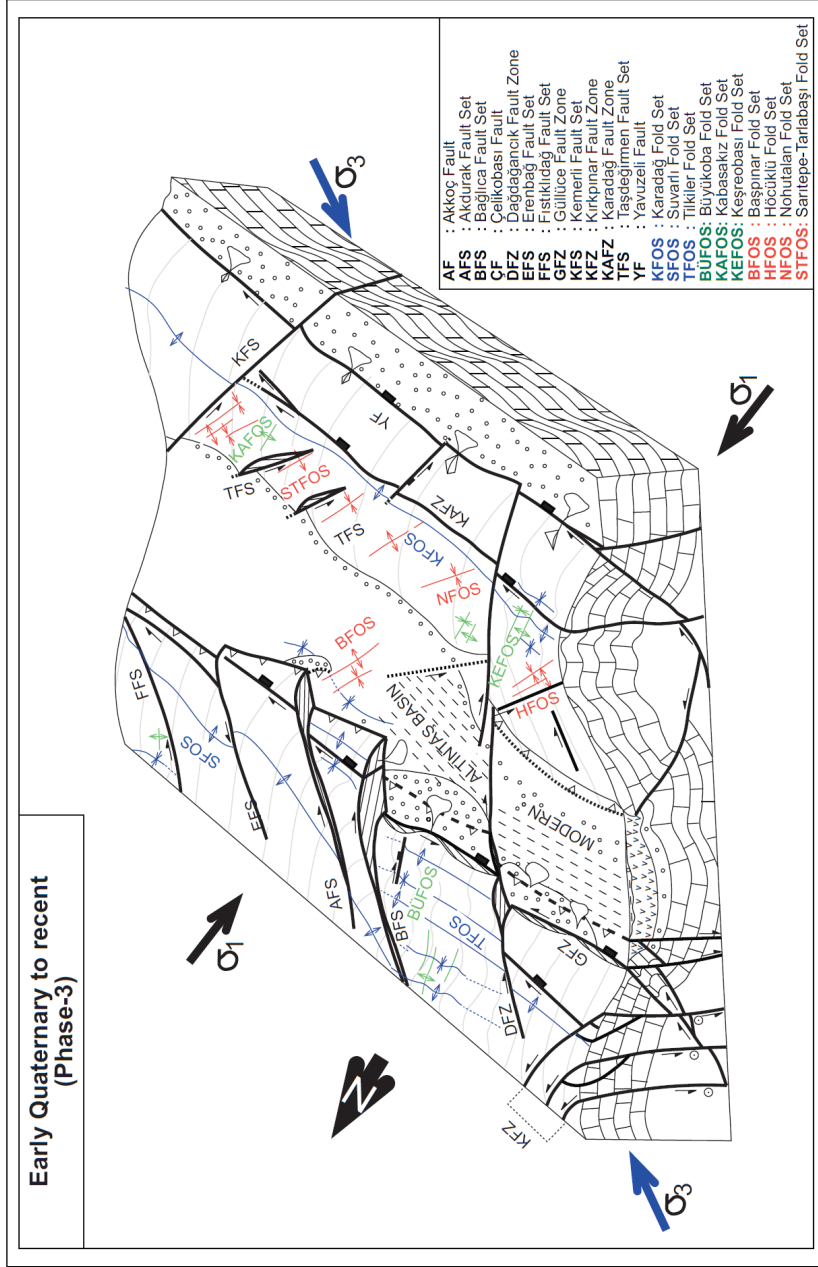


Figure 79. Sketch block diagram depicting development history of the pre-modern Altıntaş basin during the Quaternary.

4.3. Quaternary Strike-slip Neotectonic Phase (Phase-3)

Starting from the Early Quaternary, the Phase-2 deformational period was replaced by a new strike-slip neotectonic regime (Phase-3), which is still lasting in southeastern Anatolia. The early formed and deformed pre-modern Altıntaş basin and its significant elements such as the pre-modern basin fill and the major structures have been re-deformed by the occurrence of the strike-slip neotectonic regime. And so, a new basin began to appear as a modern Altıntaş basin restricted to a small area with respect to its earlier configuration under the control of the phase-3. Particularly, the marginal sections of older basin continued to be uplifted, dissected and inverted, as its central parts were being subsided in lowlands, in which the modern basin fill (the Lahti group) began to be deposited under the control of the strike-slip neotectonic regime (Appendices-A, B and Figure 79).

The development of the modern Altıntaş basin, sedimentation in it, and the activity along its margin-boundary faults have been lasting under the control of strike-slip style of deformation since Early Quaternary. The onset of a new tectonic regime and the inversion in the operation direction of stress system or faulting pattern are evidenced strongly by: (a) a regional angular unconformity that separates the underlying deformed pre-modern basin fill from the overlying nearly horizontal modern basin fill of Quaternary age, (b) paleostress analyses of slip-plane data, (c) focal mechanism solutions of earthquakes occurred in and adjacent to the study area (Ökeler, 2003; Aktuğ et al., 2016), (d) records of significant lateral offsets accumulated on both the NE- and NW-trending sinistral to dextral strike-slip faults respectively, (e) the clear difference in between the configurations and occurrence patterns of older and modern Altıntaş basins, and (f) a significant change-over in the plate tectonic configuration of Middle East resulted from the occurrence of the Anatolian platelet and its west-southwestwards escape along the newly-formed two intra-continental transform fault system, namely the dextral North Anatolian and the sinistral East Anatolian Fault Systems.

The phase-3 is characterized by a strike-slip faulting pattern originated from a stress system operating in approximately N-S direction. Based on this stress system a series of dextral and sinistral strike-slip faults and numerous N-S-trending oblique-slip normal faults formed even if some of older structures reactivate. Inversion in the style of deformation can be attributed to the westward escape of Anatolian Platelet and northward motion of the Arabian Plate. Additionally, the escape of the Anatolian Plate is expected to increase the lateral space needed for the formation of the Araban Block and decrease magnitude of previous lateral stress System. Consequently the N-S-operating stress system became prominent and the strike-slip neotectonic regime (phase-3) gained its present day state of stress during Quaternary (Figure 79). Additionally, this neotectonic period also includes occurrences of some major geological events in a broad area. Some of them are: (1) intensified marine extension along the Red Sea, Gulf of Aden following the sea floor spreading events and continental extension along the Ethiopia (or as a whole along the Afar Tripple Junction-ATJ (Hempton, 1987; Bayer et al., 1998; Ghebreab, 1998; Garfunkel and Beyth, 2006; Trifonov et al., 2011 and some references therein), (2) faster movement along the DSFS (Quennel, 1958; Şaroğlu et al., 1987; Şaroğlu et al., 1992 a, b; İmamoğlu, 1993; Zanchi et al., 2002; Rukieh et al., 2005; Garfunkel and Beyth, 2006; Herece 2009; Trifonov et al., 2011 and some references therein), (3) formation of the North Anatolian Fault System (NAFS) (Alpar and Yaltırak, 2002; Koçyiğit et al. 2005) and EAFS (Şaroğlu et al., 1992 a, b; İmamoğlu, 1993; Herece, 2009), (4) formation and escape of Anatolian Platelet towards W to SW along the (NAFS) to the north and EAFS to the south (McKenzie, 1972; Hempton, 1987; Bozkurt, 2001 and some references therein), (5) onset of Quaternary volcanism along the ATJ (Volker et al., 1997; Chorowicz, 2005 and some references therein), the DSFS (Çapan et al., 1987; Yürür and Chorowicz, 1998; Rojay et al., 2001; Toprak et al., 2002; Lustrino and Sharkov, 2006; Trifonov et al., 2011 and some references therein), the EAFS (Çapan et al., 1987; Ulu et al., 1991; 2001; Yürür and Chorowicz, 1998; Rojay et al, 2001; Toprak et al 2002), the NAFS (Tatar et al.,

2007) and some references therein), the Anatolian Platelet (or Collage) (e.g. Şen et al. 2003; Temel et al. 1998 and some references there in), the East Anatolian Plateau (Ekici et al., 2009), the northern margin of the Arabian Plate (Keskin et al., 2012a, b; Lustrino et al., 2012) and Armenia (Neill et al., 2013). All these processes strongly imply to a significant inversion in the style and pattern of the paleotectonic regime and the onset of a neotectonic regime during Quaternary.

All of the above-mentioned relatively local events included in the phase-3 seems to contemporaneous with some complex large-scale events. These are most probably (1) Global Climate Changes and related events (Potter and Szatmari, 2009; Miller et al., 1987; Zachos et al., 2001), (2) the delayed effect of possible intensification on the activity of the east African Super Plume during the Late Miocene to Early Pliocene (Potter and Szatmari, 2009; Courtillot et al., 2003), (3) renewal of previously existing opening rates along the Gulf of Aden ridge (Baker et al., 1997; Hempton, 1987; Garfunkel and Beyth, 2006; Trifonov et al., 2011), (4) onset of the sea floor spreading along the Red Sea (Baker et al., 1997; Hempton, 1987; Garfunkel and Beyth, 2006; Trifonov et al., 2011), (5) intensified extension rates on the east African Rift and related NNE to NE-trending faster motion of the Arabian Plate towards north (Baker et al., 1997; Hempton, 1987; Garfunkel and Beyth, 2006; Trifonov et al., 2011), (6) reactivation of Palmyra Zone during Late Miocene -Early Pliocene and its regional effects (Dewey and Burke, 1973; Dewey and Şengör, 1979; Şengör and Yılmaz, 1981), (7) renewal of strike-slip motion along the DSTFS (Quennel, 1958; Perinçek and Eren, 1990), and (8) relaxation of the Arabian block and the Arabian plate due to escape tectonics. These events altogether might have triggered the onset of the Early Quaternary strike-slip tectonic regime and related Phase-3 deformation. However, all these relationships must be verified by extra research.

CHAPTER 5

DISCUSSION

First of all, the main scope and aim of this thesis is to illuminate neotectonic development of the Altıntaş Basin located in the Araban Block of the SE Anatolian region (Figure 3). This area is also located on the border of “*Area of Strike-slip Neotectonic Regime with normal component and Area of Strike-slip Neotectonic Regime with reverse component*” (Figures 2). Newly obtained and presented raw data in previous chapters were analyzed, discussed and a development model for the Altıntaş Basin has been suggested so as to contribute to the commencement age of the neotectonic period, deformation mode, structural properties and seismicity of the Altıntaş Basin located at the northwestern margin of the Arabian Plate.

In order to understand the source of the latest phase of deformation, first of all the latest paleotectonic and the neotectonic units in the study area were mapped in detail at a 1/25000 scale, hundreds of slip-plane data and some mesoscopic scale structures were measured and analyzed on 31 stations in the present study. In addition to these, regional stratigraphic correlations, deformation in terms of field geological mapping, measured stratigraphic columnar sections and analysis of faults reveal that the Altıntaş basin has a complex development history accompanied by multiphase deformation. The separation of phases is based on stratigraphic, structural and geophysical data. data such as regional angular unconformity between Quaternary (according to major modification in Quaternary period in 2009 by ICS) and pre-Quaternary units, structural data such as folds, reverse to thrust faults oblique-slip normal faults, strike-slip faults and geophysical data such as focal mechanism solutions inside and outside of the study area. The the refolded folds, overprinting lenations These are (1) Middle Eocene (?) to Early

Pliocene Phase-1 (contractional) deformation, (2) the late Early Pliocene to Early Quaternary Phase-2 deformation (or dominantly WNW and NW-trending strike-slip phase), (3) Early Pliocene to Early Quaternary to recent Phase-3 deformation (or strike-slip neotectonic phase). Although the geological data related to basic geological concepts of SE Anatolia is very much due to significant petroleum exploration studies, there are only a few detailed geological studies about the neotectonics of this region. Its age, origin and mode has become the core of many hot debates particularly since 1970's. Up to now, It is well-agreed that the neotectonics of SE Turkey (or the northwestern margin of the Arabian Plate) is the interplay of the continent-continent collision between Eurasian Plate to the north and Arabian Plate to the south (e.g. Şengör and Dewey, 1979) and escape of the Anatolian (e.g. Şengör and Dewey, 1979). However, there are some major contradictions on the age and style of deformation. The proposals for the initiation age of the neotectonic regime in SE Anatolia falls into four main groups: (1) Middle Miocene or Late Miocene (e.g. Şengör and Dewey, 1979; Yoldemir, 1988), (2) Early Pliocene (e.g. Yusufoglu, 2013) and (3) Early Quaternary (e.g. Koçyiğit and Özacar, 2003; Boulton and Robertson, 2008). In addition to these, the style of deformation debates also falls into two categories, namely, (1) contractional (Dewey et al. 1986) and (2) strike-slip in character (Koçyiğit et al. 2001; Bulut et al. 2012).

Beyond the neotectonics of the Altıntaş basin, the neotectonics of the SE Anatolia also shed light to the onset age of neotectonics of Turkey. The age range also falls into 4 groups. (1) Early (?) - Middle Miocene (e.g. Şengör, 1980), (2) Early Pliocene (e.g. Yusufoglu, 2013) and (3) Early Quaternary (e.g. İmamoğlu, 1993; Koçyiğit et al. 2001).

When the tectonic development of the Altıntaş Basin is considered in the context of the above-mentioned explanations, initiation age of the neotectonic regime in Turkey fits well to the Early Quaternary age. What is interesting to note that the initiation age, style of deformation and causes of neotectonic regime of the Altıntaş basin and SE Anatolia also coincide with some larger events. This is

because; there is a large number of data suggesting that the major tectonic changeover in the global tectonic regime or the initiation age of the global neotectonic period is a few million years (Ollier, 2006). According to this study, almost all of the major mountain belts such as Alps (Trumpy, 1980), Himalayas (Gansser, 1991; Kalvoda, 1992; Zhang, 1998), Andes (Kroonenberg et al., 1990; Holingsworth and Rutland, 1968; Walker, 1949; Coltorti and Ollier, 2000), Jura Mountains (Holmes, 1965), Apennines (Coltorti and Pierruccini, 2000), Pyrenees, (Sala, 1984a; Calvet, 1994), Cordilleras of Spain (Sala, 1984b), Carpathians, (Zuchiewicz, 2000), (Rádoane et al., 2003), Caucasus (Bridges, 1990), Tien Shan (Holmes, 1965), Japanese Mountains (Hoshino, 1998), Taiwan (Chai, 1972; Ho, 1986), Sierra Nevada (Axelrod, 1962), Basin and Range (Nitchman et al., 1990), Rocky Mountains (Eaton, 1987), Canadian Coast Ranges (Farley et al., 2001), New Zealand Mountains (Sugatte, 1982), East Australia (Ollier and Taylor, 1988), Antarctica (Behrendt and Cooper, 1991), Ural Mountains (Bridges, 1990), Sudeten (Migon and Lach, 1999), Tibetan Plateau (Wu et al., 2001) and many others recorded some major peculiarities in their uplift history since the Pliocene to Early Quaternary. In addition to the uplift history, this time also corresponds to the change in some other geological agents all across the whole world such as climate (e.g. Ruddimann and Raymo, 1988; Zachos et al. 2001; Miller et al. 2005; Ollier, 2006), flow of the lower crust (e.g. Arger et al. 2000; Demir et al. 2008), acceleration of the supermantle plumes (e.g. Potter and Szatmari, 2009), reorganization of the Atlantic and Pasific mid-ocean ridges (e.g. Cloetingh et al. 1990; Pollitz, 1986). However, the relationship between all these fitting events should be checked with various scientific methods in detail.

CHAPTER 6

CONCLUSION

Under the light of both literature survey and the newly obtained field data the followings are concluded:

(1) The Altıntaş basin has experienced three phases of deformation during its Eocene-Quaternary development history. These are, from oldest to youngest: (1) the Middle Eocene-Early Pliocene real contraction phase operated in an approximately N-S direction, (2) the Pliocene strike-slip phase operated in an approximately E-W to NW direction, and (3) the Quaternary strike-slip phase operated again in approximately N-S direction. The phase-3 is still lasting. Therefore it is also known as the strike-slip neotectonic regime or neotectonic phase of deformation.

(2) The early configuration of the Altıntaş depositional setting was evolved to in a passive marginal site of a foreland basin during the phase-1 deformation in the Eocene-Late-Early Pliocene time interval. At the end of this phase, the earlier large-scale foreland basin was dissected into at least two smaller basins such as the Altıntaş and Yavuzeli ramp basins. During the Phase-2, these two ramp basins and their early accumulated fills were deformed into a series of anticlines and synclines and displaced in both vertical and lateral directions by the strike-slip tectonic regime and related structures. Additionally, the deformed older basin fill uplifted and left open to the erosional processes.

(3) The change in the tectonic regime at the beginning of Quaternary is not confined to the study area. It seems larger-scale event as indicated by the inversion of various geological phenomena.

(4) Older structures have a significant role as much as the newly formed neotectonic structures in the development of both the paleotectonic and neotectonic configurations of the Altıntaş basin.

(5) The findings supports that the Araban Block was broken-up from the northwestern margin of the Arabian Plate along the East Anatolian Transform Fault System to the west and Bozova Fault Zone to the east most probably during Early Pliocene.

REFERENCES

- Adiyaman, Ö. And Chorowicz, J. 2002. Late Cenozoic tectonics and volcanics in the northwestern corner of the Arabian plate: a consequence of the strike-slip Dead Sea Fault Zone and lateral escape of Anatolia, *Journal of Volcanology and Geothermal Research*, 117. 327-345.
- Allmendinger, R. W. 1999. Introduction to Structural Geology. *Lecture notes*. 279 p.
- Allmendinger, R. W., Cardozo, N. C., and Fisher, D., 2013. Structural Geology Algorithms: Vectors & Tensors: Cambridge, England, Cambridge University Press, 289 p.
- Alpar, B. and Yaltırak, C. 2002. Characteristic features of the North Anatolian Fault in the eastern Marmara region and its tectonic evolution. *Marine Geology*, 190, 329-350.
- Alpaslan, M. 2007. Early to Middle Miocene Intracontinental basaltic volcanism in the northern margin of the Arabian Plate, SE Anatolia, Turkey: geochemistry and petrogenesis. *Geological Magazine*. 144 (5), 867-882.
- Amrouch, K., Lacombe, O., Bellahsen, N., Daniel, J. M. and Callot, J. P. 2010. Stress and strain patterns, kinematics and deformation mechanisms in a basement-cored anticline: Sheep Mountain Anticline, Wyoming. *Tectonics*, 29, TC1005, doi:10.1029/2009TC002525.
- Angelier, J. (1990), Inversion of field data in fault tectonics to obtain the regional stress. III: A new rapid direct inversion method by analytical means, *Geophys. J. Int.*, 103, 363-376, doi:10.1111/j.1365-246X.1990.tb01777.x.
- Arger, J., Michel, J. and Westaway, R.W.C. 2000. Neogene and Quaternary volcanics of southeastern Turkey. *The Geological Society, London, Special Publications*, 173,459-487.

- Arpat, E. and Şarođlu, F., 1972. The East Anatolian Fault System: thoughts on its development. *Bulletin of Mineral Research and Exploration (MTA) Institute of Turkey*, 78, 33-39.
- Axelrod, D.I. 1962. Post-Pliocene uplift of the Sierra Nevada, California, *Bullettin of Geological. Society of America*, 73, 183-198.
- Ayaz, İ. 1958. 1/50000 Geological Map of N38b Sheet. Esso (Turkey) INC.
- Baker, J.A., Menzies, M.A., Thirlwall, M.F., MacPherson, C.G., 1997. Petrogenesis of Quaternary intraplate volcanism, Sana'a, Yemen: implications for plume-lithosphere interaction and polybaric melt hybridization. *Journal of Petrology*, 36, 1359-1390.
- Bayer, H. J., Hötzl, G., Jado, A. R., Röscher, B., Voggenreiter, W., 1998. Sedimentary and structural evolution of the northwest Arabian Red Sea margin. *Tectonophysics*, 153, 137-151.
- Behrendt, J.C. and A. Cooper 1991. Evidence of rapid Cenozoic uplift of the shoulder escarpment of the Cenozoic West Antarctic Rift System and a speculation on possible climatic forcing, *Geology*, 19, 315-319.
- Biddle, K.T., Bultman, T.R., Fairchild, L.H. and Yılmaz, P.O. 1987. An approach to structural interpretation of the SE Turkey fold and thrust belt. *Proceeding in 7th Biannual Petroleum Congress of Turkey*, 89-102. [in Turkish with English abstract]
- Bolat, A., 2012. Adıyaman ili kuzeyinin jeolojisi ve petrol olanakları. *Çukurova University, MSc Thesis*, 112p. [in Turkish with English abstract].
- Bolgi, T., 1961. V. Petrol Bölgesi Seksiyon ölçümleri AR/TPO/261 nolu saha ile Reşan Dodan arası batısındaki sahanın strüktürel etüdları. (TPAO Exploration Group, Report No: 162), 52 p.

- Boulton, S., J. and Robertson, A. H. F., 2008. The Neogene-Recent Hatay Graben, South Central Turkey: graben formation in a setting of oblique extension (transtension) related to post-collisional tectonic escape. *Geological Magazine*, 145, 6, 800-821.
- Bozkurt, E. 2001. Neotectonics of Turkey - a synthesis: *Geodinamica Acta*, 14, 3-30.
- Bridges, E.M. 1990. World Geomorphology *Cambridge University Press, Cambridge*, pp. 260.
- Bryant, G. F., 1960. Stratigraphic report on the Amanus Mountains area. Petroleum District VI and VII, Southeast Turkey (American Overseas Petroleum [AMOSEAS] Report): *General Directorate of Petroleum Affairs of Turkey Technical Archive*, Box No: 398, Report No: 3, 67 p. (TPAO Exploration Group, Report No: 906).
- Bulut, F., Bohnhoff, M., Eken, T., Janssen, C., Kılıç, T., and Dresen, G., 2012. The East Anatolian Fault Zone: Seismotectonic setting and spatiotemporal characteristics of seismicity based on precise earthquake locations, *Journal of Geophysical Research*, 117, B07304, doi:10.1029/2011JB008966.
- Calvet, M. 1994. Les Pyrénées Orientales, *These de Doctorat d'Etat Université de Paris I*, 31-38.
- Cardozo, N., and Allmendinger, R. W., 2013, Spherical projections with OSXStereonet: *Computers & Geosciences*, v. 51, no. 0, p. 193- 05, doi: 10.1016/j.cageo.2012.07.021.
- Chai, B.H.T. 1972. Structure and tectonic evolution of Taiwan, *American Journal of Science*, 272, 389-422.
- Chorowicz, J. Luxey, P., Lyberis, N., Carvalho, J., Parrot, J-F., Yürür, T. and Gündoğdu, N., 1994. The Maraş triple junction (Southern Turkey) based on digital elevation model and satellite imagery interpretation. *Journal of Geophysical Research*, 99, A3, 20225-20242.

- Chorowicz, J., 2005. The East African rift system. *Journal of African Earth Sciences*, 43, 379-410.
- Cloetingh, S., Gradstein, F.M., Kooi, H., Grant, A.C., Kaminski, M., 1990. Plate reorganization; a cause of rapid late Neogene subsidence and sedimentation around the North Atlantic. *Journal of the Geological Society, London*, 147, 495-506.
- Coltorti, M. and C.D. Ollier 2000. Geomorphic and tectonic evolution of the Ecuadorian Andes, *Geomorphology*, 32, 1-19.
- Coltorti, M. and P. Pieruccini 2000. A Late Lower Pliocene planation surface across the Italian Peninsula. a key tool in neotectonic studies, *Journal of Geodynamics*, 29, 323-328.
- Coşkun, B. and Coşkun, B., 2000. The Dead Sea Fault and related subsurface structures, Gaziantep basin, southeast Turkey. *Geological Magazine*, 137 (2), 175-192.
- Courtillot, V., Davaille, A., Besse, J., Stock, J., 2003. Three distinct types of hotspots in the Earth's mantle. *Earth and Planetary Letters*, 205, 295-308.
- Çabalar, A.F., 2006. An overview of earthquake ground response analysis: A case study of Gaziantep city, Turkey. *Geological Society, London, Engineering Geology Special Publications*, 22 [On CD-Rom insert, paper 753], In: Culshaw, M.G., Reeves, H.J., Jeffersen, I. and Spink, T.W. (eds). *Engineering Geology for Tomorrow's cities*.
- Çabalar, A.F. 2008. An assessment of earthquake hazard in Gaziantep, Turkey. *Electronic Journal of Geotechnical Engineering*, 13, Bund. E, 1-14.
- Çapan U.Z., Vidal P., Cantagrel J.M., 1987. K-Ar, Nd, Sr and Pb Isotopic study of the Quaternary volcanism in Karasu Rift (Hatay), N-end of Dead sea rift zone in SE Turkey, *Hacettepe University Earth Sciences*, 14, 165-178.

- Çemen, İ. 1987. Structural geology of the western part of the Araban block: Implications concerning Petroleum potential of the region. *TPAO Exploration Group*, Report No: 2239.
- Çemen, İ. 1990. Araban tektonik bloğu doğu kısmının yapısal jeolojisi ve petrol potansiyeli. TPAO Report No: 2727.
- Çemen, İ., Perinçek, D., Ediger, V.Ş. and Akça, L. 1990a. Güneydoğu Anadolu'daki Bozova Doğrultu Atımlı Fayı: Üzerindeki ilk hareket ters faylanma olan faylara ait bir örnek. *Proceedings in 8th Petroleum Congress of Turkey*, 169-179. [in Turkish with English abstract]
- Çemen., İ., Perincek, D., and Drake, R. E., 1990b, Tectonics of the Araban block, southeastern Anatolia: Syn and post-collisional structures formed in a foreland; *EOS, Transactions American Geophysical Union*, 71, 17, 637-638.
- Demir, T., Seyrek, A., Westaway, R., Bridgland, D. and Beck, A. 2008. Late Cenozoic surface uplift revealed by incision by the River Euphrates at Birecik, South East Turkey. *Quaternary International*, 186, 132-163.
- Demirel, İ. H. Yurtsever, T.S. and Güneri, S. 2001. Petroleum systems of Adıyaman region, Southeastern Anatolia, Turkey. *Marine and Petroleum Geology*, 18, 391-410.
- Geophoto Services, INC. Denver, Colorado, 1958. 1/100.000 Structure Map of Gaziantep N38, N39 Sheet.
- Dewey, J. F. and K. C. Burke, 1973. Tibetan, Variscan, and Precambrian basement reactivation: Products of continental collision, *Journal of Geology*, 81, 683-692.

- Dewey, J. F., and A.M. C. Şengör, 1979. Aegean and surrounding regions: Complex multiplate and continuum tectonics in a convergent zone, *Geological Society of America Bulletin*, 90, 84-92.
- Dewey, F. J., Hempton, M. R., Kidd, W. S. F., Şaroğlu, F. and Şengör, A. M. C. 1986. Shortening of continental lithosphere: the neotectonics of eastern Anatolia - a young collision zone, In: COWARD, M. P. and RIES, A. C. (eds) *Collision Tectonics, Geological Society, London, Special Publication*, 19, 3-36.
- Dunne, W. M. and Hancock, P. L. 1994. Paleostress analysis of small-scale brittle structures. 101-120 [in P. L. Hancock, (ed.) 1994. *Continental Deformation. Pergamon Press, Oxford*, 421 p.].
- Duran, O., Şemşir, D., Sezgin, İ., and Perinçek, D., 1989. Güney Doğu Anadolu'da Midyat ve sylvan Gruplarının stratigrafisi, sedimentolojisi, paleocoğrafyası, paleontolojisi, jeoloji tarihi, rezervuar ve diyajenez özellikleri ve olası petrol potansiyeli. *TPAO Exploration Group*, Report No: 2563, 78 p.
- Eaton, G.P. 1987. Topography and origin of the Southern Rocky Mountains and Alvarado Ridge, in *Continental Extensional Tectonics*, edited by M.P. Coward, J.F. Dewey and P.L. Hancock, *Geological Society London, Special Publications*, 28, 355-369.
- Ekici, T., Alpaslan, M., Parlak, O. and Uçurum, A., 2009; Geochemistry of the Middle Miocene Collision-Related Yamadaği (Eastern Anatolia) Calc-Alkaline Volcanics, Turkey, *Turkish Journal of Earth Sciences*, 18, 511-528.
- Ercan, A. 1979. Doğu Anadolu Fayı üzerinde Deprem Çalışmaları. *Yeryuvarı ve İnsan*, 2, 21-30. [in Turkish with English abstract].
- Eyal, Y. and Reches, Z., 1983. Tectonic analysis of the Dead Sea Rift region since the Late-Cretaceous based on mesostructures. *Tectonics*, 2, 2, 167-185.

- Faccenna, C., Becker, T. W., Jolivet, L. and Keskin, M. 2013. Mantle convection in the Middle East: Reconciling Afar upwelling, Arabia indentation and Aegean trench rollback. *Earth and Planetary Science Letters*, 375, 254-269.
- Farley, K.A., M.E. Rusmore and S.W. Bogue 2001. Post-10 Myr uplift and exhumation of the Northern Coast Mountains, British Columbia, *Geology*, 29, 99-102.
- Gansser, A. 1991. Facts and theories on the Himalayas, *Eclogae Geologicae Helvetiae*, 84, 33-59.
- Garfunkel, Z., Beyth, M., 2006. Constraints on the structural development of Afar imposed by the kinematics of the major surrounding plates. In: Yirgu, G., Ebinger, C.J., Maguire, P. K. H. (Eds.), *The Afar Volcanic Province Within the East African Rift System*, 259, Geological Society of London, Special Publication, 23-42.
- Ghebreab, W., 1998. Tectonics of the Red Sea region reassessed. *Earth Science Review*, 45, 1-44.
- Golding and Conolly, 1962. Stylolites In Volcanic Rocks. *Journal of Sedimentary Petrology*, 32, 3, 534-538.
- Gossage, D.W., 1956. Compiled progress report on the geology of part of Petroleum District VI, SE Turkey: *N.V. Turkse Shell*, Report no.: GRT. 2, 22 p.
- Gülen, L., Barka, A., Toksöz, M.N., 1987. Kıtaların çarpışması ve ilgili kompleks deformasyon: Maraş üçlü eklemi ve çevre yapıları. *Yerbilimleri*, 14, 319-336.
- Güven, A., Dinçer, A., Tuna, M. E., Çoruh, T., 1991. Güneydoğu Anadolu Kampaniyen - Paleosen otokton istifin stratigrafisi, TPAO Report No: 2828, 133p.

- Gürsoy, H., Tatar, O., Piper, J.D.A., Koçbulut, F. and Mesci, B.L. 2007. Anadolu bloğu-Arap Levhasının Neotektonik dönem çarpışma sürecinde gelişen kabuksal deformasyonun Paleomanyetik yöntemlerle analizi. *TÜBİTAK, Project No: CAYDAG-104Y262*, 92p. [Unpublished]. [in Turkish with English abstract]
- Hancock, P. L., 1985. Brittle Microtectonics: Principles and Practice: *Journal of Structural Geology*, 7, 437-457.
- Hancock, P. L. and Barka, A., 1987. Kinematic indicators on active normal faults in western Turkey. *Journal of Structural Geology*, 9, 573-584.
- Hempton, M.R., 1987. Constraints on Arabian plate motion and extensional history of the Red Sea. *Tectonics* 6, 687-705.
- Herece, E. and Akay, E. 1992. Karlıova-Çelikhan arasında Doğu Anadolu Fayı. *Proceedings in 9th Petroleum Congress of Turkey*, Ankara, 361-372. [in Turkish with English abstract]
- Herece, E., 2009. Left-lateral offset and age of the East Anatolian Fault System. *62th Geological Congress of Turkey*, Abstract book.
- Hisarlı, Z. M., Çinku, M. C., Ustaömer, T., Keskin, M. and Orbay, N. 2016. Neotectonic deformation in the Eurasia-Arabia collision zone, the East Anatolian Plateau, E Turkey: evidence from palaeomagnetic study of Neogene-Quaternary volcanic rocks. *International Journal of Earth Sciences (Geol Rundsch)*, 105, 139-165. DOI 10.1007/s00531-015-1245-4.
- Ho, C.S. 1986. A synthesis of the geological evolution of Taiwan, *Tectonophysics*, 125, 1-16.
- Holingsworth, S.E. and R.W.R. Rutland 1968. Studies of Andean Uplift, Part 1. Post-Cretaceous evolution of the San Bartelo area, North Chile, *Geological Journal*, 6, 49-62.

- Holmes, A. 1965. Principles of Physical Geology. *Nelson, London, 2nd edition*, pp. 1288.
- Hoshino, M. 1998. The Expanding Earth. Evidence, Causes and Effects. *Tokai Univ. Press, Tokyo*.
- Huesing, S.K., Zachariasse, W.J., Hinsbergen, D.J.J., Krijgsman, W., İnceöz, M., Harzhauser, M., Mandic, O. and Kroh, A. 2009. Oligocene-Miocene basin evolution in SE Anatolia, Turkey: constraints on the closure of the eastern Tethys gateway. *The Geological Society, London, Special Publications*, 311, 107-132.
- İmamoğlu, M. Ş., 1993. Gölbaşı (Adıyaman)-Pazarcık-Narlı (K.Maraş) Arasındaki Sahada Doğu Anadolu Fayı'nın Neotektonik İncelemesi, PhD Thesis, Ankara University. 137p.
- Kalvoda, J. 1992. Geomorphological Record of the Quaternary Orogeny in the Himalaya and the Karakoram *Elsevier, Amsterdam*, pp. 316.
- Kartal, R.F., Kadiroğlu, F.T. and Apak, A. 2014. 19/09/2012 Pazarcık Kahramanmaraş depremi ve artçı deprem aktivitesinin bölgenin neotektoniği ile ilişkisi. *Proceedings' in the 67th Geological Congress of Turkey*, 1-16.
- Kaymakçı, N., İnceöz, M., Ertepinar, P. and Koç, A. 2010. Late Cretaceous to recent kinematics of SE Anatolia (Turkey). *Geological Society, London*, 340, 409-435.
- Kellogg, H.E., 1960. Stratigraphic report, Hazro area, Petroleum District V, SE Turkey. (American Overseas Petroleum [AMOSEAS] Report): *General Directorate of Petroleum Affairs of Turkey Technical Archive*, Box No: 126, Report No: 1, 42 p.
- Keskin M., Chugaev A., Lebedev V.A., Sharkov E., Oyan V., Kavak O., 2012a. The Geochronology and Origin of Mantle Sources for Late Cenozoic

Intraplate Volcanism in the Frontal Part of the Arabian Plate in the Karacada Neovolcanic Area of Turkey. Part 2. The Results of Geochemical and Isotope (Sr-Nd-Pb) Studies, *Journal of Volcanology and Seismology*, 6, 361-382.

Keskin, M., Chugaev A., Lebedev V.A., Sharkov E., Oyan V., Kavak O., 2012b. The Geochronology and Origin of Mantle Sources for Late Cenozoic Intraplate Volcanism in the Frontal Part of the Arabian Plate in the Karacada Neovolcanic Area of Turkey. Part 1. The Results of Isotope Geochronological Studies, *Journal of Volcanology and Seismology*, 6, 31-42.

Koç, A. and Kaymakçı, N. 2013. Kinematics of Sürgü Fault Zone (Malatya,Turkey): A Remote sensing study. *Journal of Geodynamics*, 65, 292-307.

Koçyiğit, A., Yusufoglu, H. and Bozkurt, E. 1999. Evidence from the Gediz graben for episodic two-stage extension in western Turkey. *Journal of the Geological Society, London* 156, 605–616.

Koçyiğit A., Ünay, E. & Saraç, G. 2000. Episodic graben formation and extensional neotectonic regime in west Central Anatolia and the Isparta Angle: a key study in the Akşehir-Afyon graben, Turkey. *Geological Society, London, Special Publication* 173, 405-421.

Koçyiğit, A., Yılmaz, A., Adamia, S. and Kuloshvili, S. 2001. Neotectonics of East Anatolian Plateau (Turkey) and Lesser Caucasus: implications for transition from thrusting to strike-slip faulting. *Geodinamica Acta* 14-177-195.

Koçyiğit, A., Aksoy, E. and İnceöz, M. 2003. Basic neotectonic characteristics of the Sivrice Fault Zone in the Sivrice-Palu Area, East Anatolian Fault System (EAFS), Turkey. *A pre workshop excursion guide-book (International Workshop on the North Anatolian, East Anatolian and Dead Sea Fault Systems: Recent Progress in Tectonics and Paleoseismology, and Field Training Course in Paleoseismology, 31 August-12 September, 2003 Middle East Technical University-METU, Ankara, Turkey)*, 20p.

Koçyiğit, A. & Özacar, A. 2003. Extensional Neotectonic Regime through the NE Edge of the Outer Isparta Angle, SW Turkey: New field and seismic Data. *Turkish Journal of Earth Sciences* 12, 67-90.

Koçyiğit, A., Deveci, Ş., Biryol, B., Arca, S., Aktürk, Ö., Ayhan, E., Demir, C., Lenk, O., Kılıçoğlu, A., Aktuğ, B., Açıkgöz, M., Çetin, H. and Günaydın, O., and Aytun, A., 2005. Kuzey Anadolu Fay Sisteminin (KAFFS) İsmetpaşa-Gerede ve Mengen Arasındaki Kesiminin Depremselliği. *TÜBİTAK Report No: YDABAG: 102Y053*. 180p. [Unpublished]

Koçyiğit, A., Aksoy, E., İmamoğlu, Ş. and Deveci Gürboğa, Ş. 2010. Doğu Anadolu Fay Sistemi'nin Gölbaşı Kesiminde Saha Gözlemleri ve Teknik İnceleme. *14th Workshop of the Active Tectonics Research Group*, [Supplementary Book], 14 p. [in Turkish]

Koçyiğit, A. 2013. New field and seismic data about the intraplate strike-slip deformation in Van region, East Anatolian plateau, E. Turkey. *Journal of Asian Earth Science*, 62, 586-605.

Koehn, D. and Renard, F., Toussaint, R. and Passchier, C.W., 2007. Growth of stylolite teeth patterns depending on normal stress and finite compaction. *Earth and Planetary Science Letters* 257, 582-595.

Kroonenberg, S.B., J.G.M. Bakker and M. Van Der Wiel 1990. Late Cenozoic uplift and paleogeography of the Colombian Andes. constraints on the development of the high-andean biota, *Geologie en Mijnbouw*, 69, 279-290.

Kuşçu, İ., Gençlioğlu-Kuşçu, G., Tosdal, R. M., Ulrich, T. D. and Friedman, R. 2010. Magmatism in the southeastern Anatolian orogenic belt: transition from arc to post-collisional setting in an evolving orogen. In: Sosson, M., Kaymakçı, N., Stephenson, R. A., Bergerat, F. and Starostenko, V. (eds) *Sedimentary Basin Tectonics from the Black Sea and Caucasus to the Arabian Platform*. Geological Society, London, Special Publications, 340, 437-460.

- Kuzucuođlu, C., Fontunge, M. and Mourolis, D., 2004. Holocene Terraces in the Middle Euphrates Valley between Halfeti and Karkemish (Gaziantep, Turkey). *Quaternaire*, 15 (1-2), 195-206.
- Külah, T. 2006. Uđurca (Gaziantep) civarı Tersiyer istifinin Mikropaleontolojik incelenmesi ve ortamsal yorumu. *Çukurova University, MSc Thesis*, 62p. [Adana]. [in Turkish with English abstract]
- Lustrino, M. and Sharkov, E. 2006. Neogene volcanic activity of western Syria and its relationship with Arabian plate kinematics. *Journal of Geodynamics*, 42, 115-139.
- Lustrino M., Keskin M., Mattioli M., Kavak O., 2012. Heterogeneous mantle sources feeding the volcanic activity of Mt. Karacadađ (SE Turkey), *Journal of Asian Earth Sciences*, 6, 120-139.
- Lyberis, N., Yürür, T., Chorowicz, J., Kasapođlu, E. and Gündođdu, N. 1992. The East Anatolian Fault: an oblique collision belt. *Tectonophysics*, 204, 1-15.
- Maxson, J. H., 1936, Geology and petroleum possibilities of the Hermis dome. *MTA Report No: 255*, 25 p.
- Maxson ve Tromp., 1940. Studies of NTS in VI. Petroleum region of Turkey.
- McKenzie D. P., 1972. Active tectonics of the Mediterranean region. *Geophysical Journal of the Royal Astronomical Society*, 30, 109-185.
- Migon, P. and J. Lach 1999. Geomorphological evidence of neotectonics in the Kaczawa sector of the Sudetic marginal fault, Southwestern Poland, in Late Cainozoic Evolution of the Sudeten and its Foreland, edited by D. Krzyszkowski, *Geologia Sudetica*, 32, 307-316.
- Miller, K.G., Fairbanks, R.G., Mountain, G.S., 1987. Tertiary oxygen isotope synthesis, sea level history, and continental margin erosion. *Paleoceanography*, 2, 1-19.

- Miller, K.G., Kominz, M.A., Browning, J.V., Wright, J.D., Mountain, G.S., Katz, M.E., Sugarman, P.J., Cramer, B.S., Christie-Blick, N., and Pekar, S.F., 2005, The Phanerozoic record of global sea-level change. *Science*, 312, 1293-1298.
- Nalbant, S.S., McClosky, J., Steacy, S. and Barka, A. A. 2002. Stress accumulation and increased seismic risk in eastern Turkey. *Earth and Planetary Science Letters*, 195, 291-298.
- Neill, I., Meliksetian, Kh., Allen, M.B., Navarsardyan, G. and Karapetyan, S., 2013. Pliocene-Quaternary volcanic rocks of NW Armenia: Magmatism and lithospheric dynamics within an active orogenic plateau. *Lithos* 180-181 (2013) 200-215
- Nitchman, S.P., S.J. Caskey and T.L. Sawyer, 1990. Change in Great Basin tectonics at 3-4 Myr - A hypothesis, *Geological Society of America, Cordilleran Section*, 33 3, p. 72.
- Ökeler, A., 2003. Kliskya Bölgesi'nin Güncel Depremselliği ve Gerilme Analizi. *Istanbul Technical University, İstanbul, Graduate School of Sciences, Engineering and Technology, MSc Thesis*, 110p. [Unpublished]. [in Turkish with English abstract].
- Ollier, C.D. and D. Taylor 1988. Major geomorphic features of the Kosciusko-Bega region, *BMR J. Australian geology and geophysics*, 10, 357-362.
- Ollier, C. D. 2006. Mountain uplift and the Neotectonic Period. *Annals of Geophysics, Supplement to Volume*, 49, 1, 437-450.
- Över, S., Özden, S., Ünlügenç, U.C., Yılmaz, H. Vergely, P. and Bellier, O., 2003. Adana ve Kahramanmaraş arasında kalan bölgenin Miyosen sonrası tektoniği ve depremselliği. *TÜBİTAK, Report No: YDABAG 100Y095*, 78p. [Unpublished]. [in Turkish with English abstract].

- Park, W.C., and Schot, E.K., 1968, Stylolites: their nature and origin: *Journal of Sedimentary Petrology*, 38, 175-191.
- Passchier, C. W. and Trouw, R. A. J., 1996. *Microtectonics*. Springer, New York, 289 p.
- Peksu, M. 1976. M40c, M40d, N39a, N39b, N40a, N40b 1/50000 scale geological maps: TPAO Archive [Unpublished]. [in Turkish]
- Perinçek, 1978. V-VI-IX. Bölge (GDA otokton-allokon birimler) jeoloji sembolleri: *TPAO Exploration Group*, Report No: 6657.
- Perinçek, D., Günay, Y., and Kozlu, H. 1987. New Observations on strike-slip faults in east and southeast Anatolia. *Proceedings in 7th Biannual Petroleum Congress of Turkey*, 89-103. [in Turkish with English Abstract]
- Perinçek, D., and Çemen, İ. 1990. The structural relationship between the East Anatolian and Dead Sea Fault Zones in Southeastern Turkey. *Tectonophysics*, 172, 331-340.
- Perinçek, D. and Eren, A, 1990, Doğrultu Atımlı Doğu Anadolu ve Ölü Deniz Fay Zonları Etki Alanında Gelişen Amik Havzasının Kökeni. *Proceedings in 8th Petroleum Congress of Turkey*, 180-192. [in Turkish with English abstract]
- Perinçek, D., Duran, O., Bozdoğan, N., and Çoruh, T., 1991. Stratigraphy and the paleogeographic evolution of the autochthonous sedimentary rocks in SE Turkey, *in the Proceedings of Ozan Sungurlu Symposium prepared by Ozan Sungurlu Foundation for Science, Education and Aid, Tectonics and hydrocarbon potential of Anatolia and surrounding regions*, 274-305.
- Pollitz F. F. 1986. Pliocene change in Pacific plate motion. *Nature*, 320:738-741.

- Petit, J.P., Mattauer, M., 1995. Palaeostress superimposition deduced from mesoscale structures in limestone: the Matelles exposure, Languedoc, France. *Journal of Structural Geology* 17, 245-256.
- Potter, P., E. and Szatmari, P., 2009. Global Miocene tectonics and the modern world. *Earth-Science Reviews*, 96, 279-295.
- Quennel, A.M. 1958. The structural and geomorphic evolution of the Dead Sea Rift. *Quarterly Journal of the Geological Society of London*, 114, 1-24.
- Rădoane, M., N. Radoane and D. Dumitru 2003. Geomorphological evolution of longitudinal river profiles in the Carpathians, *Geomorphology*, 50, 293-306.
- Railsback, L. B. 2003. Stylolites. 690-692. [in *Encyclopedia of Sediments and Sedimentary Rocks* edited by Middleton, J. C., Coniglio, M., Hardie, L. A., Longstaffe, F. J. 2003] Kluwer Academic Publishers, Dordrecht, 821 p .
- Ramsay, J.G. and Huber, M.I. 1983. The techniques of modern structural geology, 1: Strain analysis. Academic Press, London.
- Ramsay, J.G. and Huber, M.I. 1987. The techniques of modern structural geology, II: Folds and Fractures. Academic Press, London.
- Rojay, B., Heimann, A. and Toprak, V., 2001. Neotectonic and volcanic characteristics of the Karasu fault zone (Anatolia, Turkey): The transition zone between the Dead Sea transform and the East Anatolian fault zone. *Geodinamica Acta*, 14, 197-212.
- Ruddimann, W. F. and Raymo, M. E. 1988. Northern hemisphere climate regimes during the past 3 Ma: possible tectonic connections. *Philosophical Transactions of the Royal Society of London*, B 318, 411-430.
- Rukieh, M., Trifonov, V.G., Dodonov, A.E., Minini, H., Ammar, O., Ivanova, T.P., Zaza, T., Ysef, A., Al-Shara, M., Jobaili, Y., 2005. Neotectonic map

- of Syria and some aspects of Late Cenozoic evolution of the northwestern boundary zone of the Arabian plate. *Journal of Geodynamics*, 40, 135-256.
- Rutter, E.H., 1983. Pressure solution in nature, theory and experiment. *Journal of the Geological Society of London* 140, 725-740.
- Sala, M. 1984a. Pyrenees and Ebro Basin Complex, in *Geomorphology of Europe*, edited by C. Embleton, *Macmillan, London*, 269-293.
- Sala, M. 1984b. The Iberian Massif, in *Geomorphology of Europe*, edited by C. Embleton *Macmillan, London*, 294-322.
- Schmidt, K., 1935. First report over geological and paleontological. *MTA Report No: 1532*, 11 p.
- Seymen, I. and Aydın, A. 1972. Bingöl deprem fayı ve bunun Kuzey Anadolu Fayı ile ilişkisi. *Bulletin of Mineral Research and Exploration (MTA) Institute of Turkey*, 79, 1-8. [in Turkish with English abstract]
- Sonel, N. and Sarbay, N. 1988. Definition of Petroleum traps around Narlı (Kahramanmaraş) using seismic methods. *Common. Fac. Sci. Univ. Ank. Serie C*, 6, 257-287.
- Stcephsky, V. 1943a. Maraş-Gaziantep bölgesi jeolojisi. *Bulletin of Mineral Research and Exploration (MTA)of Turkey* 29, 110-125. [in Turkish with English abstract]
- Stcephsky, V. 1943b. Gaziantep Deniz Oligoseni (Cenup Türkiye). *Bulletin of Mineral Research and Exploration (MTA)of Turkey*, 30, 323-349.
- Stel, H. and De Ruig, M. J., 1989. Opposite vergence of a kink fold and pressure solution cleavage, Southeast Spain: a study of the relation between paleostress and fold kinematics. *Tectonophysics* 165, 117-124.

- Sugatte, R.P. 1982. The geological perspective, in Landforms of New Zealand, edited by J.M. Soons and M.J. Selby, *Longman Paul*, Auckland, 1-13.
- Sungurlu, O., 1973. VI. Bölge Gölbaşı-Gerger arasındaki sahanın jeolojisi: *TPAO Exploration Group*, Report no. 802, 30 p.
- Sungurlu, O., 1974. VI Bölge kuzeyinin jeolojisi ve petrol imkanlari. In: H. Okay and E. Dilekoz, (Editors), *2nd Turkish Petroleum Congress*, Ankara, 85-107. [in Turkish with English abstract]
- Suppe, J., 1985. Principles of Structural Geology. *Prentice-Hall*, New Jersey, 537 p.
- Şaroğlu, F., Emre, Ö. and Boray A., 1987. Türkiye'nin Diri Fayları ve Depremsellikleri. *MTA Report No: 8174*.
- Şaroğlu, F., Emre, Ö. and Kuşçu, İ. 1992a. The East Anatolian Fault Zone of Turkey. *Annales Tectonicae*, 6, 99-125. [Special Issue]
- Şaroğlu, F., Emre, Ö. and Kuşçu, İ., 1992b. Active Fault Map of Turkey. *General Directorate of Mineral Research and Exploration (MTA) of Turkey. Publication*, 1992.
- Şen, E., Kürkçüoğlu, B., Aydar, E., Gourgau, A., ve Vincent, P. M. 2003. Volcanological evolution of Mount Erciyes stratovolcano and origin of the Valibaba Tepe ignimbrite (Central Anatolia, Turkey). *Journal of Volcanology and Geothermal Research*, 125, 225-246.
- Şengör, A.M.C. (1979). The North Anatolian transform fault: its age, offset and tectonic significance. *Journal of the Geological Society of London*, 136, 269-282.
- Şengör, A.M.C., White, G.W. and Dewey, J.F., 1979. Tectonic evolution of the Bitlis Suture, southeastern Turkey: implications for the tectonics of the Eastern Mediterranean. *Rapp. Comm. Int. Mer Medit.*, 25/26-2a: 95-97.

- Şengör, A.M.C. 1980. Türkiyenin neotektoniğinin esasları. *Geological Society of Turkey, Conference series*, 2, Ankara.
- Şengör, A.M.C., and Yılmaz, Y., 1981, Tethyan evolution of Turkey, A plate tectonic approach: *Tectonophysics*, 75, 181-241.
- Şengör, A. M. C., Görür, N. and Şaroğlu, F. 1985. Strike-slip faulting and related basin formation in zones of tectonic escape: Turkey as a case study. In: Biddle, K. T. and Christie-Blick, N. (eds) Strike-Slip Deformation, Basin Formation and Sedimentation. *Society of Economic Paleontology and Mineralogy, Special Publications*, 37, 227-264.
- Şengör, A.M.C. 1987a. Tectonics of the Tethysides: Orogenic collage development in a collisional setting: *Ann. Rev. Earth Planet. Sci.* 15, 213-244.
- Şengör, A.M.C. 1987b. Tectonic subdivisions and evolution of Asia: *Bull. Tech. Univ. Istanbul.* 40, 355-435.
- Taşman, C. E., 1930. Mardin ve Siirt vilayetindeki bazı aksamının jeoloji ve petrol ihtimalatı hakkında rapor. *MTA Report No: 215*, 21p.
- Tatar, O., Gürsoy, H. Piper, J.D.A, Heinmann, A., Parlak, O., Yurtmen, S., Koçbulut, F. and Mesci, B.L. 2004. Ölüdeniz ve Doğu Anadolu Fay Zonlarının Kesişim bölgesinde kabuksal deformasyonun Paleomanyetik ve jeokronolojik açıdan incelenmesi. *TÜBİTAK, Report No: YDABAG-101Y023*, 129p. [in Turkish with English abstract]
- Tatar, O., Yurtmen, S., Temiz, H., Gürsoy, H., Koçbulut, F., Mesci, B.L. and Guezou, J.C. 2007. Intracontinental Quaternary volcanism in the Nıksar pull-apart basin, North Anatolian Fault Zone, Turkey. *Turkish Journal of Earth Sciences*, 16, 417-440.

- Taymaz, T., Jackson, J., McKenzie, D.P., 1991. Active tectonics of the North and Central Aegean Sea, *Geophysical Journal International* 106 433-490.
- Temel, A., Gündođdu, M.N., Gourgaud, A. and Le Pennec, J.-L., 1998. Ignimbrites of Cappadocia _Central Anatolia, Turkey: petrology and geochemistry. *Journal of Volcanology and Geothermal Research*, 85, 447-471.
- Telsiz, S., Temel, A., Gaurgaud, A., and Alpaslan, M., 2007. Geochemical properties of Miocene basaltic rocks from Yavuzeli-Araban-Narlı region, South East Anatolia, Turkey. *Goldschmidt Geochemistry Conference Abstracts, Geochim. Cosmochim. Acta*, 71, 15, Supplement 1, A1012.
- Terlemez, H.Ç.İ., Şentürk, L., Ateş, Ş., Sümengen, M. and Oral, A.1992. Gaziantep dolayının ve Pazarcık-Sakçagöz-Kilis-Elbeyli-Oğuzeli arası jeolojisi. *MTA, Report No: 9526*, 112p. [Unpublished]. [in Turkish]
- Tertemiz, G. 1958. 1/50000 Geological Map of N38c Sheet. Esso (Turkey) INC.
- Tolun, N., 1956. Pazarcık (Maraş) Birecik ve Gaziantep dolaylarının jeolojik incelemesi. *MTA Report No: 2389*, 79p. [Unpublished]. [in Turkish]
- Toprak, V., Rojay, B. and Heimann, A. 2002. Hatay Grabeni'nin neotektonik evrimi ve Ölü Deniz Fay Kuşağı ile ilişkisi. *Tübitak Report No: YDABÇAG-391 (196T083)*, 57p.
- Trifonov, V.G., Dodono, A.E., Sharkov, E.V., Golovin, D.I., Chernyshev, I.V., Lebedev, V.A., Ivanova, T.P., Bachmanov, D.M., Rukieh, M., Ammar, O. Minini, H., Al-Kafri, A.-M. and Ali, O. 2011. New data on the Late Cenozoic basaltic volcanism in Syria, applied to its origin. *Journal of Volcanology and Geothermal Research*, 199, 177-192.
- Tromp, S.W. 1943. Üst Kretasenin mikrofaunaları ile Cenubi Türkiye'de Urfa ve Gaziantep havalilerindeki (Arap fasiyesinin) üçüncü devir maktaları. *Bulletin of Mineral Research and Exploration (MTA)of Turkey*, 29, 126-141.

- Trumpy, R. 1980. An Outline of the Geology of Switzerland (Wepf, Basel), 280p.
- Tuna, D., 1973. VI. Bölge Litostratigrafi Birimleri Adlamasının Açıklayıcı Raporu. *TPAO Report No: 813*.
- Türkkan, A., 2011. Yavuzeli-Araban (Gaziantep) dolayının stratigrafisi ve Fırat formasyonu resifal kireçtaşlarının doğal yapı malzemesi olarak kullanılabilirliğinin araştırılması. *Çukurova University, Adana, Natural Sciences Institute, MSc Thesis, 72p*. [Unpublished]. [in Turkish with English abstract]
- Ulu, Ü., Genç, Ş., Giray, S., Metin, Y., Çörekçioğlu, E., Örçen, S., Ercan, T., Yaşar, T. and Karabıyıköğlu, M. 1991. Belveren-Araban-Yavuzeli-Nizip-Birecik alanının jeolojisi, Senozoyik yaşlı volkanik kayaların petrolojisi ve bölgesel yayılımı. *MTA, Report No: 9226, 225p*. [Unpublished]. [in Turkish]
- Volker, F., Altherr, R., Jochum, K.-P., McCulloch, M.T., 1997. Quaternary volcanic activity of the southern Red Sea: new data and assessment of models on magma sources and Afar plume-lithosphere interaction. *Tectonophysics, 278, 15-29*.
- Walker, E.H. 1949. Andean uplift and erosion surfaces near Uncia, Bolivia, *American Journal of Science, 247, 646-663*.
- Westaway, R., and Arger, J. 1996. The Gölbaşı basin, southeastern Turkey: a complex discontinuity in a major strike-slip fault zone. *Journal of the Geological Society, 153, 729-744*.
- Westaway, R., 2004. Kinematic consistency between the Dead Sea Fault Zone and the Neogene-Quaternary left-lateral faulting in SE Turkey. *Tectonophysics, 391, 203-237*.

- Wilson, H. H., and Krummenacher, R., 1959. Geology and oil prospects of the Gaziantep region, SE Turkey. (*N. V. Turkse Shell Report*): *General Directorate of Petroleum Affairs of Turkey Technical Archive* Box No: 351, Report No: 2, 53p. (*TPAO Exploration Group Report No: 839*),
- Wu, Y., Z. Cui, G. Liu, D. Ge, J. Yin, Q. Xu and Q. Pang 2001. Quaternary geomorphological evolution of the Kunlun Pass area and uplift of the Qinghai-Xizang Tibet Plateau, *Geomorphology*, 36, 203-216.
- Yalçın, N., 1979. Doğu Anadolu yarılımı'nın Türkoğlu-Karaağaç (K.Maraş) arasındaki kesiminin özellikleri ve bölgedeki yerleşim alanları. *Türkiye Jeoloji Kurumu. Altın Simpozyumu*, 49-56.
- Yılmaz, Y., Demirkol, C., Yalçın, N., Yiğitbaş, E., Gürpınar, O., Yetiş, C., Günay, Y. and Sarıtaş, B. 1984. The geology of the Amanos mountains, II Ophiolite. *İstanbul Teknik Üniversitesi Mühendislik Fakültesi* 351.
- Yılmaz, E., and Duran, O., 1997. Güney Doğu Anadolu Bölgesi Otokton ve Allohton Birimler Stratigrafi Adlana Sözlüğü "Lexicon". *TPAO Education Publications Series No: 31*.
- Yılmaz, Y. 1993. New evidence and model on the evolution of the southeast Anatolian orogen. *Geological Society of America Bulletin*, 105, 251-271.
- Yılmaz, Y., Yiğitbaş, E. and Genç, S.C. 1993. Ophiolitic and metamorphic assemblages of southeast Anatolia and their significance in the geological evolution of the orogenic belt. *Tectonics*, 12, 1280-1297.
- Yılmaz, H., Över, S. and Özden, S. 2006. Kinematic of the East Anatolian Fault zone between Türkoğlu (Kahramanmaraş) and Çelikhan (Adiyaman), eastern Turkey. *Earth Planets Space*, 58, 1463-1473.
- Yiğitbaş, E., Yılmaz, Y. and Genç, S.C. 1992. Eocene nappe emplacement in the SE Anatolian orogenic belt: *Proceedings in 9th Petroleum Congress of Turkey*, Ankara, 307-318. [in Turkish with English abstract].

- Yiğitbaş, E. and Yılmaz, Y. 1996a. Post-Late Cretaceous strike-slip tectonics and its implications for the SE Anatolian Orogen, Turkey. *International Geology Review*, 38, 818-831.
- Yiğitbaş, E. and Yılmaz, Y. 1996b. New evidence and solution to the Maden complex controversy of the southeast Anatolian orogenic belt (Turkey). *Geologisches Rundschau*, 85, 250-263.
- Yoldemir, O. 1987. Suvarlı-Haydarlı-Narlı-Gaziantep arasında kalan alanın jeolojisi, yapısal durumu ve petrol olanakları. *TPAO Exploration Group*, Report No: 2275, 60p [Unpublished]. [in Turkish]
- Yoldemir, O. 1988. Sakçagöze, Kartal, Yaylacık (Gaziantep) batısı civarının jeolojisi, yapısal durumu ve petrol olanakları. *TPAO Exploration Group*, Report No: 2453, 24p. [Unpublished]. [in Turkish]
- Yoldemir, O. and Perinçek, D. 1990. Güneydoğu anadolunun batısında (Gaziantep-Adıyaman arası) Paleosen yaşlı graben oluşumu ve diğer tektono - stratigrafik bulgular. *Proceedings in 8th Petroleum Congress of Turkey*, 113-127. [in Turkish with English abstract]
- Yönlü, Ö., Altunel, E. Karabacak, V. and Akyüz, H.S., 2013. Evolution of the Gölbaşı basin and its implications for the long-term offset on the east Anatolian Fault zone, Turkey. *Journal of Geodynamics*, 65, 272, 281.
- Yusufoğlu, H. 2013. An intramontane pull-apart basin in tectonic escape deformation: Elbistan Basin, Eastern Taurides, Turkey. *Journal of Geodynamics*, 65, 308- 329.
- Yürür, M.T. and Chorowicz, J., 1998. Recent volcanism, tectonics and plate kinematics near the junction of the African, Arabian and Anatolian plates in the Eastern Mediterranean. *Journal of Volcanology and Geothermal Research*, 85, 1-15.

- Zachos, J., Pagani, M., Sloan, L., Thomas, E., Billups, K., 2001. Trends, rhythms, and aberrations in global climate 65 Ma to present. *Science*, 292, 686-692.
- Zanchi, A., Crosta, G. B. and Darkal, A. N., 2002. Paleostress analyses in NW Syria: constraints on the Cenozoic evolution of the northwestern margin of the Arabian plate, *Tectonophysics*, 357, 1, 255-278.
- Zhang, D.D. 1998. Geomorphological problems of the middle reaches of the Tsangpo River, Tibet, *Earth Surface Processes and Landforms*, 23, 889-903.
- Zuchiewicz, W. 2000. Morphotectonics of the outer East Carpathians of Poland in the light of cartometric studies, *Studia Geomorphologica Carpatho-Balcanica*, 34, 5-26.

APPENDICES:

Appendix-A:

Included inside the box.

Appendix-B:

Included inside the box at the back.

CURRICULUM VITAE

PERSONAL INFORMATION

Surname, Name : ÇİÇEK, Aydın
Nationality : Turkish (TC)
Date and Place of Birth : 16 August 1982, Kırcaali
Marital Status : Married
Phone : +90 530 541 69 65
e-mail : e156299@metu.edu.tr

EDUCATION

Degree	Institution	Year of Graduation
MSc	METU Geological Engineering	2009
BSc	HU Geological Engineering	2006
High School	Yenibosna High School, İstanbul	2000

WORK EXPERIENCE

Year	Place	Enrollment
2010-	Maden Tetkik ve Arama (MTA) Genel Müdürlüğü	Geological Engineer
2009-2010	Ministry of Environment and Forestry	Engineer
2007-2009	METU Geological Engineering	Research Assistant

FOREIGN LANGUAGES

Advanced English

PUBLICATIONS

1. Çiçek A. and Koçyiğit A. "A NNE-trending active graben in the Isparta Angle, SW Turkey: Karamık Graben, its geometry, age and earthquake potential", *Trabajos de Geologia, Universidad de Oviedo*, 29, 168-174 (2009).

HOBBIES

Reading Book, Chess, Basketball.

